Post-Conference Excursion

Post-Conference Field Trip: South-Eastern Bohemia, Czech Republic; August 10–13, 2011

HP/UHP Metamorphic Rocks in the Moldanubian Zone

During the three-day field trip in the Moldanubian Zone, three areas with occurrences of granulite massifs, each of which contain HP/UHP mafic and ultramafic rocks, will be visited. As shown on the simplified geological map (Fig. 1), these include the South Bohemian granulite massifs (A), the Gföhl unit (B) and the Kutná Hora Complex (C). In total we will visit 13 localities (8 garnet peridotites with garnet pyroxenites and eclogites), 2 eclogites and 1 spinel peridotites with eclogite and 1 garnet gneiss. Most of these HP/UHP rocks are part of high-grade units with granulite, but 2 will be from the amphibolite facies units.

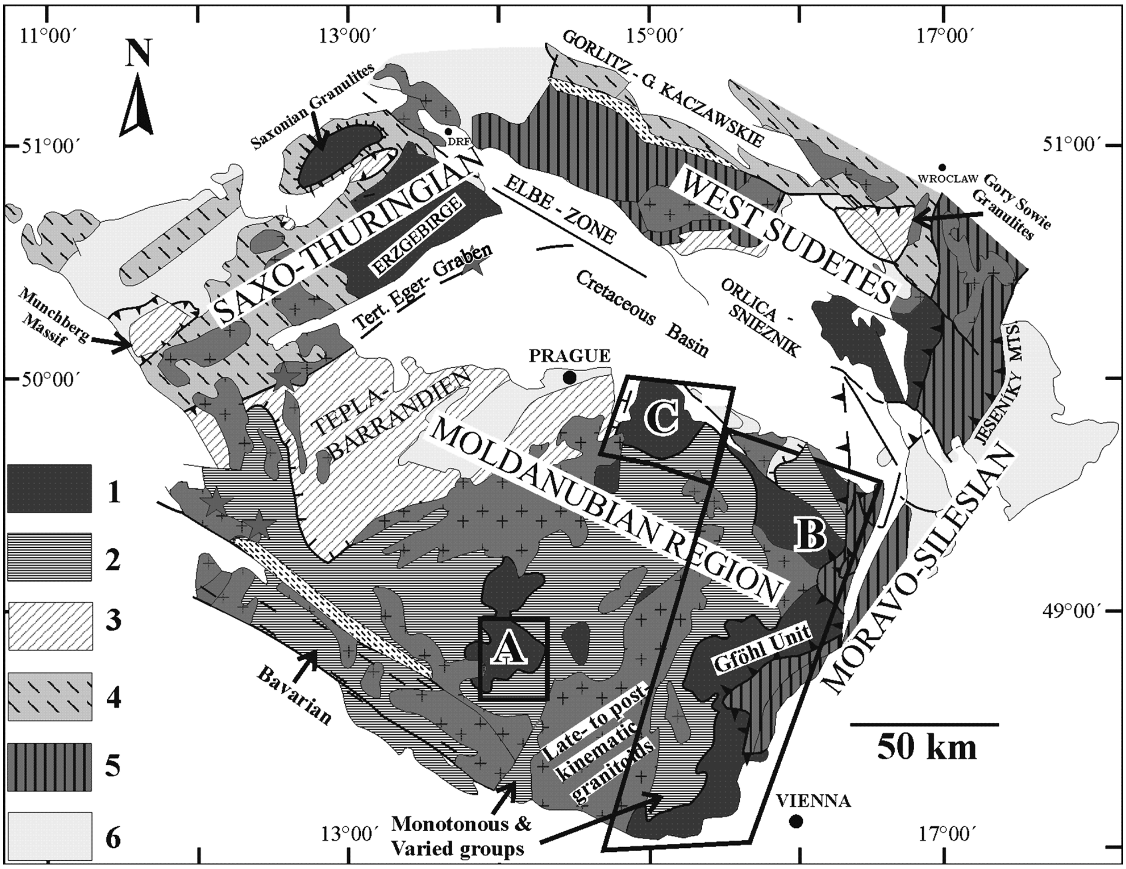

■ **Fig. 1.** Simplified geological map of the Bohemian Massif (modified from Willner et al., 2002), indicating the three main field trip areas: A, the south Bohemian granulite massifs; B, the Gföhl unit; and C, the Kutná Hora complex. 1 – HP-UHP units (360–340 Ma); 2 – Monotonous and Varied groups with MT-MP/HP rocks; 3 – units with MP rocks (400–370 Ma); 4 – low-grade units of Saxothuringia and the Sudetes, including LP-HP rocks; 5 – medium-grade units of the Sudetes and Moravo-Silesia; 6 – Upper Proterozoic to Lower Carboniferous sedimentary rocks. Stars are selected eclogite occurrences in the Moldanubian zone outside of the Gföhl unit.

South Bohemian HP Granulites with Lenses of HP/UHP Mafic and Ultramafic Rocks

Shah Wali FARYAD[1], Jan FRANĚK[2], Stanislav VRÁNA[2] and Martin SVOJTKA[3]

[1] Institute of Petrology and Structural Geology, Charles University, Albertov 2, 128 43 Prague 2, Czech Republic
[2] Czech Geological Survey, Klárov 3, 118 21 Prague 1, Czech Republic
[3] Institute of Geology, Academy of Sciences v.v.i, Rozvojová 269, 165 00 Prague 6, Czech Republic

Position and structure of the granulite massifs

Granulite facies rocks (mostly felsic granulites and granulitic gneisses) with lenses and boudins of serpentinized garnet and spinel peridotite, pyroxenite, retrogressed eclogite comprise- several large, oval-shaped massifs (the Blanský Les, Křišťanov, Prachatice, Lišov, and Krasejovka Granulite Massifs) in the south-western part of the Moldanubian zone (Fig. 1). The granulite massifs also contain lenses of pyroxene-bearing granulite of intermediate composition, whose relation to felsic granulite is unclear (Kodym, 1972; Vrána, 1992). The garnet or spinel peridotites and garnet pyroxenites systematically form discontinuous lenses along the margins of all the granulite massifs. Similar to other granulites in the Moldanubian zone, the southern Bohemian granulites are assigned to the high-grade Gföhl Unit. The granulite massifs are surrounded by amphibolite facies metamorphic rocks of the Monotonous and Varied groups (e.g., Rajlich et al., 1986).

The Blanský Les Granulite Massif preserves the most complete structural record. The oldest fabric is represented by scarce remnants of a compositional banding (Vrána, 1979; Franěk et al., 2006). The subsequent, better-preserved fabric developed under granulite facies conditions. This is a mylonitic foliation, dipping moderately to steeply to the W or E, are defined by elongation of Qtz ribbons and Bt aggregates emphasized by a weak compositional banding. The early fabrics were extensively reworked by steep amphibolite facies mylonitic foliation, which constitutes an ~18-km-wide sigmoidal asymmetric fold parallel to the margins of the massif. Both of the steep fabrics developed during the two-step exhumation of the granulites from lower-crustal conditions to their present tectonic position.

The oldest fabric preserved in the Křišťanov and Prachatice bodies correspond to the steep amphibolite-facies foliation described above. Compared with the Blanský Les, the orientation of these fabrics is less complex. They form between ~15 and ~7 km-wide, large-scale, single folds parallel to the margins of each massif. The folds are characterised by steep axes and roughly N to S-trending, steep axial planes, similar to the Blanský Les Granulite. This arcuate steep fabric was heterogeneously reworked by a younger ductile deformation, which resulted in development of shallowly NW-dipping to flat-lying foliation.

The rocks in the Monotonous and Varied groups are characterised by steep amphibolite facies foliation, generally trending NNE–SSW, which is similar to and concordant with that in granulites (Vrána, 1979). The steep foliation in the Lhenice Zone forms a tight, vertical, N–S elongated, fan-like pattern, while in the Libín Zone it dips steeply to the SW beneath the Křišťanov granulite. Regionally, the most prominent fabric is a flat foliation that generally strikes NE–SW, dipping at gentle angles mainly to the NW. Only in the vicinity of the granulite massifs does it get disturbed and "flow" around the individual bodies. The Lhenice Zone, with a generally higher degree of partial melting, probably represents a remnant of Variscan lower-crustal meta-sediments trapped by felsic granulites during their ascent and exhumation.

Four localities will be visited in the southern part of the Bohemian Massif (Fig. 1), which include two stops (4-1and 5-1) in granulite massifs with HP granulites and lenses of HP/UHP mafic and ultramafic rocks, a stop (4-2) in high-grade gneiss that is structurally beneath the granulite massifs, and a stop (4-3) in eclogites in the Monotonous Unit.

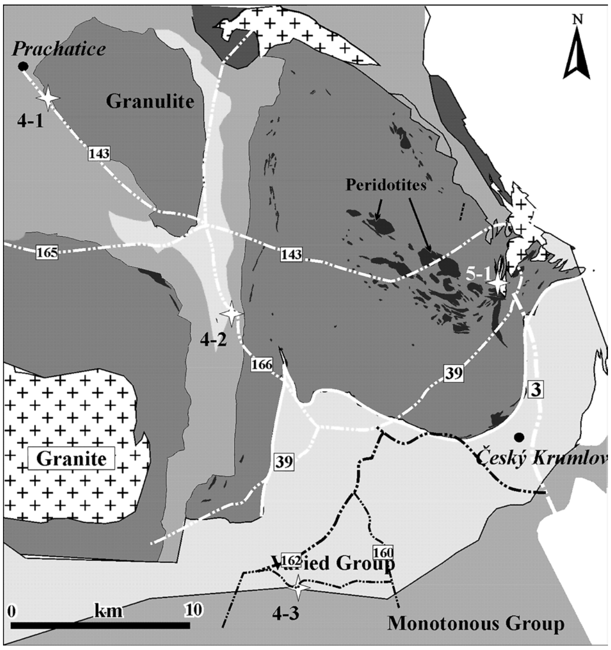

■ **Fig. 2.** Localities of field trip stops in garnet peridotites, garnet pyroxenites and eclogites in the southern Moldanubian granulite massif and adjacent units (area A in Fig. 1 of the Introduction to part III). Stops 4-1 and 5-1: peridotites in granulite massifs; 4-2: garnet-rich gneiss (kinzigite); 4-3: eclogite in the Monotonous group. Dot-dash lines with numbers indicate highways and main roads.

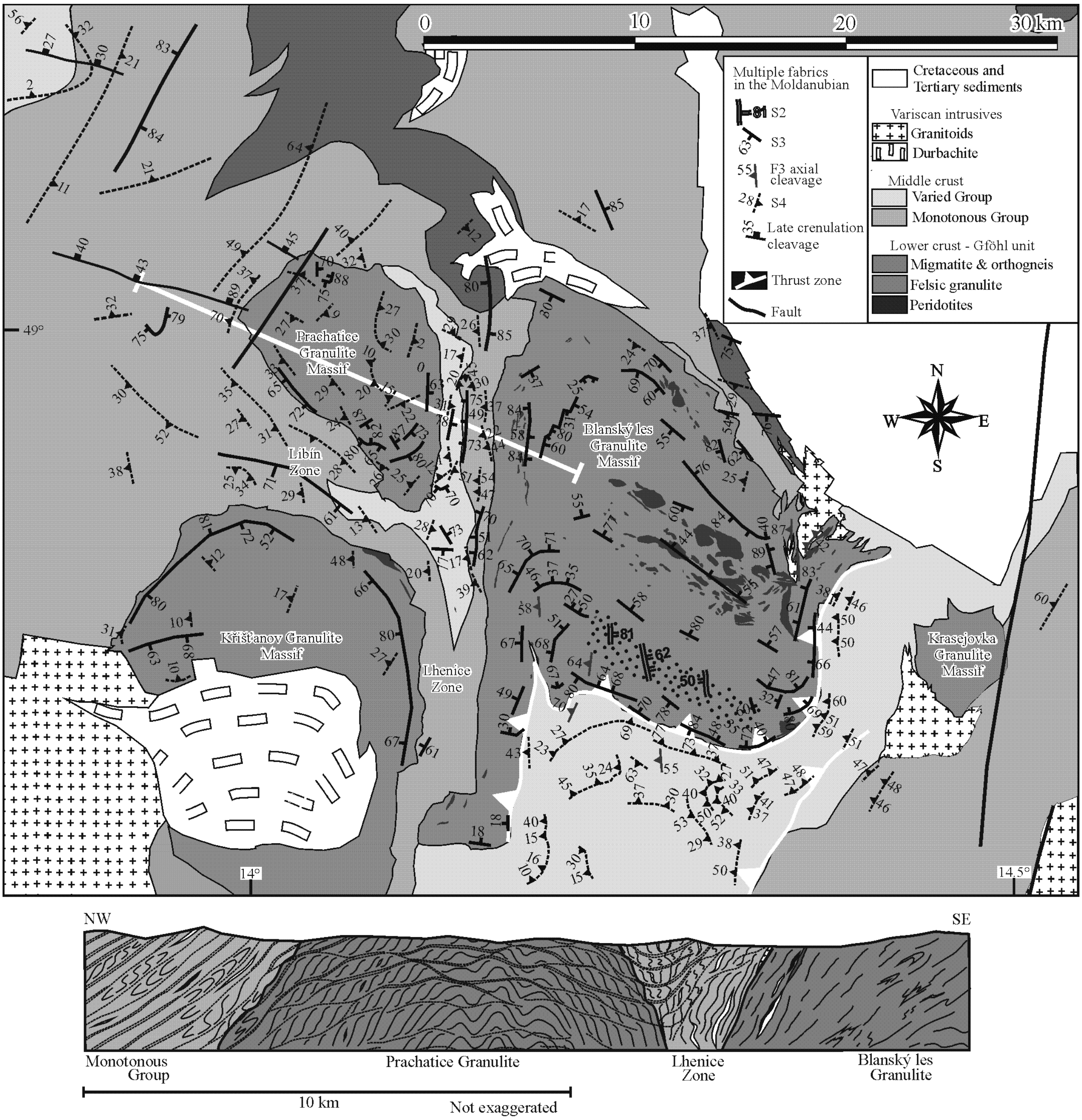

■ **Fig. 2.** Simplified structural map of the South Bohemian Moldanubian region and a NW-SE structural profile, showing the fold-like shape of steep fabrics and their overprint by a flat-lying foliation (Franěk et al., 2006).

Granulite petrology

The origins and protoliths of granulites in the Bohemian Massif have long been a subject of discussion. According to Fiala et al. (1987), the granulites were derived from felsic volcanics or volcanosedimentary rocks. Alternatively, it has been proposed that granulite originated from dry, HP-HT partial melting of sedimentary lithologies (Vrána, 1989; Jakeš, 1997; Kotková and Harley 1999, 2010) or of granitoid/acid volcanic rocks (Vrána, 1989; Janoušek et al., 2004). The granulites have been extensively re-equilibrated under lower-pressure granulite and subsequent amphibolite facies conditions. Relatively well-preserved felsic varieties, which consist of two feldspars, quartz, garnet, kyanite, and rutile, are present in the Blanský Les Massif (Vrána, 1992; Fiala et.al., 1987). The presence and amount of biotite and sillimanite or spinel depend on the degree of re-equilibration. Garnet has a composition in the range, Alm48-62Prp26-.32Grs25-04Sps1-2, and is usually compositionally zoned, with a decrease of Ca and XMg toward the rim. However, some dark, Ca-rich varieties may preserve prograde zoning in the central part, where Mn and XFe decrease outward, but Ca remains constant (Fig. 3). The rims of garnet show a strong

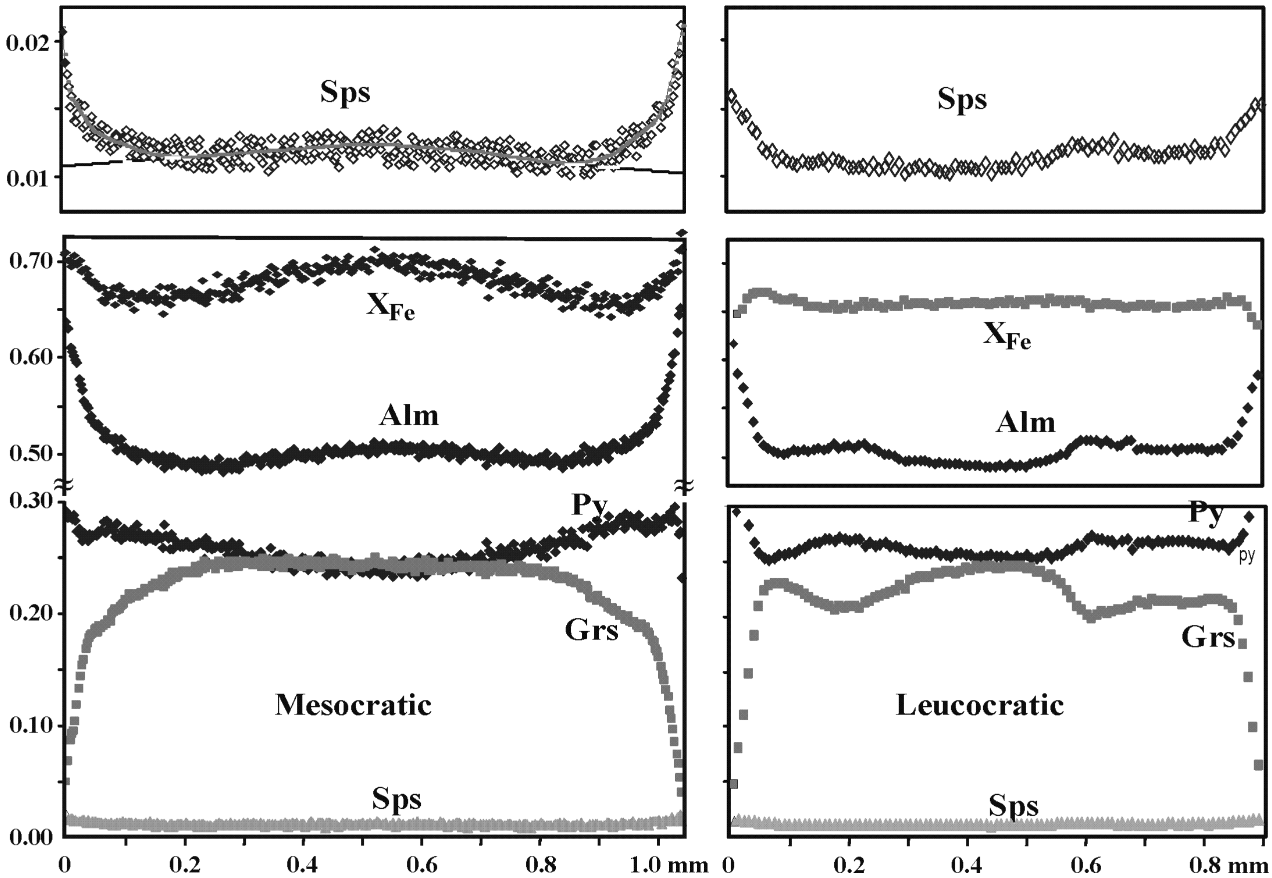

■ **Fig. 3.** Compositional profiles of almandine, pyrope, grossular, and spessartine contents and X_{Fe}=Fe/(Fe+Mg) from prograde-zoned garnets in mesocratic and leucocratic layers of granulitic gneiss. Note that Mn zoning is shown by a vertical scale enlargement in the top figure.

retrograde zoning, with a decrease in Ca and Mg, an increase in Fe, and a slight increase in Mn. In addition to rutile, garnet contains columnar or euhedral inclusions filled mostly by albite, but K-feldspar and plagioclase (An14 and An43) also occur (Figs. 4a, b). These inclusions occur in the Ca-rich internal parts of garnet and usually contain a mixture of Fe oxide + titanite. They are interpreted as pseudomorphs after a Na-rich phase, such as jadeite, paragonite, or glaucophane , or, in the case of plagioclase, after a mixture of paragonite and margarite, which were stable during the prograde PT path to eclogite facies metamorphism (Faryad et al., 2010).

The intermediate compositional variety of granulite consists of quartz, garnet, clinopyroxene, orthopyroxene, mesoperthite, plagioclase, biotite, quartz, rutile, and ilmenite. The garnet shows a flat profile in the core, with a composition of Grs32, Prp25, Alm45, and retrograde zoning near the rim (Grs24, Prp21, Alm51). Omphacite (Jd28) occurs as an inclusion in garnet (Fig. 4c), and symplectite of diopside and plagioclase after omphacite is partly enclosed in the outer part of the garnet. Clinopyroxene in the matrix is diopside, with XMg about 0.78. Orthopyroxene occurs in a corona around quartz in contact with garnet (Fig. 4d), and its XMg value ranges from 0.52 to 0.60.

PT conditions estimated for both felsic and mafic granulites are in the range of 850–1050 °C and 15–20 kbar (Carswell and O'Brien, 1993; Owen. and Dostal, 1996; Kotková and Harley, 1999; Štípská and Powell, 2005). A higher pressure of 2.5 GPa at 700 °C during the prograde stage was proposed by Faryad et al. (2010). The granulites subsequently followed a nearly isothermal decompression path to mid-crustal level pressures with an overprint at 800–900 °C and 8–12 kbar and and a final, near-isobaric cooling.

Most U-Pb ages for metamorphic zircon and monazite from felsic granulites yield ca. 338–340 Ma (van Breemen et al., 1982; Aftalion et al., 1989; Wendt et al., 1994; Kröner et al., 2000; Sláma et al., 2008; Svojtka et al., 2009). However, some older ages of 340–350 Ma by U-Pb zircon and Sm-Nd dating were obtained by Kröner et al., 2000 and Wendt et al., 1994. U-Pb ages for protolith magmatic zircon are ca. 370 Ma (Wendt et al., 1994). Zircons from amphibolite facies Crd patches in granulite yield an age of 338.2 ±3.2 Ma (Kröner et al., 2000). Similar ages of 337 Ma by U-Pb on zircon for felsic granulites were obtained by Sláma et al. (2007).

References

CARSWELL D.A. and O'BRIEN P.J., 1993. Thermobarometry and Geotectonic Significance of High-Pressure Granulites – Examples From the Moldanubian Zone of the Bohemian Massif in Lower Austria. *Journal of Petrology*, 34(3): 427-459.

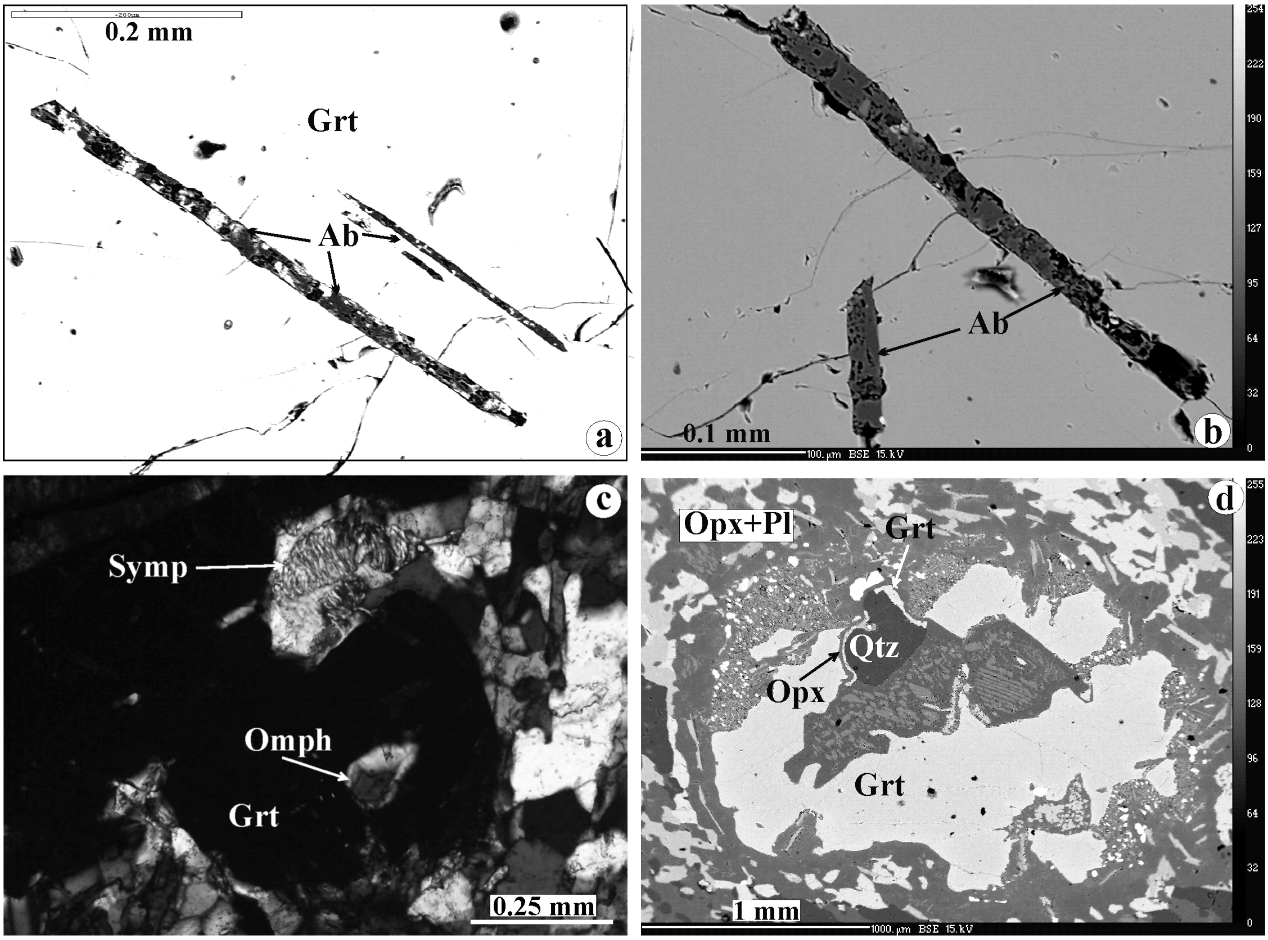

■ **Fig. 4.** Backscattered electron images of garnet crystals with inclusions of albite + Fe-oxides (after clinopyroxene, Na-amphibole, or paragonite?).

FARYAD S.W. NAHODILOVÁ R. and DOLEJŠ D., 2010. Incipient eclogite facies metamorphism in the Moldanubian granulites revealed by mineral inclusions in garnet. *Lithos*, 114: 54–69.

FIALA J., MATĚJOVSKÁ O. and VAŇKOVÁ V., 1987. Moldanubian granulites: source material and petrogenetic considerations. *Neues Jahrbuch fur Mineralogie, Abhandlungen*, 157(2): 133-165.

FRANĚK J., SCHULMAN K. and LEXA O., 2006. Kinematic and rheological model of exhumation of high pressure granulites in the Variscan orogenic root: Example of the Blanský les granulite, Bohemian Massif, Czech Republic. *Mineralogy and Petrology*, 86(3-4) : 253-276.

JAKEŠ P., 1997. Melting in high-P region – Case of Bohemian granulites. *Acta Universitatis Carolinae, Geologica*, 41(3-4): 113-125.

JANOUŠEK V., FINGER F., FRÝDA J., PIN C. and DOLEJŠ D., 2004. Deciphering the petrogenesis of deeply buried granites: whole-rock geochemical constraints on the origin of largely undepleted felsic granulites from the Moldanubian Zone of the Bohemian Massif. *Transactions of the Royal Society of Edinburgh-Earth Sciences*, 95: 141-159.

JANOUŠEK V. and HOLUB F.V., 2007. The causal link between HP-HT metamorphism and ultrapotassic magmatism in collisional orogens: case study from the Moldanubian Zone of the Bohemian Massif. *Proceedings of the Geologists Association*, 118: 75-86.

KODYM O., 1972. Multiphase deformation in the Blanský les granulite massif (South Bohemia). *Krystalinikum*, 9: 91-105.

KOTKOVÁ J. and HARLEY S.L., 1999. Formation and evolution of high-pressure leucogranulites: Experimental constraints and unresolved issues. Physics and Chemistry of the Earth Part a-Solid *Earth and Geodesy*, 24(3) : 299-304.

KRÖNER A., O'BRIEN P.J., NEMCHIN A.A. and PIDGEON R.T., 2000. Zircon ages for high pressure granulites from South Bohemia, Czech Republic, and their connection to Carboniferous high temperature processes. *Contributions to Mineralogy and Petrology*, 138(2) :127-142.

OWEN J.V. and DOSTAL J., 1996. Contrasting corona structures in mafic granulite from the Blansky Les complex, Bohemian Massif, Czech Republic. *Canadian Mineralogist*, 34(5) : 959-966.

RAJLICH P., SYNEK J., SARBACH, M. and SCHULMANN K., 1986. Hercynian-Thrust Related Shear Zones and Deformation of the Varied Group on the Contact of Granulites Southern Moldanubian, Bohemian Massif. *Geologische Rundschau*, 75(3) : 665-683.

SLÁMA J., KOŠLER J. and PEDERSEN R. B., 2007. Behaviour of zircon in high-grade metamorphic rocks: Evidence from Hf isotopes, trace elements and textural studies. *Contributions to Mineralogy and Petrology,* 154(3) : 335-356.
ŠTÍPSKÁ P. and POWELL R., 2005. Does ternary feldspar constrain the metamorphic conditions of high-grade meta-igneous rocks? Evidence from orthopyroxene granulites, Bohemian Massif. *Journal of Metamorphic Geology*, 23(8): 627-647.
SVOJTKA M., KOŠLER J. and VENERA Z., 2002. Dating granulite-facies structures and the exhumation of lower crust in the Moldanubian Zone of the Bohemian Massif. *Geol Rundsch*, 91: 373–385.
VAN BREEMEN O. et al., 1982. Geochronological studies of the Bohemian massif, Czechoslovakia, and their significancein the evolution of Central Europe. *Trans. R. Soc. Edinburgh, Earth Sci.*, 73: 89-108.
VRÁNA S., 1989. Perpotassic granulites from southern Bohemia. A new rock type derived from partial melting of crustal rocks under upper mantle conditions. *Contrib. Mineral. Petrol*., 103: 510-522.
VRÁNA S., 1992. The moldanubian zone in southern Bohemia: polyphase evolution of imbricated crustal and upper mantle segments. In: KUKAL Z (Editors) P 1 Int C Boh Mass P, Czech Geol Surv, Prague, 331-336.
VRÁNA S., 1979. Polyphase shear folding and thrusting in the Moldanubicum of southern Bohemia. *Bull. Czech Geol. Survey*, 54: 75-86
WENDT J.I., KRÖNER A., FIALA J. and TODT W., 1994. U-Pb zircon and Sm-Nd dating of Moldanubian high-P/high-T granulites from south Bohemia, Czechoslovakia: London. *Journal of the Geological Society*, 151:83–90.

Stop 4-1 (Day 4). Garnet Peridotites and Pyroxenites, Quarry Pod Libínem

Coordinates: N48°59′59.4″ E14°01′21.0″

Shah Wali FARYAD[1], Jan FRANĚK[2] and Stanislav VRÁNA[2]

[1] Institute of Petrology and Structural Geology, Charles University, Albertov 2, 128 43 Prague 2, Czech Republic
[2] Czech Geological Survey, Klárov 3, 118 21 Prague 1, Czech Republic

The large active quarry Pod Libínem is located directly at the SW margin of the Prachatice Granulite Massif (Fig. 1). The felsic granulites exhibit penetrative steep fabric and contain bodies of partially serpentinized Grt peridotites and pyroxenites, which form up to 10-m-large boudins. Granulite consists of feldspars, quartz, garnet, biotite, and kyanite (sillimanite), cordierite and accessory, spinel, rutile, zircon, graphite and apatite. Quartz forms mostly platy grains that define foliation of the rocks. Grain boundaries of quartz grains are followed by fine-grained perthitic K-feldspar, plagioclase and locally by biotite and relics of kyanite. Garnet is replaced by biotite or by cordierite, and kyanite is rimmed by spinel or totally replaced by sillimanite. Cordierite occurs along thin veins but mostly forms corona around garnet and finally replaced the whole garnet. Plagioclase forming symplectite with sapphirine is also present. Granulite is locally penetrated by granitic veins.

Garnet peridotites are strongly serpentinized. Pyroxene-rich varieties may contain up to 5- to 7-cm-large garnet porphyroblasts that are mostly replaced by symplectites of pyroxene + amphibole + spinel. They contain inclusions of clinopyroxene. In addition to isolated red-brown spinel, symplectites of spinel + orthopyroxene (former garnet), overgrown by amphibole, are also present. Garnet in peridotite forms relic grains, which have homogeneous composition with Mg and Cr con-

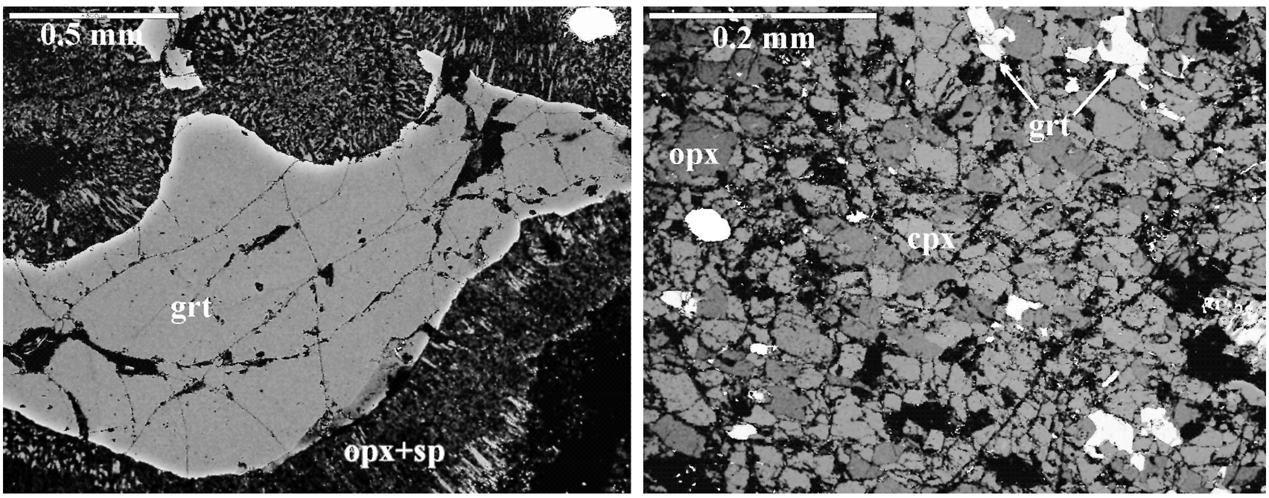

■ **Fig. 1.** BSE images from garnet peridotite and garnet pyroxenite within garnulites (stop 3-1). (a) garnet with corona of opx+sp symplectite from garnet peridotite. (b) microtexture of garnet pyroxenite.

tent (Prp_{70} Alm_{15} Grs_6 Uv_7). Orthopyroxene, clinopyroxene, and olivine show weak zoning. Core-to-rim grains of ? orthopyroxene show an increase in Al and Mg and a decrease of Cr, and clinopyroxene exhibits a decrease in Na from (Jd_8) to (Jd_5). Olivine has forsterite content 0.89. Spinel has X_{Al}=Al/(Cr+Al+Fe^{3+}) ratio 0.37. PT conditions, calculated based on garnet-olivine (O'Neill & Wood, 1980; O'Neill, 1981), two-pyroxene (Brey and Kohler, 1990; Taylor, 1998) thermometry, and Grt-Opx (Brey and Kohler, 1990), Cr-in Cpx (Nimis and Taylor, 2000) are in the range 1080–1115 °C at 2.9–3.0 GPa.

References

BREY G.P. and KÖHLER T.P., 1990. Geothermobarometry in 4-phase lherzolites. 2. New thermobarometers, and practical assesment of existing thermometers. *Journal of Petrology,* 31: 1353–1378.

NIMIS P. and TAYLOR W.R., 2000. Single clinopyroxene thermobarometry for garnet peridotites. Part I. Calibration and testing of a Cr-in-Cpx barometer and an enstatite-in-Cpx thermometer. *Contributions to Mineralogy and Petrology,* 139: 541–554.

O'NEILL H.S.C., 1981. The transition between spinel lherzolite and garnet lherzolite, and its use as a geobarome. *Contribution to Mineralogy and Petrology,* 77: 185–194.

O'NEILL H.S.C. and WOOD B.J., 1980. An experimental study of Fe-Mg partitioning between garnet and olivine and its calibration as a geothermometer. *Contribution to Mineralogy and Petrology,* 70: 59–70; *erratum in Contribution to Mineralogy and Petrology*, 72: 337.

TAYLOR W.R., 1998. An experimental test of some geothermometer and geobarometer formulations for upper mantle peridotites with application to the thermobarometry of fertile lherzolite and garnet websterite. *Neues Jahrbuch fuer Mineralogie Abh*., 172: 381–408.

Stop 5-1 (Day 5). Granulite and Garnet Peridotite, Plešovice Quarry, 5 km NNE of Český Krumlov

Coordinates: N48°55′25.20″, E14°20′28.10″

Martin SVOJTKA[1], Takao HIRAJIMA[2], Stanislav VRÁNA[3] and Kosuke NAEMURA[2]

[1] Institute of Geology, Academy of Sciences v.v.i, Rozvojová 269, 165 00 Prague 6, Czech Republic
[2] Department of Geology and Mineralogy, Graduate School of Science, Kyoto University, Kyoto 6069-8502, Japan
[3] Czech Geological Survey, Klárov 3, 118 21 Prague 1, Czech Republic

The main rock types in the Plešovice quarry are felsic granulites and granulitic gneisses, similar to those at stop 4-1, but minor amounts of garnetiferous perpotassic granulites and veins of aplites and pegmatites also occur. Garnet peridotite occurs as an isolated boudins in the granulites. The highly potassic granulites (with K_2O content up to 13 wt.%) occur in foliated layers up to 2 m thick, which are concordant with the predominant felsic calc-alkaline granulites (Vrána, 1989; Janoušek et al., 2007; for description of the predominant felsic granulites – see the Post-Conference Excursion Guide, Day 1). Perpotassic granulites consist of K-feldspar (up to 93%), quartz and pyrope-rich (~30 molar%) garnet with accesory zircon (up to 1 000 ppm Zr), apatite and monazite. Characteristic are high concentrations of Cs, Rb, Ba and U and variable enrichments in Zr and Hf (Vrána, 1989; Janoušek et al., 2007). The perpotassic granulites are interpreted as the product of non-eutectic melt (Vrána, 1989; Janoušek et al., 2007), possibly derived from the protolith of the adjacent felsic granulites in the BLGM (Janoušek et al., 2007).

The spinel-garnet peridotite (Fig. 1), which has been studied in detail, occurs as an elongated lens (20 m × 5 m), which is exposed in the western part of the present-day fifth level of the quarry. The peridotite has an inequigranular texture, in which large spheroidal garnet grains (extensively kelyphitized) are set in a fine-grained matrix of olivine (Ol), orthopyroxene (Opx), minor clinopyroxene (Cpx), and Cr-rich spinel (Spl). The large spheroidal garnet grains locally enclose Ba- and Sr-rich phlogopite and apatite (Ap) inclusions (Naemura et al., 2008). Thorianite (ThO_2) occurs as a member of multiphase solid inclusions, consisting of phlogopite + carbonates + apatite + graphite + rutile + monazite + thorianite, in chromian spinel. The CHIME U-Th-Pb dating of the thorianite yielded a weighted mean age of 333.8 ±4.5 Ma (2 sigma, Table 1), which is the

analyses no.	UO_2 [wt%]	ThO_2 [wt%]	PbO [wt%]	ThO_2* [wt%]	Age ± 2σ [Ma]
1	17.628	77.210	1.889	134.714	331.3 ± 6.6
2	18.094	76.910	1.918	135.942	333.3 ± 6.6
3	17.758	77.240	1.927	135.193	336.7 ± 6.7
4	18.836	75.730	1.938	137.183	333.8 ± 6.6
weighted average					333.7 ± 5.5

■ **Tab. 1**. Results of electron microprobe dating of thorianite from the Plešovice peridotite. From Naemura et al., 2008.

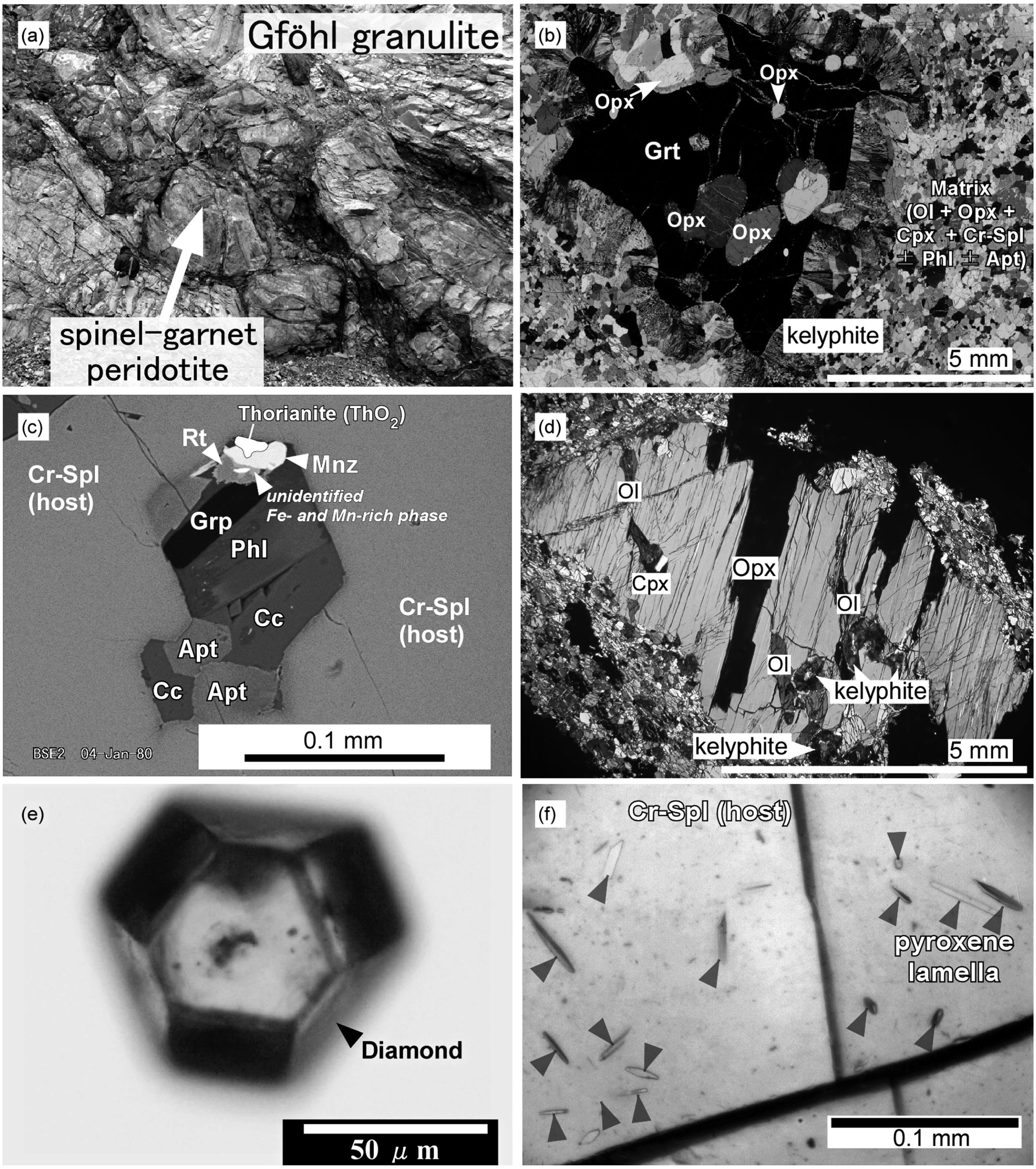

■ **Fig. 1.** (a) The spinel–garnet peridotite outcrop within prevailing felsic granulite in the Plešovice quarry; (b) A large garnet (Grt) with rounded orthopyroxene inclusions (Opx), the fine-grained matrix is composed of olivine (Ol) + orthopyroxene (Opx) + clinopyroxene (Cpx) + Cr-spinel (Cr-Spl). Phlogopite (Phl) and apatite (Apt) are present as accesories. Crossed polarized light; (c) Backscattered electron image of a multi-phase solid inclusion within chromian spinel (Cr-Spl). Inclusion consists of phlogopite (Phl), calcite (Cc), apatite (Apt), graphite (Grp), rutile (Rt), monazite (Mnz), thorianite and unidentified Fe- and Mn-rich phase; (d) Orthopyroxene (Opx) megacryst (approximately 6 mm in diameter) with olivine (Ol) and clinopyroxene (Cpx) inclusions. Crossed polarized light; (e) Microphotography of diamond crystal from the Plešovice peridotite. Plane polarized light; (f) Detail of the core of large chromian spinel (Cr-Spl) inclusion in kelyphitized garnet. Note that there are many lamellae in the Cr-Spl, which were identified as diopside crystals with minor clino-enstatite. Plane polarized light.

same within error as the age of H*P* metamorphism determined for felsic granulites in southern Bohemia (Naemura et al., 2008, see the text above).

Naemura et al. (2009) described three equilibrium stages for the Plešovice peridotite. The temperature of Stage I was estimated to be 1020 ± 15 °C, using the Al-Cr orthopyroxene thermometer (Witt-Eickschen and Seck 1991) for orthopyroxene megacrysts. Stage II is defined by the spinel-garnet lherzolite assemblage in the matrix, and equilibrium conditions were estimated to be 23–35 kbar and 850–1030 °C, based on the application of two-pyroxene and Grt-Cpx thermometry, Grt-Opx and Grt-Cpx barometry, and an empirical Spl barometer for Spl-Grt lherzolite. Stage III is defined by the presence of aluminous ortho- and clinopyroxene, aluminious spinel, and amphibole and phlogopite in kelyphite. Temperature conditions for stage III were estimated to be 730–770 (±27) °C at 8–15 kbar. The mineral assemblage in the multiphase solid inclusions (MSI) in chromian spinel is composed of phlogopite, dolomite, apatite and calcite with minor amounts of chlorite and magnesiohornblende. Crystallization conditions of the MSI assemblage were at relatively low-P and low-T ($T < 750$ °C; $P < 16$ kbar). The timing of crystallization of MSI appears to predate the stage II, as most MSI are completely enclosed by the host chromian spinel, which formed during stage II. These relations suggest that the Plešovice peridotite experienced cooling after Stage I and was transformed to spinel-garnet peridotite by subsequent subduction processes (Naemura et al, 2009).

Recently, Naemura et al. (in press) reported the presence of carbon phases in garnet(?), including micro-diamond that suggests ultra-deep conditions (~6 GPa) for garnet in the precursor of the Stage I(?) garnet peridotite. Synchrotron X-ray fluorescence analysis indicated that this diamond contains Fe-Ni metal (taenite) and Cu-Zn-rich phases (possibly sulfide) as inclusions. In particular, the latter phase supports the natural origin of this diamond, although the aggregation state of nitrogen in the diamond is very similar to that in synthetic diamond. Raman spectroscopy shows that graphite crystals included in garnet show upward displacements of the G-band up to 1600 cm^{-1}. Such upward displacements are most likely due to internal pressure, supporting the high-pressure origin of graphites. Another line of evidence for ultra-deep conditions is revealed by pyroxene lamellae developed in coarse-grained chromian spinel grains. EBSD analysis indicates that the pyroxene lamellae could be formed by exsolution from a high-pressure polymorph of spinel (Ca-ferrite and/or Ca-titanite structure), which may be stable under very high pressures (>12.5 GPa). The diamond-bearing Plešovice peridotite is interpreted to represent a fragment of asthenosphere (> 200 km) that was transported to relatively shallow levels by a diapiric plume and then incorporated into the Moldanubian orogenic root shortly before or during the Variscan continent-continent collision at ca. 340 Ma.

References

JANOUŠEK V., KRENN E., FINGER F., MÍKOVÁ J. and FRÝDA J., 2007. Hyperpotassic granulites from Blanský les (Moldanubian Zone, Bohemian Massif) revisited. *Journal of Geosciences*, 52: 73-112.

NAEMURA K., HISASHIMA H., HIRAJIMA T. and SVOJTKA M., 2009. An ultra-high-pressure metamorphic condition and isothermal decompression path obtained from a garnet-pyroxenite in the Horni Bory granulite of the Bohemian Massif. *Journal of Mineralogical and Petrological Sciences*, 104(3): 168-175.

NAEMURA K., YOKOYAMA K., HIRAJIMA T. and SVOJTKA M., 2008. Age determination of thorianite in phlogopite-bearing spinel-garnet peridotite in the Gföhl Unit, Moldanubian Zone of the Bohemian Massif. *Journal of Mineralogical and Petrological Sciences*, 103: 285-290.

NAEMURA K., IKUTA D., KAGI H., ODAKE S., UEDA T., OHI S., KOBAYASHI Y., SVOJTKA M., HIRAJIMA T., (2011, in press). Diamond and other possible ultra-deep evidence discovered in the orogenic spinel-garnet peridotite from the Moldanubian Zone of the Bohemian Massif, Czech Republic, In: L. DOBRZHINETSKAYA, S.W. FARYAD, S. WALLIS and S. CUTHBERT (Editors), UHPM: 25 year after discovery of coesite and diamond, Elsevier.

VRÁNA S., 1989. Perpotassic granulites from southern Bohemia. A new rock type derived from partial melting of crustal rocks under upper mantle conditions. *Contrib. Mineral. Petrol.,* 103: 510-522.

WITT-EICKSCHEN G. and SECK H.A., 1991. Solubility of Ca and Al in orthopyroxene from spinel peridotite: an improved version of an empirical geothermometer. *Contrib. Mineral. Petrol., 106:* 431-439.

Garnet-Rich Gneisses (Kinzigites) of the Lhenice Shear Zone

Martin SVOJTKA[1], Tomoyuki KOBAYASHI[2,3] and Takao HIRAJIMA[2]

[1] Institute of Geology, Academy of Sciences v.v.i, Rozvojová 269, 165 00 Prague 6, Czech Republic
[2] Department of Geology and Mineralogy, Graduate School of Science, Kyoto University, Kyoto 6069-8502, Japan
[3] Department of Earth Sciences, Graduate School of science, Chiba University, 1-33 Yayoi, Inage, Chiba 263-8522, Japan

The garnet-rich gneisses form a ~15 km long, north-south trending, discontinuous belt having up to 100 m in thickness, which forms part of the Lhenice shear zone (Rajlich et al., 1986). The Lhenice shear zone separates the Blanský les granulite massif to the east from the Prachatice and Křišťanov granulite massifs to the west. Rajlich et al. (1986) determined that the Lhenice shear zone experienced amphibolite facies metamorphism similar to that in the Varied and Monotonous Units in Lower Austria, i.e. about 0.5 to 0.9 GPa and 700 to 840 °C (Petrakakis, 1986). Detailed gravity profiles of the Lhenice belt presented by Vrána (1979) and Vrána and Šrámek (1999) demonstrated that the Lhenice shear zone is a major N-S striking regional shear zone.

Fiala (1992) published an E-W profile of different lithological rock types across the Lhenice shear zone and assumed that the garnet-rich gneisses forms suite of the Lhenice shear zone metasediments.

Stop 4-2 (Day 4). Garnet-Rich Gneisses (Kinzigites), Ktiš Quarry, 1 km NNE of Ktiš Village

Coordinates: N48°55′25.33″ E14°8′24.15″

This locality (Fig. 1) was first described by Fiala (1992), who compared the compositions of iron- and aluminium-rich garnet-sillimanite-biotite and cordierite-bearing gneisses at Ktiš with other occurrences of kinzigites worldwide and applied the term kinzigite to the suite of Ktiš gneisses.

Ktiš kinzigites have a planar fabric (Fig. 2); they are granoblastic and have a coarse-grained to fine-grained matrix composed of cordierite, sillimanite, biotite, garnet, quartz, K-feldspar and plagioclase with accessory spinel, apatite and zircon. Biotite, sillimanite, plagioclase and kyanite occur as inclusions in garnet. Cordierite and spinel occur only in the matrix both as isolated grains and as reaction coronas around garnet.

The main foliation planes dip to the west at 35–60°, and fold axes of quartz-K-feldspar lenses trend 190° and plunge at 60°. Kinzigites were intruded by biotite-bearing granite dykes (up 1.5 m) in the eastern and central parts of the quarry.

Geological studies of the Ktiš locality

U-Pb dating of the Ktiš garnet-rich gneisses (Wendt, 1989) revealed two populations of detrital zircons. The rounded heterogeneous zircon population (ca. 1.6–2.0 Ga) indicated repeated sedimentary reworking during the Precambrian, and younger

■ **Fig. 1.** Free blocks of garnet-rich gneisses in abandoned Ktiš quarry (photo by M. Svojtka).

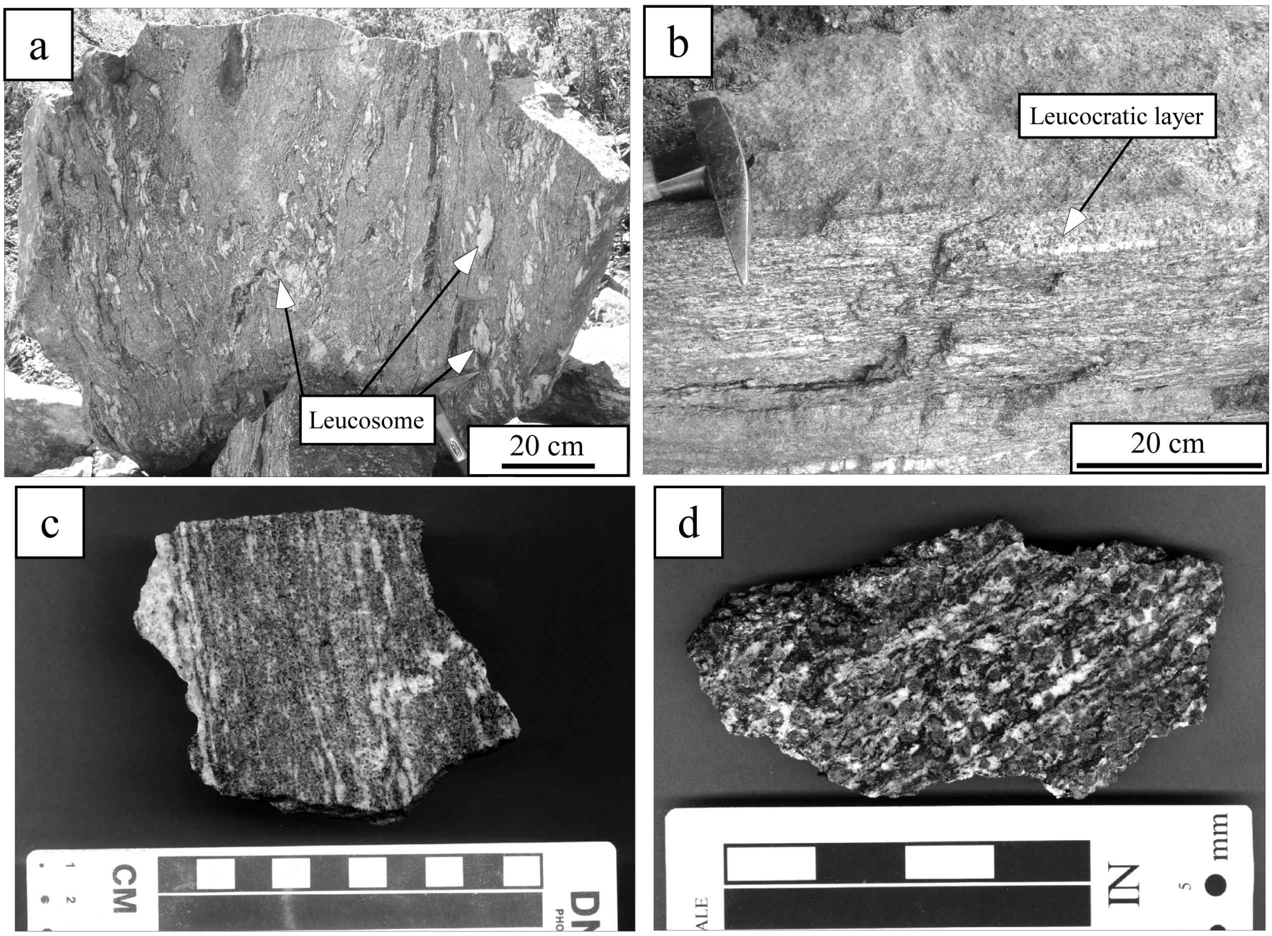

■ **Fig. 2.** Photographs (photo by T. Kobayashi) of garnet-rich gneiss at Ktiš showing various types of partial melting structures, (a) leucosomes developed parallel with the main foliation. (b) leucocratic layers defining the main foliation. (c) melanocratic layer with fine-grained garnet (0.1–1 mm) with intercalations of leucosome, and (d) melanocratic layer with coarse-grained (3–5 mm) garnet. From Kobayashi et al, 2011.

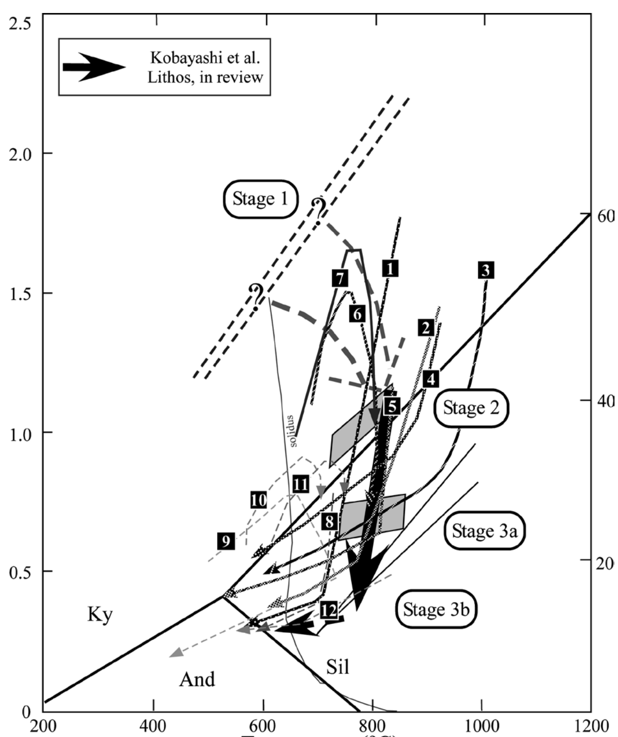

■ **Fig. 3.** Comparison of P-T paths of garnet-rich gneiss at Ktiš with those of HP-granulites from the Gföhl Unit and those of gneisses from the Varied and Monotonous Units (For cited references, cf. Fig. 11 in Kobayashi et al, 2011). 1 – Strážek Unit (Tajčmanová et al. 2006), 2 – South Bohemian granulites (Vrána 1992; Kotková and Harley 1999), 3 – granulites of the Lower Austria (Carswell and O'Brien 1993; Cooke and O'Brien 2001), 4 – Lišov granulite massif (Kotková 1998), 5 – Eastern Bohemian granulites; conglomerates (Kotková et al. 2007), 6 – Raabs Unit (eclogite and migmatite; Racek et al. 2006), 7 – granulite massif of the Gföhl Unit (Štípská and Powell 2005; Racek et al. 2008), 8 – Varied Unit (Petrakakis 1986), 9 – Monotonous Unit (Linner 1994, Büttner and Kruhl 1997), 10 – Varied Unit (Racek et al. 2006), 11 – Monotonous Unit (Racek et al. 2006), 12 – Monotonous Unit (Tropper et al. 2006).

prismatic euhedral zircons (549±5 Ma) probably went through only one sedimentary cycle, whose age likely corresponds to Cadomian (Panafrican) intrusive activity in the source area. The latter value is interpreted as a maximum age for early Paleozoic deposition of the Ktiš gneiss sedimentary precursor (Wendt, 1989; Fiala and Wendt, 1995).

Šreinová and Šrein (2000) described the petrography and mineralogy of several varieties of kinzigite from the Ktiš quarry and surrounding localities (e.g. Kozí Kámen, Ktišská Hora, Smědeč, and Lhenice). In addition to these locaties, several occurrences of kinzigites occur outside Lhenice shear zone, mainly in the margins of the Prachatice and Křišťanov granulite massifs.

Recently, multiple equilibrium stages were identified in the Ktiš garnet-rich gneisses in a detailed petrological study by Kobayashi et al. (2011). Garnet shows two different grain sizes (fine-grained up to 0.8 mm and coarse-grained up to 3–5 mm) and compositional heterogeneity in major and trace elements. While fine-grained garnets are mostly homogeneous in composition, some coarse-grained garnets are compositionally zoned, with Grs content $\{Xgrs = Ca/(Ca + Mg + Fe + Mn)\}$ decreasing from 0.27 in the grain center to 0.02 at the grain margin. Pyrope (Prp)-content varies inversely with Grs, with Prp being low and constant $\{Xprp = Mg/(Ca + Mg + Fe + Mn) = 0.03\}$ in the center of the grain and gradually increasing towards the margin (up to Xprp = 0.28), (cf. Fig. 5 in Kobayashi et al, 2011). The contours of Grs and Prp contents show symmetrical hexagonal shapes (Kobayashi et al., 2011). The distribution pattern of phosphorous, however, shows a striking contrast with Grs-content. The core of the grain is characterized by a low phosphorous content, almost below the detection limit of the EPMA analysis, but it is surrounded by a high-phosphorous rim, followed by local development of a phosphorous-poor outermost rim. The outline of the phosphorous-poor core shows a hexagonal shape, which is symmetrical to those of Grs and Prp contours, but it is located outside of the higher Grs (Xgrs = 0.27) and lower Prp (Xprp = 0.03) contours (cf. Fig. 6 in Kobayashi et al, 2011, Lithos in print). These observations suggest that the outline of the phosphorous-poor core may indicate the original shape of Grs-rich garnet developed during an early stage of metamorphism.

Based on a combination of Grt-Bt and Grt-Crd geothermometers with Grt-Als-Qtz-Pl (GASP) and Grt-Crd geobarometers, Kobayashi et al. (2011) defined the following equilibrium stages (Fig. 3): Stage 1, 1.5–2.3 GPa at 700–900 °C; Stage 2, 730–830 °C and 1.0–1.3 GPa; and Stage 3, 740–850 °C and 0.6–0.8 GPa. The *P-T* conditions for the Stage 2 are slightly higher than the peak *P-T* conditions for gneisses of the Varied/Monotonous Units in the literatures and the *P*-conditions for the Stage 1 are similar to those of H*P*-granulite in the Gföhl Unit. The inferred *P-T* conditions of the studied rock and a model petrogenetic grid suggest that the studied rock experienced the isothermal decompression at least from the Grt rim stage (Stage 2, 1.0–1.3 GPa) to the matrix stage (Stage 3, 0.6–0.8 GPa). This decompression path would overstep following dehydration melting reactions at different depths: Ms + Qtz = Grt+Bt+Sil+K fs+Liq at 1.0–1.2 GPa and Bt+Sil+Qtz = Grt+Crd+Kfs+Liq at 0.3–0.6 GPa. The high-phosphorous Grt rim should be formed through these reactions, in other words, higher-phosphorous content of Grt can be used as an indicator of partial melting of the host rock (Kobayashi et al., 2011).

References

BÜTTNER S. and D KRUHL J.H., 1997. The evolution of a late-Variscan high-T/low-P region: The south-eastern margin of the Bohemian Massif. *International Journal of Earth Sciences (Geologische Rundschau)*, 86: 21-38.

CARSWELL D.A. and O'BRIEN P.J., 1993. Thermobarometry and geotectonic significance of high-pressure granulites: examples from the Moldanubian Zone of the Bohemian Massif in Lower Austria. *Journal of Petrology*, 34: 427-459.

COOKE R.A. and O'BRIEN P.J., 2001. Resolving the relationship between high P-T rocks and gneisses in collisional terranes; an example from the Gföhl gneiss-granulite association in the Moldanubian Zone, Austria. *Lithos*, 58: 33-54.

FIALA J., 1992. Stop 3, Ktiš – kinzigites and quartzities within the Lhenice shear zone. In: J. FIALA, M. FIŠERA, E. JELÍNEK, J. SLABÝ, S. VRÁNA: High-pressure granulites – lower crustal metamorphism, 27. 6.–5. 7. 1992, Rohanov, Czechoslovakia. Excursion guide, 9-11.

FIALA J. and WENDT J.I., 1995. Moldanubian Geochronology, In: DALLMAYER et al. (Editors), Pre-Permian Geology of Central and Eastern Europe, Springer Verlag, Berlin Heidelberg, pp. 418-422.

KOBAYASHI T., HIRAJIMA T., KAWAKAMI T. and SVOJTKA M., 2011. Metamorphic history of garnet-rich gneiss at Ktiš in the Lhenice shear zone, Moldanubian Zone of the southern Bohemian Massif, inferred from inclusions and compositional zoning of garnet. *Lithos*, 124: 46-65.

KOTKOVÁ J., 1998. Garnet-bearing mafic granulites from the Lišov Granulite Massif. *Geolines*, 6: 37.

KOTKOVÁ J. and HARLEY S.L., 1999. Formation and evolution of high-pressure leucogranulites: experimental constraints and unresolved issues. *Physics and Chemistry of the Earth, Part A: Solid Earth and Geodesy*, 24: 299-304.

KOTKOVÁ J., GERDES A., PARRISH R.R. and NOVÁK M., 2007. Clasts of Variscan high-grade rocks within Upper Viséan conglomerates – constraints on exhumation history from petrology and U-Pb chronology. *Journal of Metamorphic Geology, 25: 781-801.*

LINNER M., 1994. Metamorphism and migmatization of the paragneisses of the Monotonous group, SE Moldanubium. *Mitteilungen der Österr. Mineral. Gesellschaft*, 139: 83-84.

PETRAKAKIS K., 1986. Metamorphism of high-grade gneisses from the Moldanubian Zone, Austria, with particular reference to the garnets. *Journal of Metamorphic Geology*, 4: 323-344.

RACEK M., ŠTÍPSKÁ P., PITRA P., SCHULMANN K. and LEXA O., 2006. Metamorphic record of burial and exhumation of orogenic lower and middle crust: a new tectonothermal model for the Drosendorf window (Bohemian Massif, Austria). *Mineralogy and Petrology*, 86: 221-251.

RAJLICH P., SYNEK J., ŠARBACH M. and SCHULMANN K., 1986. Hercynianthrust related shear zones and deformation of the Varied Group on the contact of granulites/Southern Moldanubian, Bohemian Massif. *Geologische Rundschau*, 75: 665-683.

ŠREINOVÁ B. and ŠREIN V., 2000. Mineralogy and petrography of the kinzigites from Lhenice and Ktiš in the South Bohemia (Czech Republic). *Acta Montana IRSM AS CR,* Ser. A, No. 17, 119:, 7-14.

TAJČMANOVÁ L., KONOPÁSEK J. and SCHULMANN K., 2006. Thermal evolution of the orogenic lower crust during exhumation within a thickened Moldanubian root of the Variscan belt of Central Europe. *Journal of Metamorphic Geology*, 24: 119-134.

TROPPER P., DEIBL I., FINGER F. and KAINDL R., 2006. *P-T-t* evolution of spinel-cordierite-garnet gneisses from the Sauwald Zone (Southern Bohemian Massif, Upper Austria): is there evidence for two independent late-Variscan low-P/high-T events in the Moldanubian Unit? *International Journal of Earth Sciences*, 95: 1019-1037.

VRÁNA S., 1992. The Moldanubian Zone in southern Bohemia: Polyphase evolution of imbricated crustal and upper mantle segments. In: Z. KUKAL (ed.) Proceedings of the 1st International Conference on the Bohemian Massif, Prague, September 26-October3 1988, Praha. Czech Geological Survey, Prague, 331-336.

VRÁNA S. and ŠRÁMEK J., 1999. Geological interpretation of detailed gravity survey of the granulite complex in southern Bohemia and its structure. *Věstník Českého geologického ústavu*, 74(3): 261-278.

VRÁNA S.*,* 1989. Perpotassic granulites from southern Bohemia: a new rock-type derived from partial melting of crustal rocks under upper mantle conditions. *Contributions to Mineralogy and Petrology*, 103: 510-522.

WENDT J.I., 1989. U-Pb Zirkondatierung und Sm-Nd Systematik sowie Petrologie und Geochemie an Granuliten und Gneisen aus den Moldanubikum Südböhmens (ČSSR). – Diplomarbeit, Institut für Geowissenschaften, Universiät Mainz.

Eclogite and Garnet Clinopyroxenite from the Monotonous Unit

In addition to garnet peridotites, garnet pyroxenites, and eclogites within granulites and granulite gneisses of the Gföhl unit, numerous bodies of ultramafic and mafic rocks are present in amphibolite facies rocks of the Monotonous and Varied units. Machart (1982) summarized almost 100 occurrences of amphibolite, eclogite (extensively retrograded) and serpentinized spinel peridotite in the Monotonous and Varied units that occur along a NE-SW zone between the Kutná Hora Complex in the north and the southern Bohemian granulite massifs in the south (Fig.1). Numerous occurrences of eclogites with garnet clinopyroxenite (O´Brien and Vrána, 1995) are present south of the South Bohemian granulite massifs.

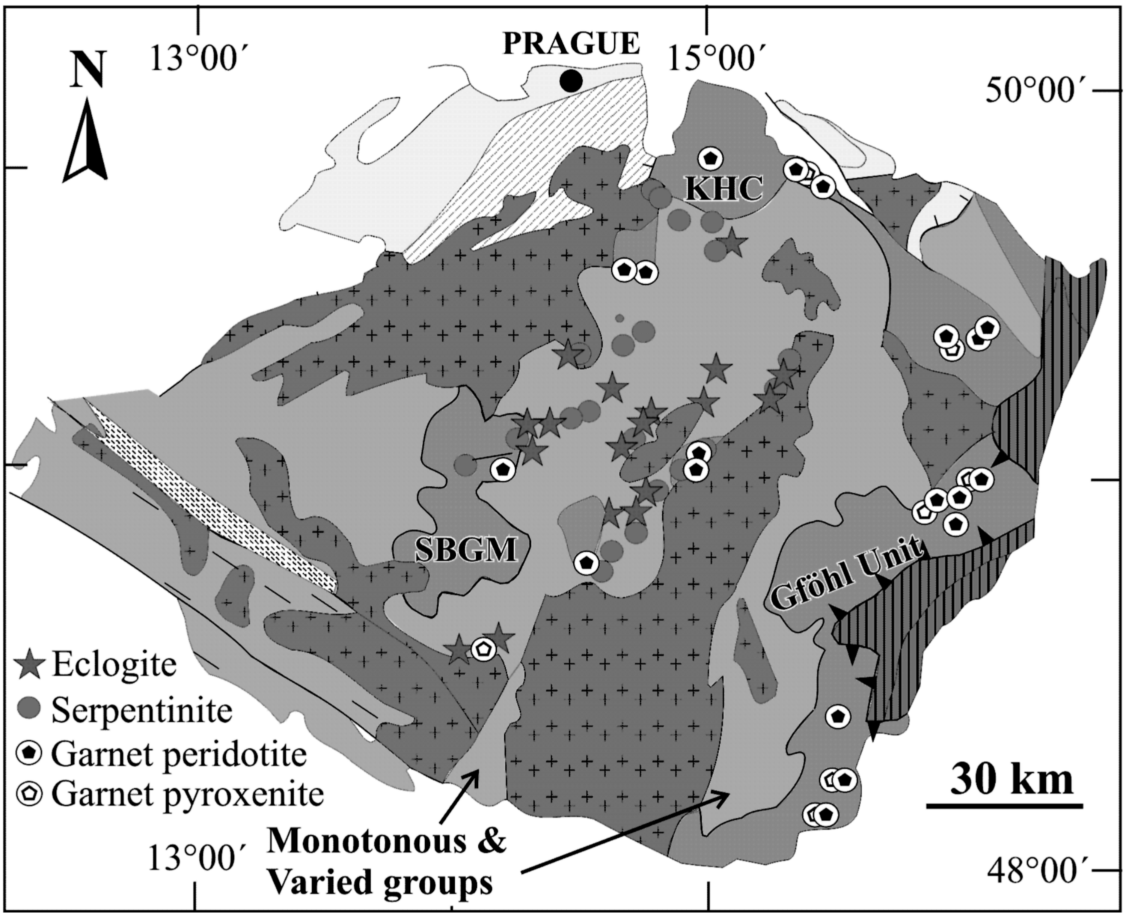

■ **Fig. 1.** Occurrences of retrograded eclogites and serpentinized peridotites in the Monotonous and Varied units in the central part of the Moldanubian zone (modified after Machart, 1982). KHC- the Kutná Hora Complex, SBGM- South Bohemian granulite massifs.

Stop 4-3 (Day 4). Eclogite, Světlík-Suš

Coordinates: N48°43′19.5″ E14°14′49.2″

Shah Wali FARYAD[1] and Stanislav VRÁNA[2]

[1] Institute of Petrology and Structural Geology, Charles University, Albertov 2, 128 43 Prague 2, Czech Republic
[2] Czech Geological Survey, Klárov 3, 118 21 Prague 1, Czech Republic

Eclogite near the village of Suš belongs to a group of lens-shaped bodies of mafic and ultramafic rocks (retrogressed eclogites, garnet pyroxenites and partly serpentinized spinel lherzolite) that occur in the Monotonous unit near its northern contacts with the Svetlik orthogneiss and the Varied unit (Fig. 2). Altogether, 11 bodies of eclogite, 6 of garnet pyroxenite, and one of spinel lherzolite are exposed in this area, where the Monotonous unit is structurally overlain by the Světlík orthogneiss and by the Varied unit. The Monotonous unit consists of migmatitic paragneisses containing biotite, K-feldspar, sillimanite and, locally, cordierite and garnet (Vrána, 1979). To the south, the Monotonous unit is gradually retrogressed to biotite + muscovite ± sillimanite gneiss, which is designated as the Kaplice unit. Occasionally, the Monotonous unit contains kyanite, but in contact with the Moldanubian pluton, cordierite and andalusite are present. Minor pods of calc-silicate rocks are also present in the Monotonous unit. Metamorphic mineral assemblages in the Kaplice unit, the Světlík orthogneiss, and in the Varied unit are representative for amphibolite facies conditions. The northeast-southwest trending units exhibit monoclinal planar fabrics due to regional re-foliation imposed by (syn-metamorphic) shearing. Relics of older structures trending N-S and WNW-ESE are locally preserved (Vrána, 1979).

The eclogite near Světlík-Suš is exposed along a forest road about 2 km west of the village of Suš, where it forms a low, 2 × 4 m outcrop surrounded by fresh eclogite boulders. About 50 m from the outcrop into the forest, boulders of partly retrogressed eclogite and garnet clinopyroxenite (with abundant retrograde magnesihornblende) can be also found.

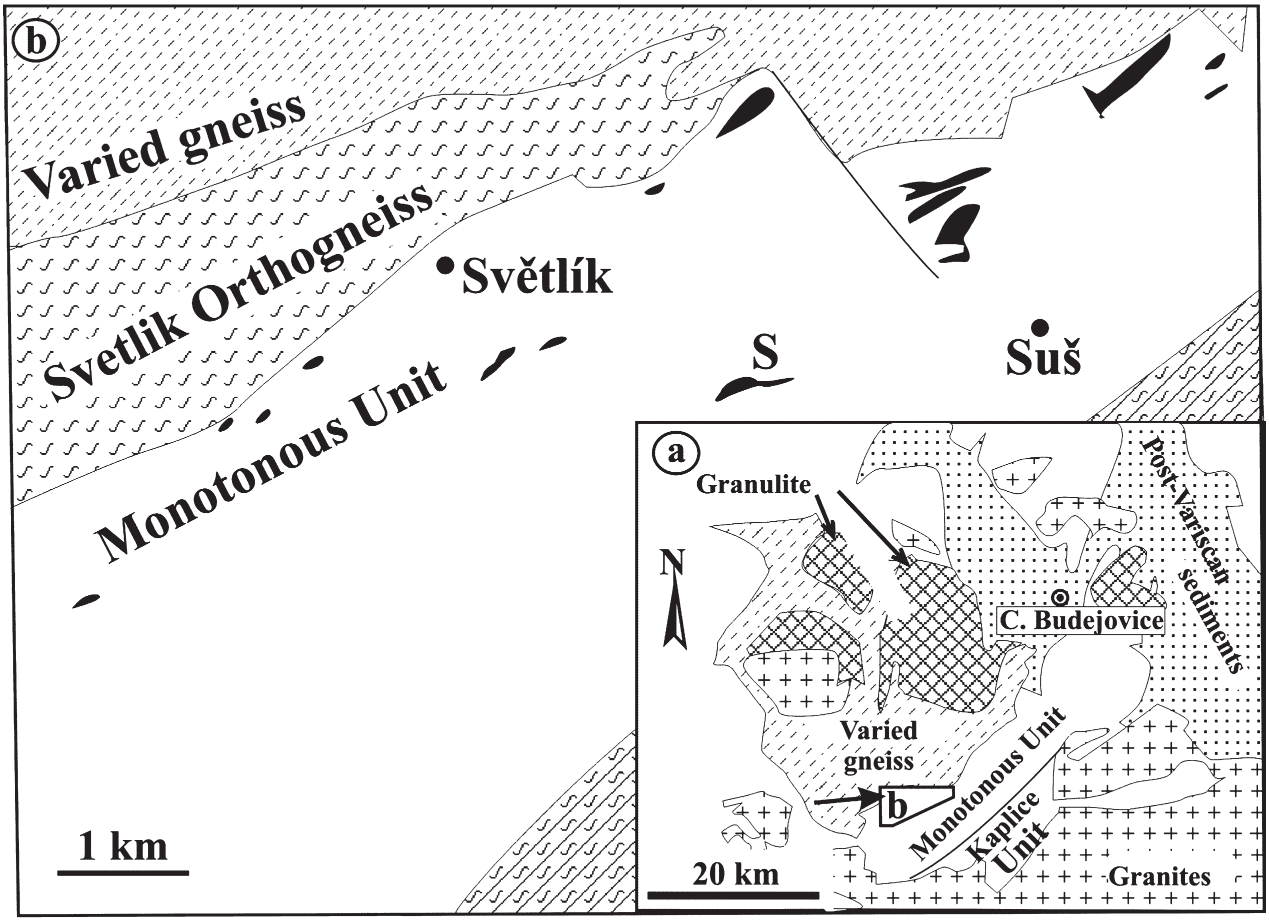

■ **Fig. 2.** a – Geological map of the southern part of the Bohemian Massif (after Vrána, 1991, simplified). b – The studied area of the Monotonous unit with eclogite bodies (black). S, Světlík-Suš (stop 3-5).

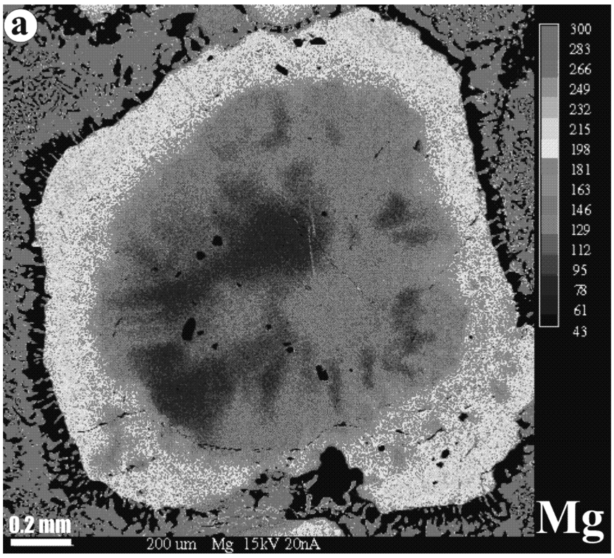

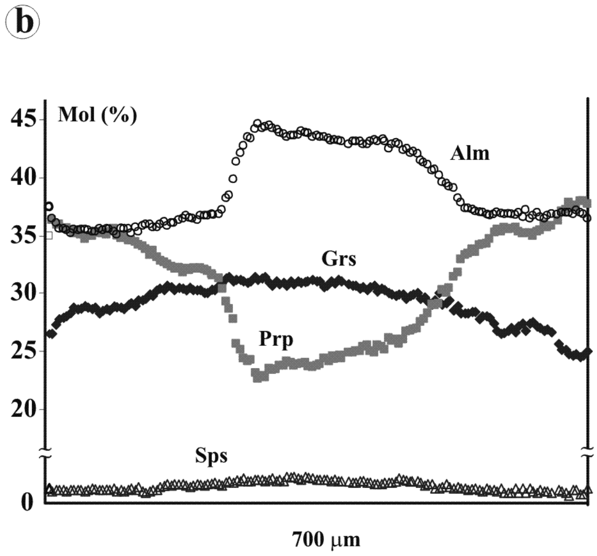

Fig. 3. a. Mg Kα X-ray map of strongly zoned garnet in Suš eclogite. b. Rim to rim compositional profiles for garnet in Světlík-Suš eclogite.

Petrography

Eclogite

Besides common bi-mineralic garnet-omphacite eclogite, quartz-(clino)zoisite-bearing eclogite is also present. Fresh eclogites are coarse-grained with garnet and omphacite up to 4 mm in size. Accessory minerals include rutile and, rarely, kyanite and titanite, both as eclogite facies phases. Some eclogites show a weak metamorphic foliation. All eclogite varieties experienced a significant degree of partial recrystallization under granulite and amphibolite facies conditions (O'Brien and Vrána, 1995; Faryad et al., 2006). Minerals formed during decompression are orthopyroxene, in reaction domains between garnet and omphacite, and anorthite + spinel ± corundum ± peraluminous sapphirine, replacing kyanite.

Garnet (Alm_{47-60},Grs_{20-36},Prp_{22-41}) is zoned with an increase in Mg and a decrease in Fe from the central part of the garnet (1/3 of the whole garnet) to the rim (Fig. 3) A slight decrease in grossular towards the rim, combined with an increase of $X_{Mg,}$ may reflect decompression and heating after peak-pressure conditions. The Jadeite content in omphacite from different samples ranges between 22 and 32 mol. %. Titanite coexisting with omphacite and Ca-rich garnet is compositionally homogeneous in individual grains, but varies slightly in Al_2O_3 (1.42–2.35 wt.%) and F (0.2–0.36 wt.%) in different grains.

The eclogites are interesting for their replacement textures that were formed during hight-temperature decompression and cooling. Omphacite is replaced by a symplectite of diopsidic clinopyroxene, plagioclase, and amphibole. Garnet may have thick, kelyphitic rims consisting of fine-grained clinopyroxene, amphibole, and plagioclase, or orthopyroxene + plagioclase rims along garnet and quartz boundaries. Ilmenite represents the main retrograde Ti-phase in most samples, which may rim or contain inclusions of rutile. Titanite coexisting with omphacite is rimmed or replaced by symplectites of ilmenite and clinopyroxene (Fig. 4a). Na-rich pargasite and kaersutite (Ti > 0.5), with Si close to 6.00 a.p.f.u. and XMg = 0.47, occur in contact with symplectites of ilmenite + Ti-clinopyroxene. Tabular-shaped symplectites of plagioclase, biotite, and accessory spinel probably represent pseudomorphs after phengite (Figs. 4c and d). Kyanite is preserved in inclusions in garnet, but in the matrix it is replaced by symplectites of sapphirine + plagioclase or spinel + plagioclase (O'Brien and Vrána, 1995).

Garnet clinopyroxenites

In contrast to eclogites, which have composition of oceanic basalts/gabbros, garnet clinopyroxenites in the Světlík belt correspond to picritic rocks with a high MgO/FeOt ratio = 1.55–2.38 (wt. %) (O'Brien and Vrána, 1995). The whole-rock compositions of the garnet pyroxenites are similar to those described by Carswell and Scharbert (1983) from the Gföhl unit in Lower Austria. Clinopyroxene contains only 7.6 mol. % Ca-tschermakite and 6.3 mol. % jadeite, the latter reflecting the relatively low whole-rock Na content with 1.2–1.8 wt. % Na_2O (O'Brien and Vrána, 1995). Inconspicuous light-coloured garnet (c. 15–20 vol. %) has 53–58 mol. % pyrope, 21–23 % almandine, 16–20 % grossular, and 1–3 % andradite. Accessory phases are rutile, ilmenite and sulphides. Garnet clinopyroxenite samples from the Světlík belt are strongly retrogressed, containing up to 60 vol. % magnesiohornblende. Garnet is rimmed by very fine-grained spinel + orthopyroxene ± amphibole + plagioclase symplectite, which is locally replaced by magnesiohornblende.

Inclusions of disordered graphite in garnet

Disordered graphite has been identified in isolated, cuboidal micro-inclusions in garnet. Most of them are opaque, although trans-

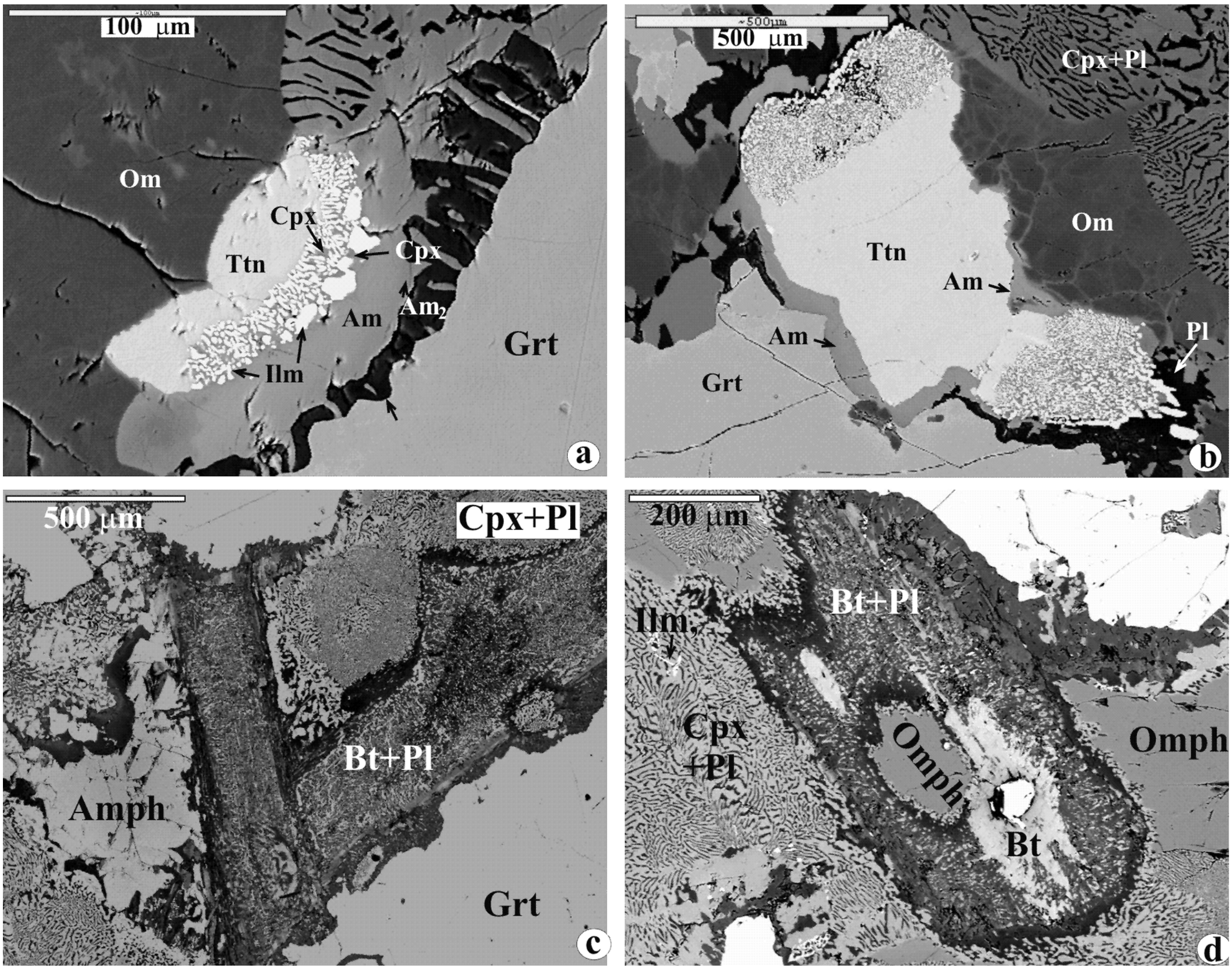

■ **Fig. 4.** (a) Titanite associated with omphacite and garnet. Note that titanite is in direct contact with omphacite. (b) Amphibole occurs between garnet and titanite. (c, d) Tabular grains of former phengite (?) replaced by symplectite of plagioclase + biotite.

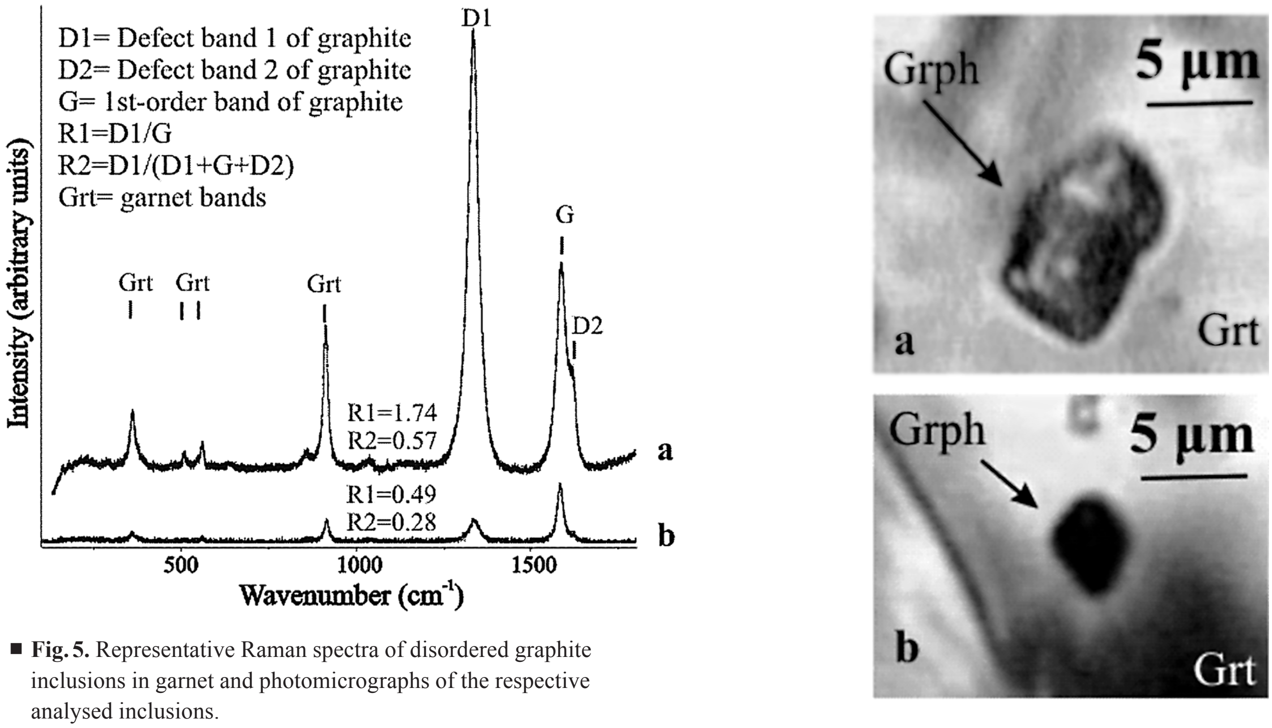

■ **Fig. 5.** Representative Raman spectra of disordered graphite inclusions in garnet and photomicrographs of the respective analysed inclusions.

parent to semi-transparent grains are also present (Fig. 5). First-order Raman spectra were analysed from 100 to 1800 cm^{-1}; in some cases the entire range from 100 to 3350 cm^{-1} was analysed in order to check the second-order Raman peaks. The analysed disordered graphites show two peaks in the first-order region, at ~1330 cm^{-1} and ~1580 cm^{-1}, with a shoulder at ~1618 cm^{-1} and a broad, second-order peak at ~2666 cm^{-1}. It is of interest that not all of the graphites show the same degree of disordering. The R1 (D1/G) and R2 [D1/(D1 + G + D2)] parameters (Beyssac et al., 2002) vary from 0.33 to 1.95 and 0.23 to 0.59, respectively. The two most likely mechanisms of formation of disordered graphite in eclogites are (1) fluid-precipitated graphite (Wopenka and Pasteris, 1993; Pasteris and Chou, 1998; Satish-Kumar, 2005) and (2) diamond-graphite phase transition (El Goresy et al., 2001; Willems et al., 2004). The distinction between these two mechanisms, i.e., whether graphite formed from transformation of previous diamond or disordered graphite grew within former fluid inclusions by precipitation, is difficult to ascertain, and crystallinity itself is insufficient to distinguish the origin of the graphite.

Geothermobarometry and interpretation

Temperatures of 700–800 °C, with a mean value of 746 ± 27 °C, and pressures of 2.0–2.4 GPa (Fig. 6) were obtained for kyanite-bearing eclogite using garnet-clinopyroxene-kyanite thermobarometry (Ganguly, 1996; Ellis and Green, 1979; Powell, 1985; Ai, 1994; Brandelik and Massonne, 2004; Ravna and Terry, 2004). Preservation of prograde zoning in garnet and formation of orthopyroxene, spinel and sapphirine suggest that the eclogites during decompression remained only briefly under granulite facies conditions (O'Brien and Vrána, 1995; Faryad et al., 2006).

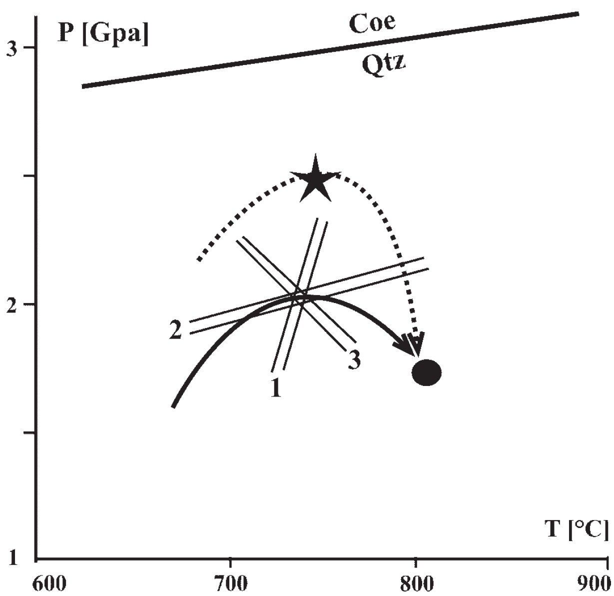

■ **Fig. 6.** Pressure and temperature conditions calculated using the PTGIBS program (Brandelik and Massonne, 2004) for kyanite-bearing eclogite with Jd-rich clinopyroxene. The star marks the intersection of reactions 1–3, obtained from the method of Ravna and Terry (2004). Arrows indicate PT paths from eclogite to HP granulite facies conditions (filled circle estimated by O'Brien and Vrána, 1995). Reactions 1–3 are:

Alm + Di = Hd + Prp	1
Grs + Alm + Qtz = Ky + Hd	2
Grs + Prp + Qtz = Ky + Di	3

PT conditions of the garnet pyroxenites have not been investigated yet. However, the presence of high-pressure metamorphic rocks in the Monotonous unit suggests that tectonic emplacement of eclogites and garnet pyroxenites into lower-grade metamorphic rocks may not be unique to the Gföhl unit. The Monotonous and Gföhl units may have been close to each other during Variscan convergence and may represent different levels in the accretionary wedge or the subduction channel.

References

AI Y. and YANG A., 1994. A revision of the garnet-clinopyroxene Fe^{2+}-Mg exchange geothermometer. *Contrib. Mineral. Petrol.*, 115: 467-473.

BEYSSAC O., GOFFE B., CHOPIN C. and ROUZAUD J.N., 2002. Raman spectra of carbonaceous material in metasediments: a new geothermometer. *J. Metamorph. Geol.,* 20: 859-871.

BRANDELIK A. and MASSONNE H.J., 2004. PTGIBBS - an EXCEL (TM) Visual Basic program for computing and visualizing thermodynamic functions and equilibria of rock-forming minerals. *Computers and Geosciences*, 30 (9-10): 909-923.

EL GORESY A., GILLET P., CHEN M., KUENSTLER F., GRAUP G. and STAEHLE V., 2001. In situ discovery of shock-induced graphite-diamond phase transition in gneisses from the Ries Crater, Germany. *Am. Mineral.*, 86: 611-621.

ELLIS D.J. and GREEN D.H., 1979. An experimental study of the effect of Ca upon garnet-clinopyroxene Fe-Mg exchange equilibria. *Contrib. Mineral. Petrol.,* 71: 13-22.

FARYAD S.W., PERRAKI M. and VRÁNA S., 2006. P-T evolution and reaction textures in retrogressed eclogites from Svetlik, the Moldanubian Zone (Czech Republic). *Mineralogy and Petrology,* 88: 297–319.

GANGULY J., CHENG W. and TIRONE M., 1996. Thermodynamics of alumosilicate garnet solid solution: new experimental data, an optimized model, and thermodynamic application. *Contrib. Mineral. Petrol.,* 126: 137-151.

O'BRIEN P. and VRÁNA S., 1995. Eclogites with a short-lived granulite facies overprint in the Moldanubian Zone, Czech Republic: petrology, geochemistry and diffusion modeling of garnet zoning. *Geol. Rundsh.*, 84: 473-488.

PASTERIS J.D. and CHOU I.M., 1998. Fluid-deposited graphitic inclusions in quartz: Comparison between KTB (German Continental Deep-Drilling) core samples and artificially reequilibrated natural inclusions. *Geochim. Cosmochim. Acta*, 62: 109-122.

POWELL R., 1985. Regression diagnostics and robust regression in geothermometer/ geobarometer calibration: the garnet-clinopyroxene geothermometer revisited. *J. Metamorph. Geol.,* 3: 231-243.

RAVNA E.J.K. and TERRY M.P., 2004. Geothermobarometry of UHP and HP eclogites and schists – an evaluation of equilibria among garnet-clinopyroxene-kyanite-phengite-coesite/quartz. *J. Metamorph. Geol.,* 22: 579-592.

SATISH-KUMAR M., 2005. Graphite-bearing CO_2-fluid inclusions in granulites: Insights on graphite precipitation and carbon isotope evolution. *Geochim. Cosmochim. Acta,* 69: 3841-3856.

SCHARBERT H.G. and CARSWELL D.A., 1983. Petrology of garnet-clinopyroxene rocks in a granulite facies environment, Bohemian Massif of Lower Austria, Austria. *Bull. Minéral.,* 106: 761–774.

VRÁNA S., 1991. Geological map 1:25000, sheet 52-234, Světlík. Czech Geol. Survey Prague.

VRÁNA S.,1979. Polyphase shear folding and thrusting in the Moldanubicum of southern Bohemia. *Bull. Czech Geol. Survey*, 54: 75-86.

WEND J.I., KRONER A., FIALA J., TODT W., 1994. U-Pb zircon and Sm-Nd dating of Moldanubian HP/HT granulites from south Bohemia, Czech Republic. *J. Geol. Soc.,* 151: 83-90.

WILLEMS B., DE CORTE K. and VAN TENDELOO G., 2004. Why does polycrystalline natural diamond turn black after annealing? *Phys. Stat. Sol*. (a), 201: 2486-2491.

WOPENKA B. and PASTERIS J.D., 1993. Structural characterization of kerogens to granulite-facies graphite: Applicability of Raman microprobe spectroscopy. *Am. Mineral*., 78: 533-577.

Eclogite, Garnet Peridotite, Garnet Pyroxenite and HP Granulite in the Gföhl Unit

Shah Wali FARYAD, Martin RACEK, and Ondrej LEXA

Institute of Petrology and Structural Geology, Charles University Prague, Czech Republic

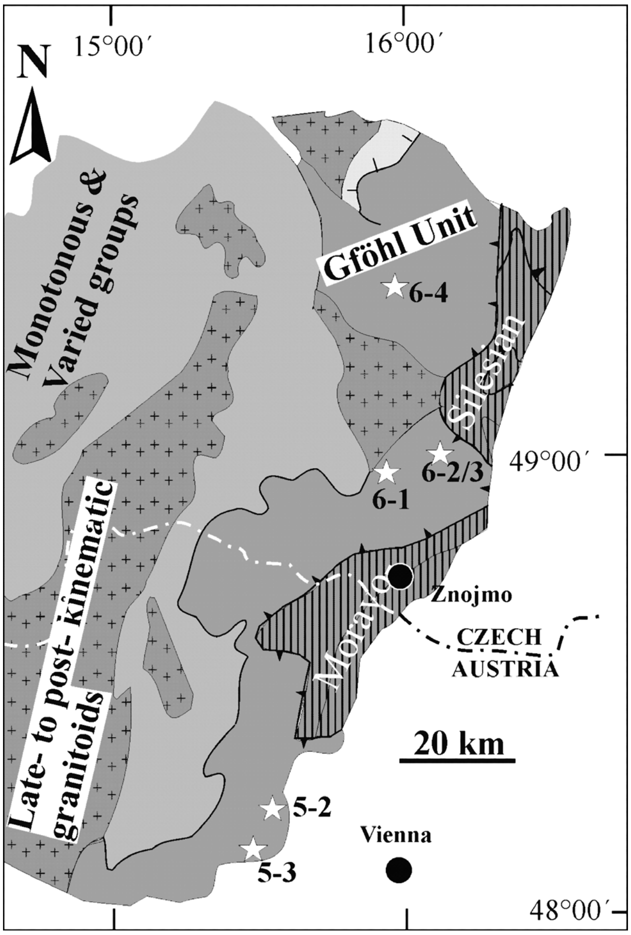

■ **Fig. 1.** Localities of field trip stops in garnet peridotites, garnet pyroxenites and eclogites in the Gföhl unit (area B in Fig. 1 of the Introduction to post-conference excursion) Stops 5-2–6-4 in the Gföhl unit with HP/UHP granulite and granulitic gneiss, garnet peridotite, garnet pyroxenite and eclogite.

The excursion to the *Gföhl unit* will start in HP granulite and associated garnet peridotite and garnet pyroxenite (stops 5-2 and 5-3) in Dunkelstein Wald (Lower Austria) about 30 km NW of Vienna (Fig. 1). We will continue to the north into the Czech Republic, where we will visit eclogite and garnet peridotite at Nové Dvory (stop 6-1), spinel peridotite and garnet peridotite at Mohelno (stops 6-2 and 6-3), and HP granulite, peridotite, and pyroxenite at Horní Bory (stop 6-4).

High-grade rocks in the eastern margin of the Bohemian massif are exposed along the contact between the Moldanubian and Brunovistulian or Moravo-Silesian domains (Fig. 2a). The Brunovistulian domain consists mostly of undeformed Late Proterozoic granitoids that are overlain by Cambrian to Carboniferous sediments with volcanic rocks (e.g., Dudek, 1960; Hartley and Otava, 2001; Kalvoda et al,. 2003). Variscan deformation caused northeastward thrusting of Moldanubian high-grade rocks over the Brunovistulian domain (Fritz and Neubauer, 1993; Schulmann et al., 1994), which are exposed in three tectonic windows in a 300-km-long and 30- to 50-km-wide belt along the eastern margin of the Bohemian Massif. Metamorphism of the Moravian Zone is tectonically inverted within imbricated orthogneiss-metasedimentary nappes from the kyanite zone in the west to the chlorite zone in the east (Štípská and Schulmann, 1995; Fritz et al., 1996; Štípská et al., 2000).

The Moldanubian domain consists of high-grade rocks of the Gföhl unit structurally overlying generally lower-grade rocks of the Varied and Monotonous groups (Fig. 2b,c), all intruded by plutonic rocks of Carboniferous age (Fuchs, 1976; Thiele, 1976). *The Gföhl unit* is dominated by migmatitic orthogneisses (the Gföhl gneisses) that are commonly associated with felsic kyanite-garnet-K-feldspar granulite and subordinate intermediate and mafic granulites, which enclose serpentinized garnet peridotites, garnet pyroxenites and retrogressed eclogites. Structurally, the lower part of the Gföhl unit, which is characterized by amphibolites interlayered with felsic metavolcanics and paragneisses, is called the Raabs group (Thiele, 1984; Fritz and Neubauer, 1993; Finger and Steyer, 1995). U-Pb zircon dating of the Gföhl orthogneiss and granulites shows an age range of 500–390 Ma for magmatic protolith of the Gföhl unit (Finger and von Quadt, 1995; Friedl et al., 2004; Schulmann et al., 2005). The Gföhl gneiss, granulite, and migmatites record HT/HP peak metamorphic conditions of 18–20 kbar and 800–1000 °C (e.g., Carswell and O'Brien, 1993; Cooke and O'Brien, 2001; Štípská and Powell, 2005a,b; Racek et al., 2006; Racek et al., 2008). According to numerous geochronological studies, the age of high-grade metamorphism in the Moldanubian domain is Carboniferous (Kröner et al., 2000; Friedl et al,. 2003, and references therein). U-Pb zircon ages ranging from ~350 to 340 Ma (van Breemen et al., 1982; Schulmann et al., 2005, and references therein) are interpreted as the age of peak metamorphic conditions, whereas Ar-Ar ages of ~330 to 325 Ma (Dallmeyer et al., 1992; Fritz et al., 1996) correspond to the cooling of the Moldanubian and Moravian zones.

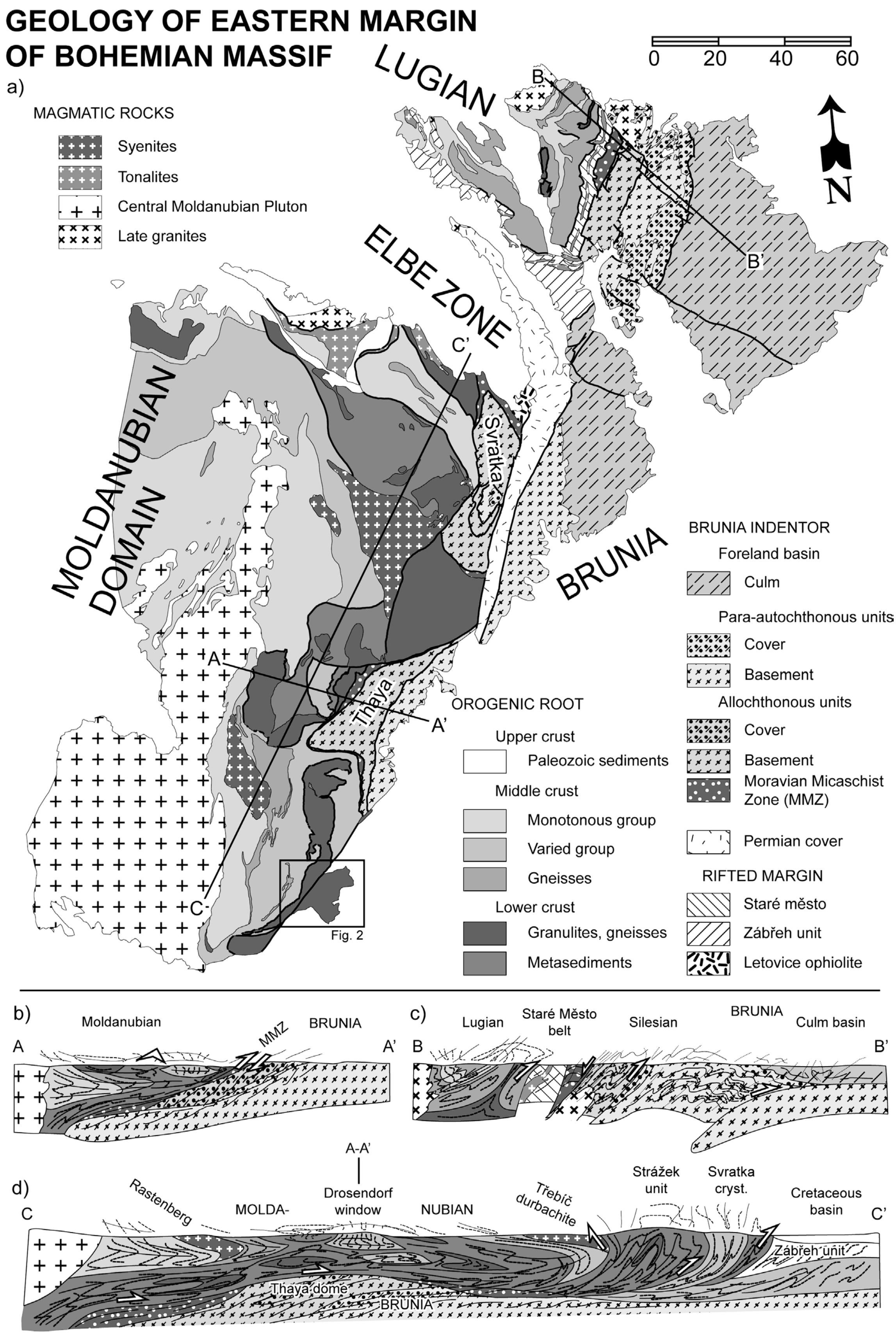

■ **Fig. 2** (a) Simplified geological map of the eastern margin of the Bohemian Massif, with three interpretative cross-sections along the marked profiles showing the inferred orogenic crustal architecture.(b) E–W cross-section of the southern Moldanubian Domain, showing flat-lying fabrics in the lower crust *vs.* steep fabrics in mid-crustal units. Dismembered orogenic middle crust forms large-scale boudins surrounded by rocks of the Gföhl unit. (c) Cross-section of the Lugian–Silesian domain. (d) North–south cross-section of the Moldanubian domain, showing strong deformation in the southern part of the system with important mixing of orogenic lower crust and orogenic middle crust due to "channel flow" processes and weak deformation in the northern part of the section.

The Varied group is composed of paragneiss with layers of quartzite, marble, graphite schist, amphibolite, and bodies of granitic gneiss. The granitic gneisses are Late Proterozoic in age and/or display a Late Proterozoic anatectic overprint. An age of 358 Ma for a felsic metavolcanite within the amphibolites (Friedl et al., 1993) suggests that sedimentation of the Varied unit is Devonian in age (Gebauer and Friedl, 1993; Friedl et al., 2004). *The Monotonous unit* is dominated by paragneisses and contains minor quartzite, calcsilicate, and mafic rocks with a presumed Late Proterozoic age of sedimentation (Kröner et al., 1988). The Varied and Monotonous groups record a prograde metamorphic evolution at P-T conditions up to 700–800 °C and 10 kbar (e.g., Petrakakis, 1997; Racek et al., 2006; Linner, 1996; Büttner and Kruhl, 1997).

The structural position of the Gföhl unit is widely interpreted as resulting from low-angle, long-distance thrusting over mid-crustal rocks of the Varied and Monotonous groups (e.g., Suess, 1918; 1976; Thiele, 1976; Tollmann, 1982; Matte, 1986; Franke, 1989). Recent models of Štípská et al., (2004), Schulmann et al. (2005; 2008), and Racek et al. (2006), however, suggest that the juxtaposition of the mid- and lower-crustal rocks in the same present-day crustal level was achieved by vertical mass transfer caused by E-W compression. This compressive phase was then followed by thrusting of the whole sequence over the Brunovistulian basement in the form of channel flow in a partially molten milieu that resulted in pervasive flat reworking and disintegration of all of units, now preserved as boudins.

Dunkelsteinwald HP granulites and garnet peridotites

The Dunkelsteinwald granulites are exposed south of the Danube River near Krems am der Donau (Fig. 3). A striking feature of the granulites is the presence of interfolded lensoidal bodies of dark-coloured garnet peridotite (Carswell, 1991).

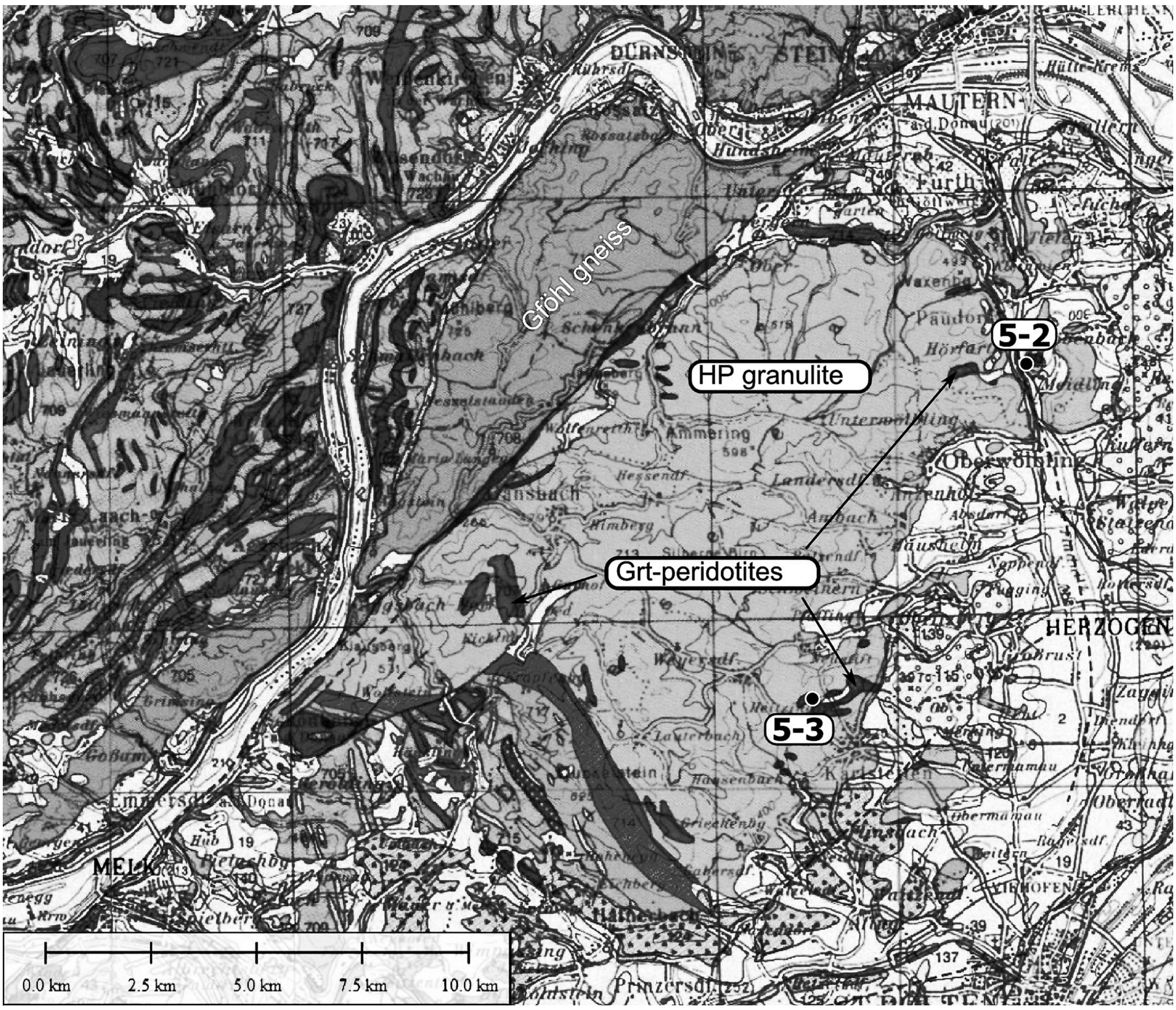

■ **Fig. 3.** Geological map of the Moldanubian Zone in Lower Austria (largely after Fuchs, 1971), showing the locations of garnet peridotites within the Dunkelsteinwald granulite and Field Trip Stops 5-2 and 5-3.

The garnet peridotites are highly deformed, with a platy fabric accentuated by late-stage serpentinisation. Boudinaged layers or lenses of pyroxenites within the peridotites are relatively unaltered and preserve high-pressure (HP) garnet-clinopyroxene assemblages.

The felsic granulites are predominant and contain almandine-rich garnet + kyanite + mesoperthite + quartz. Subordinate, intermediate granulite contains orthopyroxene and rare clinopyroxene (Scharbert and Kurat, 1974). More mafic granulites directly enclosed in felsic granulites are rare. These rocks contain garnet + sodic clinopyroxene + plagioclase, (and abundant late replacement amphibole). Granulites usually have a protomylonitic or blastomylonitic fabric, which is especially pronounced in extremely platy and lineated variants (Plattenstein) developed towards the base of the granulite unit. Granulite is extensively retrograded, with kyanite replaced by sillimanite, garnet by biotite, mesoperthite by microcline and oligoclase, and pyroxenes by amphiboles.

Garnet peridotites include lherzolite, harzburgite, and more rarely dunite (Becker, 1997). Dunite and harzburgite locally contain layers of garnet pyroxenite. Both the garnet peridotites and the spatially associated garnet pyroxenites typically display complex reaction textures that reflect a prolonged, polyphase, tectono-metamorphic history (Carswell, 1991; Carswell et al,, 1989). Garnet pyroxenites occur as millimetre- to decimetre-thick layers within the garnet peridotites. Most of them show relatively sharp contacts with the host garnet peridotite. Garnetite lenses with more than 90 vol% of garnet are also present within peridotites (Becker, 1997).

Textural and compositional relations of minerals

Garnet peridotites and garnet pyroxenites contain several textural and compositional varieties of olivine, orthopyroxene, clinopyroxene garnet, spinel, and amphibole. In addition to deep purple garnets with high Cr content (2.5 ± 7.6 wt% Cr_2O_3) in lherzolite and harzburgite, orange-brown garnets with low Cr_2O_3 contents (<1 wt% Cr_2O_3) occur in pyroxenite. Garnet shows zoning with Fe and Mn increasing and Mg decreasing from grain cores to rims. Some orthopyroxene megacrysts show exsolution lamellae of garnet and clinopyroxene and marginal recrystallisation to an assemblage of orthopyroxene + clinopyroxene + olivine (± later amphibole and spinel). Pyroxene porphyroclasts within the peridotites from Meidling-im-Tal contain garnet exsolution lamellae, and they are often recrystallized near the rims (Fig. 4). The orthopyroxene megacrysts contain 4.55 wt% Al_2O_3 and 2.19 wt% CaO. This high-Al, high-Ca orthopyroxene composition suggests an early high-temperature igneous protolith stage. Clinopyroxene I porphyroclasts recrystallized to a neoblast assemblage of clinopyroxene II ± orthopyroxene ± plagioclase. Rare clinopyroxene megacrysts (3 × 2 cm in size) in harzburgite contain millimetre-thick orthopyroxene exsolution lamellae that appear to have exsolved together with intergrown garnet lamellae.

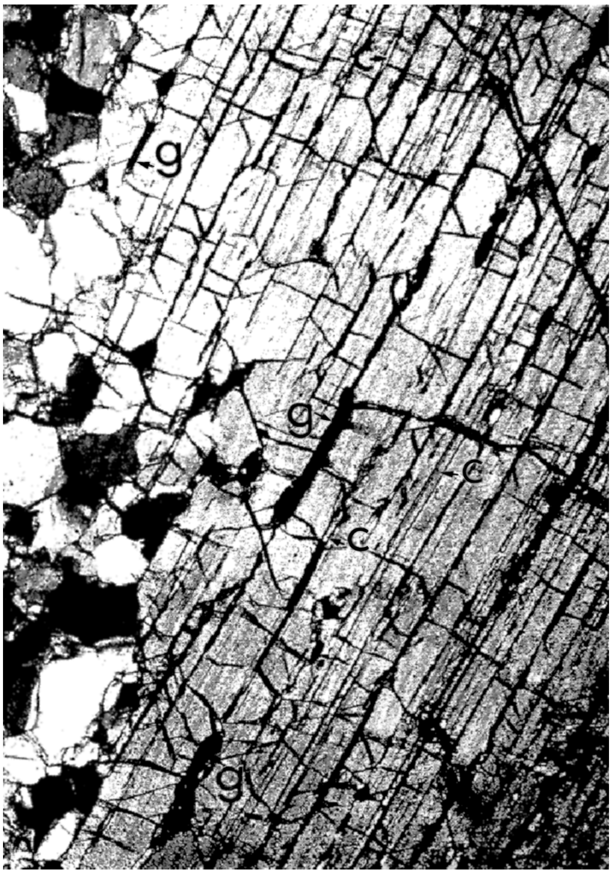

■ **Fig. 4.** Photomicrograph (crossed polarizers) of an orthopyroxene megacryst with lamellae of garnet (isotropic blebs, g) and clinopyroxene (c) from clinopyroxenite in Meidling-im-Tal, Dunkelsteinerwald (Carswell, 1991). Note marginal recrystallization along the left side of the photomicrograph. Width of field of view is approximately 5 mm. Note uneven extinction in orthopyroxene due to strain.

One sample from a pyroxenitic layer in peridotite contains garnet, with a continuous range in composition from $Py_{64-56}Alm_{23-27}Grs_{13-17}Uv_0$ to $Py_{42}Alm_{21}Grs_{33}Uv_0$, in which the low-Prp, high-Grs composition garnet occurs locally as rims on high-Prp, low-Grs garnet and as separate grains. Garnet is accompanied by omphacite, which contains 25 mol % jadeite. The high-Prp, low-Grs garnet is interesting for the presence of numerous monomineralic or multiphase inclusions, consisting of some combination of Na-Ca amphibole, alkali feldspar, phlogopite, chlorite and carbonate. The inclusions have negative crystallographic forms in garnet, suggesting the presence of former fluid-bearing phase(s). The presence of alkali with chlorine, as well as the negative forms of inclusions, suggests recrystallization of this mantle rock in a subduction zone environment with attendant fluid circulation.

Metamorphic evolution of the ultramafic rocks

Based on textural relations observed in a large number of samples, six mineralogical stages have been established in the metamorphic evolution of the Lower Austrian peridotites (Carswell, 1991). Stage 1 is representedby the assemblage, $Ol_1 + Opx_1 + Cpx_1 \pm Spl_1$, which reflects near-solidus upper-mantle conditions (Fig. 5). Stage II is represented by the garnet-bearing assemblage, $Ol_2 + Opx_2 + Cpx_2 + Grt_1$, where orthopyroxene porphyroclasts invariably show a marked decrease in Ca and an increase in Al from core to rim. PT conditions for the Stage II assemblage in garnet peridotite, using the thermobarometry of Carswell et al. (1989) and Nickel and Green (1985), are 32.2 kbar/1052 °C and 31.5 kbar/1035 °C, respectively (Carswell, 1991).

The Stage III assemblage, includes a second generation of low-Cr garnet coexisting with Cr-spinel ($Ol_3 + Opx_3 + Cpx_3 + Grt_2 + Spl_2$), although this complete assemblage cannot be explicitly demonstrated due to extensive overprinting by the later granulite facies assemblages of Stage IV, $Ol_4 + Opx_4 + Cpx_4 + Spl_3$, and amphibolite facies Stage V, $Ol_5 + Opx_5 + Amp_1 + Spl_4$. Development of the Stage IV granulite-facies assemblage is essentially restricted to the growth of fine-grained filamental kelyphites around garnets, presumably under strain-free conditions. Subsequent high-strain deformation promoted the development of the Stage V amphibolite-facies assemblage with aggregates of orthopyroxene + amphibole + spinel replacing the earlier pyroxene + spinel kelyphites.

A different PT evolution for garnet peridotite in the Dunkelsteinwald was proposed by Becker (1997). He obtained temperatures of 1400 ± 1420 °C (Stage 1 in Fig. 6) using Ca-in-orthopyroxene and two-pyroxene thermometry (Brey and Kohler, 1990). Based on such high crystallization temperatures of pyroxene megacrysts and the bulk composition of the pyroxenites, Becker (1996) suggested that the pyroxenite and megacryst cumulates crystallized in the lithosphere from hot low-degree melts, which were derived from the asthenospheric mantle from minimum depths of 180 to 200 km (ca. 5.5 to 6.0 GPa). Pressures of 3 to 3.5 GPa at 1100 °C were estimated for the assemblage garnet-orthopyroxene-clinopyroxene-olivine in garnet peridotite for stage 2. The garnet exsolution textures and growth of garnet II, interpreted to be at the expense of clinopyroxene I, are apparently restricted to pyroxenite layers and their surroundings. According to this interpretation, the exsolution textures reflect subsequent subsolidus cooling of the cumulates to the ambient lithospheric geotherm.

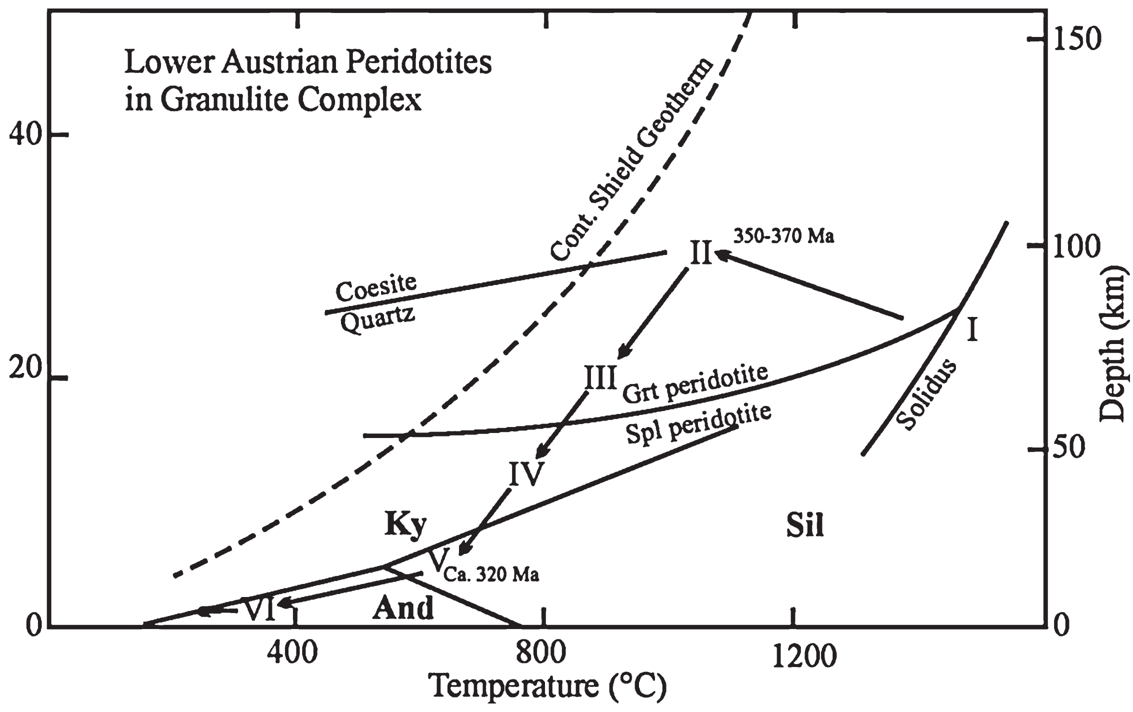

■ **Fig. 5.** Deduced pressure-temperature-time path for the six recognised stages in the metamorphic evolution of the Lower Austrian peridotits (Carswell, 1991). Spinel peridotite/Garnet peridotite reaction from O'Hara et al. (1971); Quartz/Coesite reaction from Mirwald and Massonne (1980); Al-sihcate stability fields – Ky/Sil/And from Salje (1986); "Dry" pyrolite solidus from Green and Ringwood (1967); Precambrian shield geotherm from Clark and Ringwood (1964).

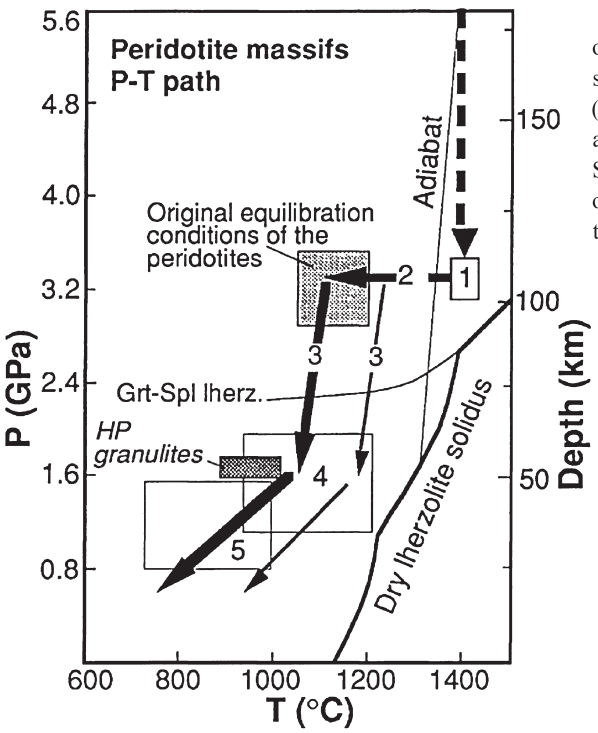

Sm/Nd garnet-clinopyroxene-whole rock isochron ages of 344 ± 10 Ma and 370 ± 15 Ma for two garnet pyroxenite samples within Dunkelsteinerwald peridotite bodies (Carswell and Jamtveit, 1990) indicate an early Variscan age for the formation of the Pmax (Stage II) assemblages. Similar U-Pb zircon ages (347 ± 9 and 367 ± 18 Ma) were obtained by Kroner et al. (1988) from granulite massifs in the southern and eastern parts of the Moldanubian Zone.

■ **Fig. 6.** P-T diagram showing the P-T paths of peridotite massifs from lower Austria (Becker, 1997). Stage 1, formation of pyroxenites and pyroxene megacrysts as high-pressure igneous cumulates; Stage 2, isobaric cooling; Stage 3, near-isothermal decompression; Stage 4, exsolution of spinel in pyroxenes and growth of coarse-grained symplectites; and Stage 5, formation of kelyphites. The dashed arrow represents isothermal interpolation to the intersection with an upper-mantle adiabat and implies fast ascent of superheated magma in the sublithospheric mantle. Thick and thin arrows indicate different paths for peridotites that followed somewhat different cooling histories. Equilibration conditions of high-pressure granulites are also shown (Carswell and O'Brien, 1993).

Stop 5-2 (Day 5). Garnet Peridotite and Garnet Pyroxenite, Granulite Quarry in Meidling-im-Tal, 6 km South from Krems am der Donau

Coordinates: N48°20′40.0″ E15°37′32.3″

The high-pressure granulite with elongated boudins of garnet peridotite exhibits a highly sheared fabric, which is homogeneously developed across the quarry and originated during the early stages of exhumation of the rocks. Felsic granulites are dominant in the quarry, consisting of feldspar, quartz, garnet, kyanite ± sillimanite, rutile, and variable amounts of biotite. Ternary feldspar (+ mesoperthite) is well preserved in garnet and occurs locally in the matrix. Some mafic varieties of granulite may contain clinopyroxene and orthopyroxene. Garnet contains oriented needles of rutile.

A large body of strongly serpentinized garnet peridotite, including lherzolite, harzburgite, and rare dunite, is exposed in the

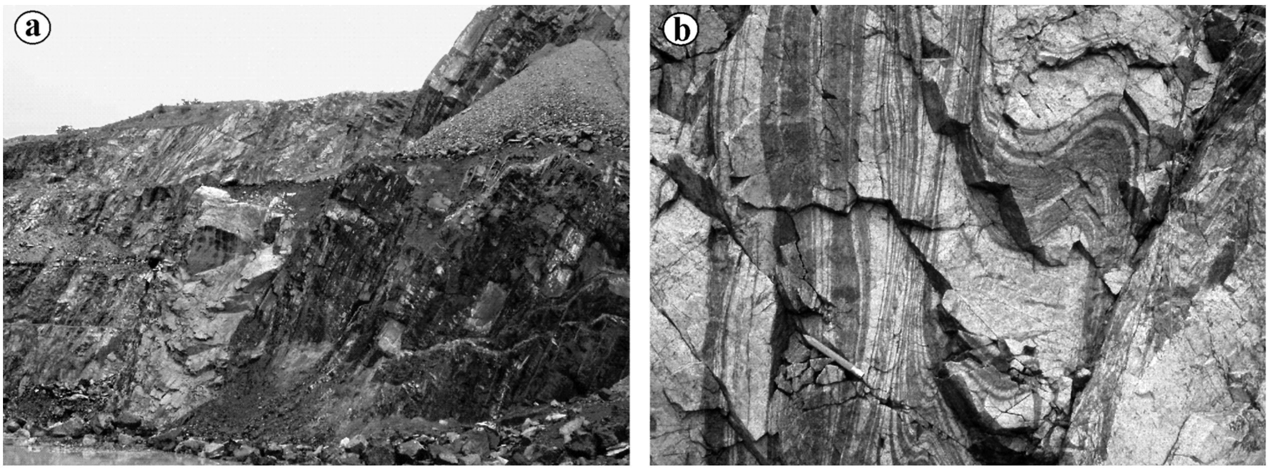

■ **Fig. 7.** Meidling-im-Tal granulites and peridotites. (a) large deformed body of peridotite within strongly foliated HP granulite; Meidling quarry. (b) relicts of early compositional layering transposed to a dominant Grt-Ky bearing granulitic fabric; Meidling quarry central part of the quarry (Fig. 7a, b) (Becker, 1997). Relict minerals in the peridotites are pyroxenes, olivine, and garnet with kelyphitic rims or kelyphite pseudomorphs after garnet. Garnet is rich in MgO (19–20 wt%) and Cr_2O_3 (3.6–7.6 wt%), and orthopyroxene has relatively high Al_2O_3 = 1.9–3.5 wt% (Table 1). Garnet pyroxenites form thin layers (millimetres to several decimetres) within garnet peridotites. They show a weak foliation, defined by alignment of pyroxenes, which together with garnet, formed by recrystallization of primary, coarse-grained Al-rich clino- or orthopyroxene, as illustrated in Fig. 4 and described by Carswell (1991). Clinopyroxene neoblasts in pyroxenite are rich in Na_2O (up to 4.16 wt%, Table 1). More details about mineral compositions and PT evolution of the ultramafic rocks are given above.

Rock	Lh	Hz	CMe	GCp	GCp	Lh	OMe	CMe	Lh	OMe	CMe	GCp	Hz	Lh	Lh
Mineral	Garnet					Orthopyroxene				Clinopyroxene			Spinel		
position	lamellae					Incl.	lamellae	kelyph	incl		lamellae	incl	matrix	in amph	in amph
SiO_2	41.76	41.28	41.24	40.82	41.74	55.71	56.14	55.75	53.47	51.98	52.32	53.27	0	0	0
TiO_2	0.28	0.13	0.15	0.2	0.1	0.09	0.06	0.06	0.2	0.19	0.25	0.38	0.07	0.05	0.03
Cr_2O_3	3.5	7.62	1.91	0.06	0.54	0.65	0.42	0.46	1.43	1.33	1.44	0.13	33.69	40.72	32.05
Al_2O_3	21.06	18.04	21.69	22.92	23.16	1.95	2.58	2.45	3.56	4.12	4.56	10.33	34.99	28.93	36.42
FeO	6.72	6.97	10.6	9.63	10.76	5.25	5.92	5.97	2.61	2.18	1.79	2.91	15.94	17.2	15.28
MnO	0.38	0.2	0.68	0.17	0.43	0.09	0.16	0.13	0.13	0.08	0.05	0.07	0.08	0.06	0.06
MgO	20.48	19.87	18.6	12.76	18.59	34.53	33.17	34.66	16.63	15.35	15.77	11.2	15.72	12.45	14.63
CaO	5.68	6.62	5.35	13.16	4.95	0.94	0.55	0.44	20.05	23.34	22.41	16.94	0.01	0.04	0.08
Na_2O	0.01	0.03	0.03	0.02	0	0.09	0.04	0.04	1.55	1	1.33	4.16			
Total	99.85	100.77	100.26	99.75	100.26	99.29	99.04	99.95	99.63	99.56	99.95	99.38	100.48	99.445	100.44

Gnt garnet, Lh lherzolite, Hz harzburgite, CMe clinopyroxene megacryst, OMe orthopyroxene megacryst, Gnt garnetite, GCp garnet clinopyroxenite)

■ **Tab. 1.** Selected mineral analyses from peridotites, megacrysts and pyroxenites (taken from Becker, 1997).

Stop 5-3 (Day 5). Garnet Peridotites, Granulite Quarry Close to Karlstetten, 9 km Northwest from St. Pölten

Coordinates: N48°16′12.9″ E15°33′12.0″

This quarry is a typical example of strongly retrogressed granulites containing boudins and rootless folds of garnet peridotite bodies (Fig. 8a,b). Structures developed in this quarry show vertical shortening affecting the granulite under middle crustal con-

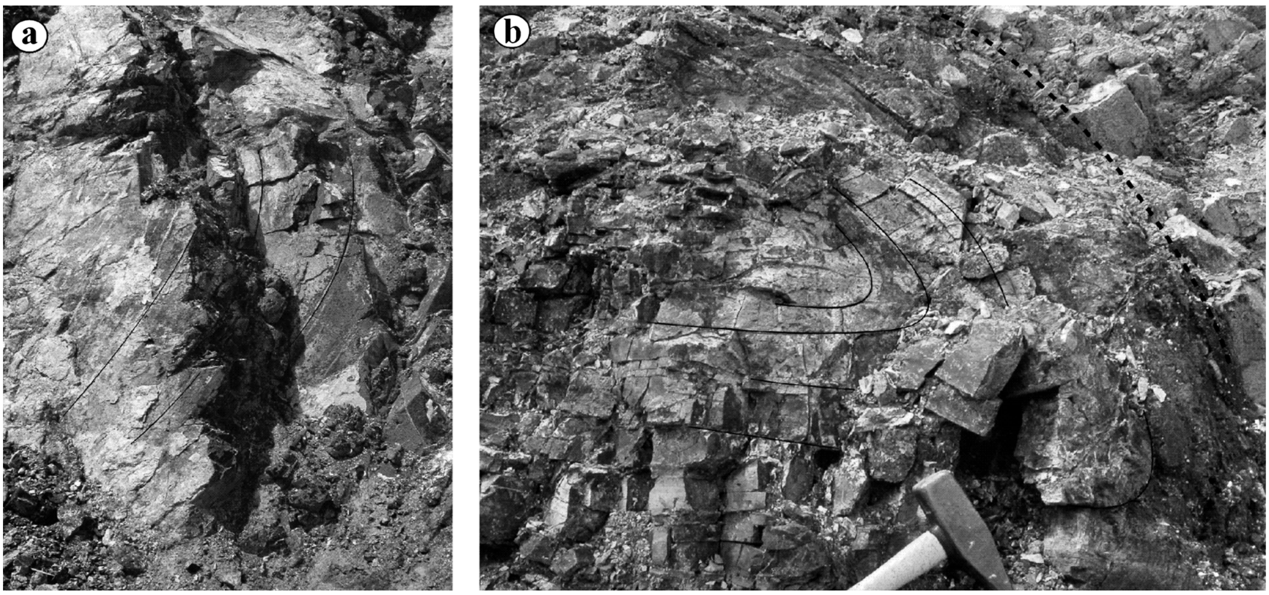

■ **Fig. 8.** Structures in granulites with serpentinized garnet peridotites. (a) isoclinal fold of serpentinized peridotite within retrograded granulite; Karlstetten quarry. (b) large open buckle fold of serpentinized garnet peridotite; Karlstetten quarry.

ditions. Flat lying fabrics in the quarry are structurally concordant with the dominant foliations in the surrounding Gföhl unit gneisses. Microtextural relations and mineral composition of the granulites and garnet peridotites are similar to those in the Meidling-im-Tal quarry, as described above.

References

BECKER H., 1996. Crustal trace element and isotopic signatures in garnet pyroxenites from garnet peridotite massifs from lower Austria. *J. Petrol.,* 37: 785-810.

BECKER H., 1997. Petrological constraints on the cooling history of high-temperature garnet peridotite massifs in lower Austria. *Contributions to Mineralogy and Petrology*, 128: 272-286.

VAN BREEMEN O., AFTALION M., BOWES D.R., DUDEK A., MÍSAŘ Z., POVONDRA P. and VRÁNA S., 1982. Geochronological studies of the Bohemian Massif, Czechoslovakia, and their significance in the evolution of Central Europe. *Transaction of the Royal Society of Edinburgh - Earth Sciences*, 73:89–108.

BREY G.P. and KÖHLER T.P., 1990. Geothermobarometry in 4-phase lherzolites. 2. New thermobarometers, and practicle assesment of existing thermometers. *Journal of Petrology,* 31: 1353–1378.

BÜTTNER S. and KRUHL J.H., 1997. The evolution of a late-Variscan high-T/low-P region: The southeastern margin of the Bohemian massif. *Geologische Rundschau*, 86: 21-38.

CARSWELL D.A., 1991. Variscan high P-T metamorphism and uplift history in the Moldanubian Zone of the Bohemian Massif in lower Austria. *European Journal of Mineralogy*, 3: 323-342.

CARSWELL D.A. and JAMTVEIT B., 1990. Variscan Sm-Nd ages for the high-pressure metamorphism in the Moldanubian Zone of the Bohemian Massif, Lower Austria. *Neues Jahrbuch Miner. Abh*.,162: 69-78.

CARSWELL D.A., MOLLER C. and O'BRIEN P.J., 1989. Origin of sapphirine- plagioclase symplectites in metabasites from Mitterbachgraben, Dunkelsteinerwald granulite complex, Lower Austria. *Eur.J. Mineral.*, 1: 455-466.

CARSWELL D.A. and O'BRIEN P.J., 1993. Thermobarometry and geotectonic significance of high-pressure granulites: examples from the Moldanubian Zone of the Bohemian Massif in Lower Austria. *Journal of Petrology*, 34: 427–459.

CLARK S.P. and RINGWOOD A.E., 1964. Density distribution and constitution of the mantle. *Rev. Geophys*., 2: 35-88.

COOKE R.A. and O'BRIEN P.J., 2001. Resolving the relationship between high P-T rocks and gneisses in collisional terranes: an example from the Gföhl gneiss-granulite association in the Moldanubian Zone, Austria. *Lithos*, 58: 33–54.

DALLMEYER R.D., NEUBAUER F. and HOCK V., 1992. Chronology of late Paleozoic tectonothermal activity in the southeastern Bohemian Massif, Austria (Moldanubian and Moravo- Silesian zones): 40Ar/39Ar mineral age controls. *Tectonophysics*, 210: 135-153.

DUDEK A., 1960. Krystalické břidlice a devon východně od Znojma. *Sborník Ústředního ústavu geologického*, 26: 101-141.

FINGER F. and STEYER H.P., 1995. A tectonic model for the eastern Variscides: indications from a chemical study of amphibolites in the south-eastern Bohemian Massif, Austria. *Geologica Carpathica*, 46: 1-14.

FINGER F. and VON QUADT A., 1995. U/Pb Ages of Zircons from a Plagiogranite-Gneiss in the South-Eastern Bohemian Massif, Austria - Further Evidence for an Important Early Paleozoic Rifting Episode in the Eastern Variscides. *Schweizerische Mineralogische und Petrologische Mitteilungen*, 75: 265-270.

FRANKE W., 1989. Tectonostratigraphic units in the Variscan belt of Central Europe. In "Terranes in the Circum-Atlantic Paleozoic Orogens" (Dallmeyer, Ed. Geological Society of America Special Paper, 230: 67-90.

FRIEDL G., VON QUADT A., OCHSNER A. and FINGER F., 1993. Timing of the Variscan orogeny in the Southern Bohemian Massif (NE Austria) deduced from new U-Pb zircon and monazite dating. *Terra Nova*, 1: 235-236.

FRIEDL G., COOKE R., FINGER F., MCNAUGHTON N.J. and FLETCHER I., 2003. U-Pb shrimp dating and trace element investigations on multiple zircons from a South-Bohemian granulite. *Journal of the Czech Geological Society*, 48: 51.

FRIEDL G., FINGER F., PAQUETTE J., VON QUADT A., McNAUGHTON N. and FLETCHER I., 2004. Pre-Variscan geological events in the Austrian part of the Bohemian Massif deduced from U-Pb zircon ages. *International Journal of Earth Sciences*, 93: 802-823

FRITZ H. and NEUBAUER F., 1993. Kinematics of crustal stacking and dispersion in the south-eastern Bohemian Massif. *Geologische Rundschau*, 82: 556-565.

FRITZ H., DALLMEYER R.D. and NEUBAUER F., 1996. Thick-skinned versus thin-skinned thrusting: Rheology controlled thrust propagation in the Variscan collisional belt (The Southeastern Bohemian Massif, Czech Republic - Austria). *Tectonics*, 15: 1389-1413.

FUCHS G., 1976. Zur Entwicklung der Böhmischen Masse. *Jahrbuch der Geologischen Bundesanstalt*, 119: 45-61.

GEBAUER D. and FRIEDL G., 1993. A 1.38 Ga protolith age for the Dobra orthogneiss (Moldanubian zone of the southern Bohemian massif, NE-Austria): evidence from ion-microprobe (SHRIMP) dating of zircon. *European Journal of Mineralogy*, 5:115.

GREEN D.H. and RINGWOOD A.E., 1967. The stability fields of aluminous pyroxene peridotite and garnet peridotite and their relevance in upper mantle structure. *Earth Planet Sci. Lett*., 3: 151-160.

HARTLEY A.J. and OTAVA J., 2001. Sediment provenance and dispersal in a deep marine foreland basin: the Lower Carboniferous Culm Basin, Czech Republic. *Journal of the Geological Society*, 158: 137-150.

KALVODA J., LEICHMANN J., BÁBEK O. and MELICHAR R., 2003. Brunovistulian Terrane (Central Europe) and Istanbul Zone (NW Turkey): Late Proterozoic and Paleozoic tectonostratigrapic development and paleogeography. *Geologica Carpathica*, 54: 139-152.

KRÖNER A., WENDT I., LIEW T.C., COMPSTON W., TODT W., FIALA J., VAŇKOVÁ V. and VANĚK J., 1988. U-Pb zircon and Sm-Nd model ages of high grade Moldanubian metasediments, Bohemian Massif, Czechoslovakia. *Contributions to Mineralogy and Petrology,* 99: 257-266.

KRÖNER A., O'BRIEN P.J., NEMCHIN A.A. and PIDGEON R.T., 2000. Zircon ages for high pressure granulites from South Bohemia, Czech Republic, and their connection to Carboniferous high temperature processes. *Contributions to Mineralogy and Petrology*, 138: 127-142.

LINNER M., 1996. Metamorphism and partial melting of paragneisses of the Monotonous Group, SE Moldanubicum (Austria). *Mineralogy and Petrology*, 58: 215-234.

MATTE P., 1986. Tectonic and plate tectonic model for the Variscan belt of Europe. *Tectonophysics,* 126: 329–374.

MIRWALD P.W. and MASSONNE H.-J., 1980. The low-high quartz and quartz-coesite transition to 40 kbar between 600 ° and 1600 °C and some reconnaissance data on the effect of $NaA1O_4$ component on the low quartz-coesite transition. *J. Geophys. Res*., 85: B12, 6983-6990.

NICKEL K.G. and GREEN D.H., 1985. Empirical geothermobarometry for garnet peridotites and implications for the nature of the lithosphere, kimberlites and diamonds. *Earth Planet. Sci. Lett*., 73: 158-170.

O'HARA M.J., RICHARDSON S.W. and WILSON G., 1971. Garnet peridotite stability and occurrence in crust and mantle. *Contrib. Mineral.Petrol.*, 32: 48-67.

PETRAKAKIS K., 1997. Evolution of Moldanubian rocks in Austria: review and synthesis. *Journal of Metamorphic Geology*, 15: 203–222.

RACEK M., ŠTÍPSKÁ P., PITRA P., SCHULMANN K. and LEXA O., 2006. Metamorphic record of burial and exhumation of orogenic lower and middle crust: new tectonothermal model for the Drosendorf window (Bohemian Massif, Austria). *Mineralogy and Petrology*, 86: 221–251.

RACEK M., ŠTÍPSKÁ P. and POWELL R., 2008. Garnet-clinopyroxene intermediate granulites in the St. Leonhard massif of the Bohemian Massif: ultrahigh-temperature metamorphism at high pressure or not? *Journal of Metamorphic Geology*, 26: 253-271.

SCHARBERT H.G. and KURAT G., 1974. Distribution of some elements between coexisting ferromagnesian minerals in Moldanubian Granulite Facies Rocks, Lower Austria, Austria. *Tsch. Mineral Petr. Mitt*., 21: 110-134.

SCHULMANN K., MELKA R., LOBKOWICZ M., LEDRU P., LARDEAUX J. M. and AUTRAN A., 1994. Contrasting Styles of Deformation During Progressive Nappe Stacking at the Southeastern Margin of the Bohemian Massif (Thaya Dome). *Journal of Structural Geology*, 16: 355-370.

SCHULMANN K., KRÖNER A., HEGNER E., WENDTI., KONOPÁSEK J., LEXA O. and ŠTÍPSKÁ P., 2005. Chronological constraints on the pre-orogenic history, burial and exhumation of deep- seated rocks along the eastern margin of the Variscan orogen, Bohemian Massif, Czech Republic. *American Journal of Science*, 305: 407–448.

SCHULMANN K., LEXA O., ŠTÍPSKÁ P., RACEK M., TAJČMANOVÁ L., KONOPÁSEK J., EDEL J.-B., PESCHLER A. and LEHMANN J., 2008. Vertical extrusion and horizontal channel flow of orogenic lower crust: key exhumation mechanisms in large hot orogens? *Journalof Metamorphic Geology*, 26: 273-297.

SUESS F.E., 1918. Bemerkungen zur neueren Literatur über die Moravischen Fenster. *Mitteilungen der Geologischen Geselschaft*, 11: 71-128.

SUESS F.E., 1926. Intrusionstektonik und Wandertektonik im variszischen Grundgebirge. *Bornträger*, Berlin, 268 pp.

ŠTÍPSKÁ P. and SCHULMANN K., 1995. Inverted metamorphic zonation in a basement-derived nappe sequence, eastern margin of the Bohemian Massif. *Geological Journal*, 30: 385-413.

ŠTÍPSKÁ P., SCHULMANN K. and HÖCK V., 2000. Complex metamorphic zonation of the Thaya dome: result of buckling and gravitational collapse of an imbricated nappe sequence. In: COSGROWE J.W. and AMEEN M.S. (Editors), Forced folds and fractures. Geological Society Special Publication, London, 197-211.

ŠTÍPSKÁ P., SCHULMANN K. and KRÖNER A., 2004. Vertical extrusion and middle crustal spreading of omphacite granulite: a model of syn-convergent exhumation (Bohemian Massif, Czech Republic). *Journal of Metamorphic Geology*, 22: 179–198.

ŠTÍPSKÁ P. and POWELL R., 2005a. Does ternary feldspar constrain the metamorphic conditions of high-grade meta-igneous rocks? Evidence from orthopyroxene granulites, Bohemian Massif. *Journal of Metamorphic Geology*, 23: 627-647.

ŠTÍPSKÁ P. and POWELL R., 2005b. Constraining the P–T path of a MORB-type eclogite using pseudosections, garnet zoning and garnet-clinopyroxene thermometry: an example from the Bohemian Massif. *Journal of Metamorphic Geology*, 23: 725–743.

THIELE O., 1976. Zur Tektonik des Waldviertels in Niederösterreich (südliche Böhmische Masse). *Nova Acta Leopoldina*, 45: 67-82.

THIELE O., 1984. Zum Deckenbau und Achsenplan des Moldanubikums der südlichen Böhmischen Masse (Österreich). *Jahrbuch der Geologischen Bundesanstalt*, 126: 513-523.

TOLLMANN A., 1982. Grossraumiger variszischer Deckenbau im Moldanubikum und neue Gedanken zum Variszikum Europas. *Geotekt. Forsch*., 64: 1–91.

The Mohelno and Nové Dvory Peridotites: Two Contrasting Types of Peridotite in the Gföhl Unit

L. Gordon MEDARIS, Jr.[1] and Emil JELÍNEK[2]

[1] Department of Geoscience, University of Wisconsin-Madison,1215 W. Dayton St., Madison, Wisconsin 53706, U.S.A.; medaris@geology.wisc.edu
[2] Institute of Geochemistry, Mineralogy and Mineral Resources, Charles University, Albertov 6, 128 43 Praha, Czech Republic

Peridotites in the Gföhl Unit

Peridotites in the Gföhl Unit display diverse characteristics and have been divided into three types, based on their lithologic associations, texture, mineralogy, elemental and isotopic chemical composition, P-T conditions, and calculated cooling rates (Medaris et al., 1990; Medaris et al., 2005; Ackerman et al., 2009). Type I, *e.g.* the Mohelno peridotite, is surrounded by granulite, consists predominantly of Mg-Cr spinel peridotite, and is devoid of eclogite lenses. Garnet, which commonly contains inclusions of spinel, occurs only in the deformed and recrystallized margins of the peridotite body or in closely associated peridotite boudins in granulite. Type II has been identified in the Horní Bory quarry and is represented by a group of Mg-Cr to Fe-Ti spinel-garnet peridotite boudins that are associated with abundant garnet pyroxenite, all of which are hosted by felsic granulite. Type III, *e.g.* the Nové Dvory peridotite, is surrounded by migmatitic gneiss, consists solely of Mg-Cr garnet peridotite, and contains prominent lenses of eclogite.

The Mohelno and Nové Dvory Peridotites

Locations and Field Characteristics

The Mohelno and Nové Dvory peridotites are located in South Moravia approximately 32 km NWN of Znojmo (Fig. 1). The Mohelno peridotite, which is the archetype for Gföhl Type I peridotite, is a folded tabular body, ~300 m thick and 4 km long, that has concordant contacts with the surrounding Náměšť granulite, with which it shares in part a common structural and metamorphic history. Serpentinized spinel peridotiteconstitutes the bulk of the Mohelno body, and garnet peridotite occurs only within a few meters of contacts with granulite, where penetrative deformation has promoted recrystallization during the Variscan Orogen. The Biskoupky peridotite (Fig. 1), which lies ~3 km east of the Mohelno peridotite, exhibits the same characteristics as those of the Mohelno body and is correlative with it.

In contrast to Mohelno, the Nové Dvory peridotite (Fig. 1), which is the archetype for Gföhl Type III peridotite, is allochthonous and allofacial with respect to surrounding migmatitic orthogneiss. The ~1 × 2.5 km body consists largely of serpentinized garnet peridotite, which contains prominent lenses of eclogite, up to 15 meters thick.

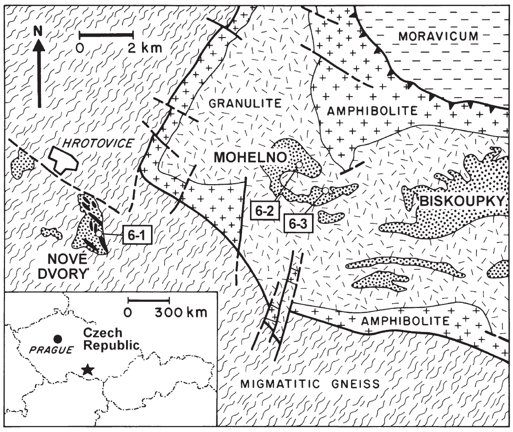

■ **Fig. 1.** Simplified geological map of the Mohelno and Nové Dvory peridotites and surrounding area. Peridotite bodies are indicated by the stipple pattern, and eclogite lenses in the Nové Dvory peridotite are in black. Excursion localities are indicated by numbers: 6-1, Nové Dvory garnet peridotite and eclogite; 6-2, Mohelno spinel peridotite; 6-3: Mohelno garnet peridotite. Locality of the map area is shown by a star in the inset.

Geochemistry

Like many other Mg-Cr mantle peridotites, the Mohelno and Nové Dvory peridotites show a decrease in concentrations of incompatible major elements, such as Al_2O_3 and CaO, with an increase in MgO (Fig. 2). Such compositional variations are commonly ascribed to partial fusion of mantle peridotite and removal of incompatible elements from the residuum by melt extraction. In the Mohelno body, garnet peridotite (MgO $\simeq$ 37.5–39 wt%) is less depleted than spinel peridotite (MgO $\simeq$ 39–43 wt%) , perhaps reflecting some degree of interaction with felsic granulite, with which it is in close proximity. For a given level of MgO, the Nové Dvory peridotite contains lower concentrations of Al_2O_3 and CaO, compared to the Mohelno body (Fig. 2). In addition, three samples of Nové Dvory peridotite contain less MgO (~34.5–36.4 wt%) than does primitive mantle, which may be due to metasomatism by transient melts, from which eclogite and pyroxenite crystallized (Medaris et al., 1995).

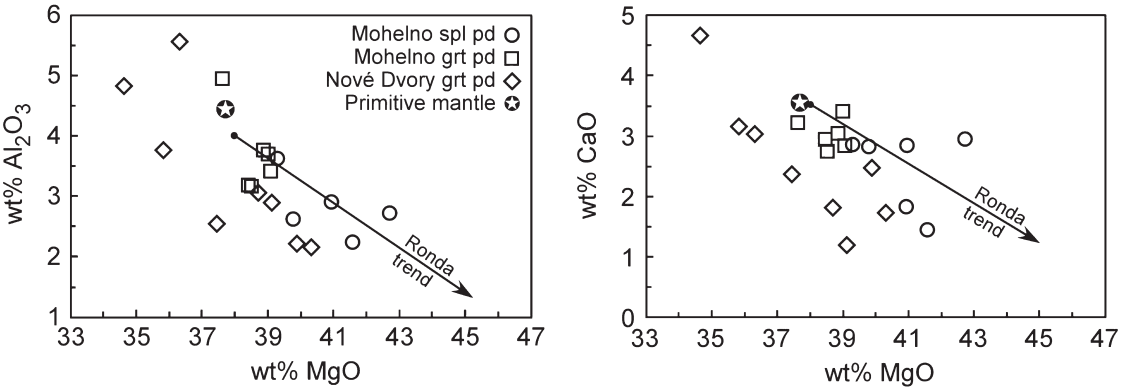

■ **Fig. 2.** Variation in wt. % Al_2O_3 and CaO relative to MgO in the Mohelno and Nové Dvory peridotites. Shown for comparison are the composition of primitive mantle (McDonough and Sun, 1995) and the variation trend for the Ronda peridotite (Frey et al., 1985).

The Mohelno and Nové Dvory peridotites are both depleted in REE, containing less than 1.0 to as little as 0.1 times that in primitive mantle. However, the two peridotites show contrasting REE patterns, with the Mohelno peridotite being consistently light-REE depleted and the Nové Dvory peridotite varying from light-REE depleted to light-REE enriched (Fig. 3). The Mohelno garnet peridotite is not as strongly light-REE depleted as spinel peridotite; again, possibly reflecting interaction with nearby felsic granulite.

With respect to Nd and Sr isotopes, clinopyroxene from the Mohelno and Nové Dvory peridotites falls into two domains (Fig. 4). Clinopyroxene from the Mohelno body and similar peridotites in Austria (Becker, 1997; Medaris, 1999) has ε_{Nd} values of +9.2 to +11.0 (at 335 Ma), which are higher than that for Depleted MORB Mantle (DMM), and relatively low values of $(^{87}Sr/^{86}Sr)_i$, 0.7024 to 0.7032. Clinopyroxene in the Nové Dvory peridotite and similar peridotites in Austria has slightly higher values of $(^{87}Sr/^{86}Sr)_i$, 0.7033 to 0.7034, and lower ε_{Nd} values, +4.1 to +6.6. When the isotopic compositions of clinopyroxene from pyroxenite and eclogite lenses in Nové Dvory-type peridotites are included (Fig. 4; Medaris et al., 2006a), the field for isotopic covariation is seen to be convex downward, with compositions of peridotite clinopyroxene plotting near the top of the pyroxenite and eclogite field. Such a covariation trend has been successfully modelled by mixing between mantle peridotite and oceanic clay (Medaris et al., 1995).

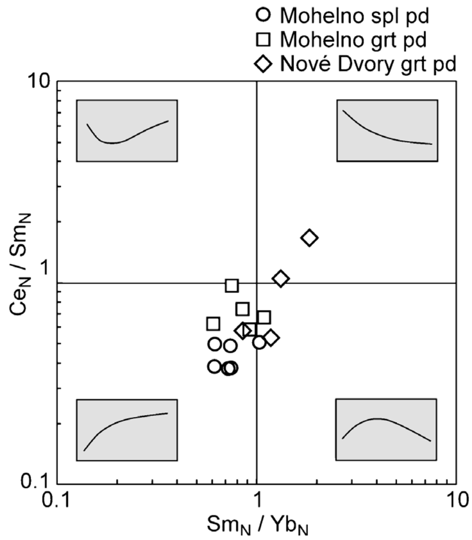

■ **Fig. 3.** Ratios of (Ce/Sm) *vs*. (Sm/Yb) for the Mohelno and Nové Dvory peridotites, normalized to primitive mantle (McDonough and Sun, 1995).

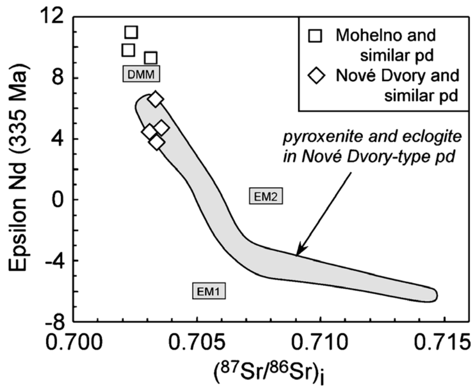

■ **Fig. 4.** Variation in ε_{Nd} and $[^{87}Sr/^{86}Sr]_i$ (at 335 Ma) for clinopyroxene in the Mohelno and Nové Dvory peridotites. The field is for clinopyroxene in garnet pyroxenite and eclogite from Nové Dvory-type peridotite. Abbreviations: DMM, depleted MORB mantle; EM1, enriched mantle 1; EM2, enriched mantle 2 (Hart 1988).

Mineralogy

Minerals in the Mohelno and Nové Dvory peridotites consist of variable proportions of forsterite, pyrope-rich garnet, enstatite, chrome diopside, and $MgAl_2O_4$-rich spinel, reflecting the magnesian composition of their host rocks.

The Mohelno peridotite contains a sequence of four different mineral assemblages (neglecting late-stage serpentinization), whose schematic P-T relations are shown in Figure 5, which is a projection from forsterite and H_2O onto the plane, spl-opx-cpx, in the CMASH system. Assemblage M1, ol+spl+opx+cpx, is the predominant mineral assemblage in the interior and bulk of the peridotite. Assemblage M2, ol+grt+opx+cpx, occurs only within a few meters of the contact with felsic granulite, and spinel inclusions in garnet demonstrate that Assemblage 2 formed later than Assemblage 1. Assemblage 3, spl+opx+cpx, and Assemblage 4, spl+opx+am, occur in kelyphite around garnet, where fine-grained minerals of Assemblage 3 constitute the kelphite rims, and very fine-grained, symplectitic intergrowths of Assemblage 4 minerals are confined to the kelyphite interiors.

In contrast to Mohelno, the Nové Dvory peridotite contains only two mineral assemblages (again, neglecting late-stage serpentinization). The bulk of the body consists of assemblage ND1 (Fig. 5), ol+grt+opx+cpx, followed by assemblage ND2, spl+opx+am, which occurs locally as thin, very fine-grained kelephite rims on garnet.

Additional mineralogical distinctions between the Mohelno and Nové Dvory peridotites are seen in their pyroxene compositions (Fig. 6). Mohelno clinopyroxene and orthopyroxene are both highly aluminous, which is characteristic for pyroxenes in high-temperature and moderate- to low-pressure peridotites. Note however, that orthopyroxene in equilibrium with garnet (assemblage M2) is slightly less aluminous and chromiferous than orthopyroxene in equilibrium with spinel (assemblage M1). In contrast, Al_2O_3 contents and Al_2O_3/Cr_2O_3 ratios are much lower in pyroxenes in the Nové Dvory peridotite (assemblage ND1), which was derived from a different mantle source and equilibrated under different conditions (mainly higher pressure) than those of the Mohelno body.

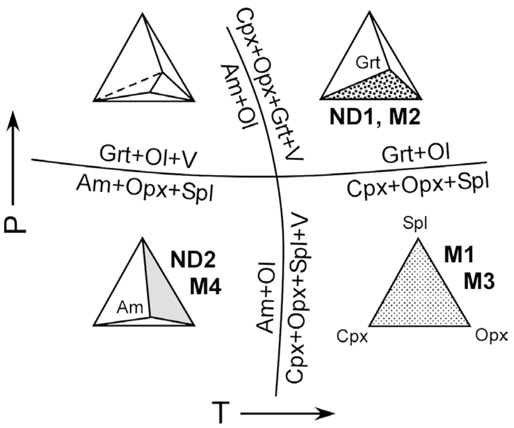

■ **Fig. 5.** Schematic P-T grid for mineral assemblages in the system, CMASH, projected from forsterite and H_2O on to the plane, $MgAl_2O_4$ - $CaMgSi_2O_6$ - $Mg_2Si_2O_6$. Successive mineral assemblages in the Mohelno (M) and Nové Dvory (ND) peridotites are numbered and indicated by different patterns.

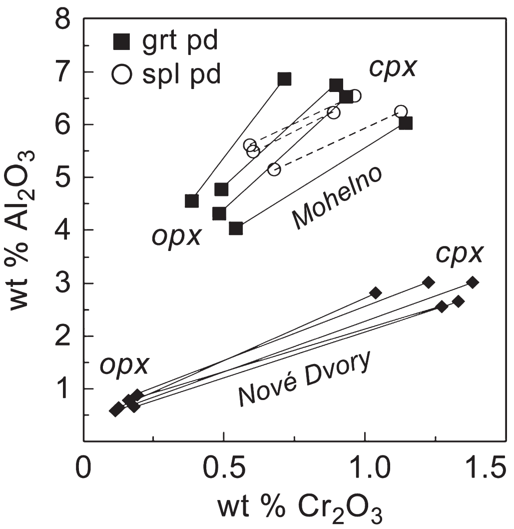

■ **Fig. 6.** Al_2O_3 and Cr_2O_3 contents of coexisting clinopyroxene and orthopyroxene in the Mohelno spinel and garnet peridotites, compared to those in the Nové Dvory garnet peridotite.

Pressure-Temperature Estimates and History

The P-T equilibration conditions for garnet-bearing assemblages in the Mohelno and Nové Dvory peridotites (assemblages M2 and ND1, respectively) are best estimated by a combination of the Fe-Mg exchange geothermometer for olivine and garnet and the Al-in-orthopyroxene geobarometer . Previously, Medaris et al. (2005) made such estimates by applying calibrations of the olivine-garnet geothermometer by O'Neill and Wood (1979) and O'Neill (1981) and the Al-in-orthopyroxene geobarometer by Brey and Köhler (1990). Results from these previous P-T estimates are shown in Figure 7, where they are compared with newer estimates based on the Wu and Zhao (2007) calibration of the olivine-garnet geothermometer and the Brey, Bulatov and Girnis (2008) calibration of the Al-in-orthopyroxene geobarometer. Compared to the previous P-T results, the newer temperature estimates are significantly lower for the Mohelno samples and slightly higher for the Nové Dvory samples. However, regardless of the specific P-T values obtained from the different calibrations, the Mohelno and Nové Dvory samples still define two contrasting field gradients, i.e., a relatively low P/T array for Mohelno and a relatively high P/T array for Nové Dvory, which extends into the stability field for majoritic garnet.

Cooling rates for garnet peridotite have been calculated by solution of the diffusion equation for compositional zoning in garnet adjacent to olivine inclusions (Medaris et al., 2005; Fig. 8). Bilinear cooling rates are required to achieve acceptable fits between the calculated and measured compositional profile, i.e. to match both the core and rim compositions of the zoned garnet grains. For Mohelno, an extremely rapid initial cooling rate, 5000 °C/m.y., is necessary to preserve the garnet core composition, and slower second stage rates, 1–50 °C/m.y., are required to attain the garnet rim composition. The initial cooling rate may reflect tectonic juxtaposition of hot peridotite and cooler granulite, rather than cooling related to exhumation of the terrane. However, the second stage cooling rates (1 to 50 °C/m.y.) are consistent with those expected during exhumation, and they are comparable to, but slightly slower than, those obtained in the Kutná Hora Complex from eclogite garnet zoning (~100 °C/m.y.) and stratigraphic constraints (100–150 °C/m.y.; Medaris et al., 2006b). Compositional zoning in Nové Dvory garnet has a smaller amplitude and longer decay distance than that in Mohelno garnet, thus yielding a slower initial cooling rate of 10 °C/m.y. and a second stage rate of 0.5 °C/m.y.. Such different model cooling rates for the Mohelno and Nové Dvory peridotites further emphasize the distinction between these two types of Czech peridotite.

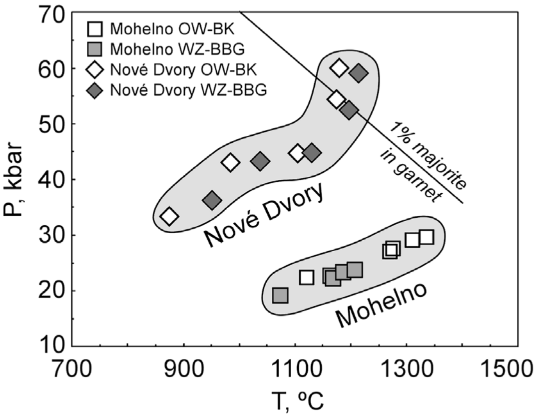

■ **Fig. 7.** Pressure-temperature estimates for the Mohelno and Nové Dvory garnet peridotites, based on the Al-in-orthopyroxene goebarometer (BK, Brey and Köhler, 1990; BBG, Brey, Bulatov and Girnis, 2008) and the olivine-garnet Fe-Mg exchange geothermometer (OW, O'Neill and Wood, 1979; O'Neill, 1980; WZ, Wu and Zhao, 2007).

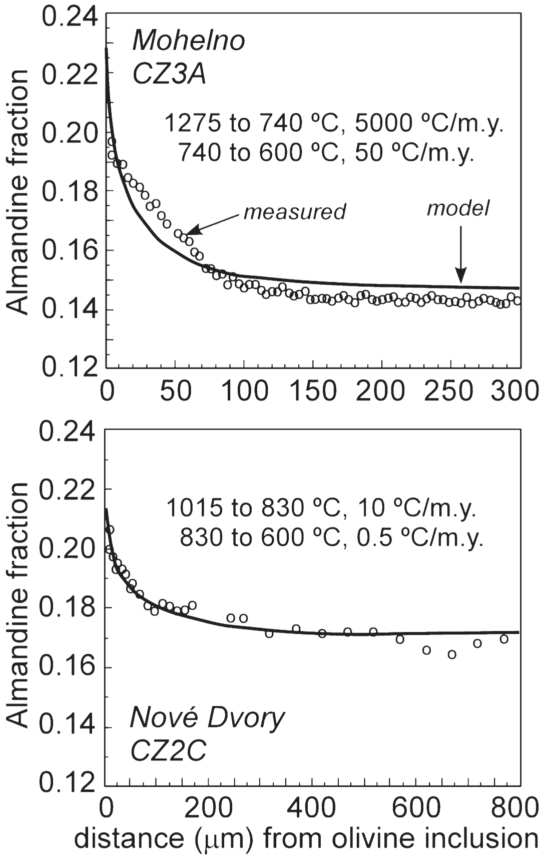

■ **Fig. 8.** Variation of almandine contents in garnet grains adjacent to olivine inclusions in two samples of garnet peridotite: Mohelno, sample CZ3A, and Nové Dvory, sample CZ2C. Symbols, measured compositions; solid curves, compositional profiles calculated from diffusion modelling. Bilinear cooling rate estimates are given in the insets.

The P-T histories for the Mohelno and Nové Dvory peridotites are summarized in Figure 9. For Mohelno, Stage 1 (assemblage M1, ol+spl+opx+cpx) represents the inferred origin of the peridotites as residua from partial melting of mantle in the spinel stability field. The interior of the peridotite body escaped penetrative deformation during Variscan HP metamorphism, resulting in metastable preservation of assemblage M1, except for intracrystalline re-equilibration and exsolution during cooling. Deformation along the margin of the peridotite promoted recrystallization and development of the garnetiferous assemblage M2 (ol+grt+opx+cpx) in response to Stage 2 Variscan metamorphism at high temperatures and pressures at ~20–25 kbar. Continued deformation and influx of H_2O along the margins of the peridotite promoted development of the Stage 3 (assemblage M3, spl-opx-cpx) and Stage 4 (assemblage M4, spl-opx-am) kelyphites during cooling and exhumation, which can be correlated with retrograde stages in the associated Náměšť granulite.

The bulk of the Nové Dvory peridotite consists of assemblage ND1 (ol+grt+opx+cpx), which yields P-T conditions of ~34–60 kbar, 850–1150 °C (Fig. 9). Such high pressures are consistent with calculated pressures of ~34–47 kbar for garnet websterite, orthopyroxene eclogite, and kyanite eclogite, which occur as lenses in the peridotite (Medaris et al., 2006a; Nakamura et al., 2004). The thin kelyphite rims on garnet, assemblage ND2 (spl+opx+am), represent a limited stage of partial recrystallization at ~8 kbar, 700 °C.

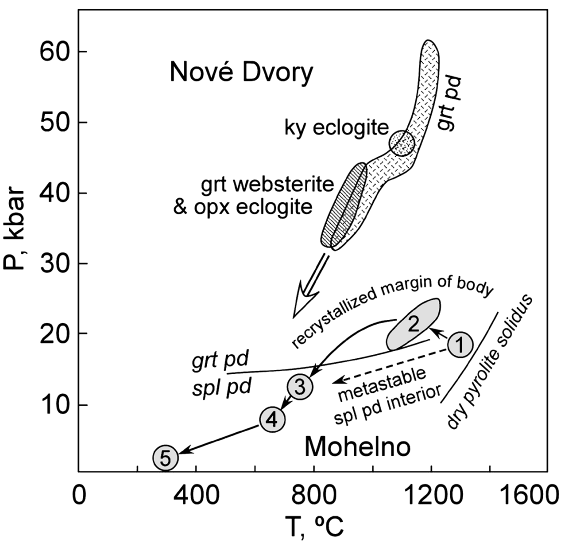

■ **Fig. 9.** Proposed P-T histories for the Mohelno and Nové peridotites. Numbers for the Mohelno body correspond to the mineral assemblages shown in Fig. 5, except for stage 5, which indicates late-stage serpentinization. Stage 1 represents the inferred conditions of origin as the residuum from partial melting of primitive mantle in the spinel stability field. The field for Nové Dvory garnet peridotite includes the range of P-T estimates for assemblage ND1, to which are compared P-T estimates for associated garnet websterite, orthopyroxene eclogite, and kyanite eclogite.

Tectonometamorphic Scenario

Based on elemental and isotopic compositions and P-T conditions, the Mohelno peridotite is interpreted as suboceanic lithospheric and, possibly, asthenospheric mantle, and the Nové Dvory peridotite most likely represents subcontinental lithospheric mantle (Medaris et al., 2005). It was proposed that the Mohelno peridotite originated in Devonian (Frasnian) time in a small ocean basin between Bohemia (Tepla-Barrandia) and Moldanubia (northern Gondwana). With Carboniferous (Tournaisian) closure of the ocean basin and collision of Bohemia and Moldanubia, imbrication of lithospheric/asthenospheric mantle, oceanic crust, and continental crust may have occurred in the vicinity of a subducted spreading center, giving rise to the lithologic association of the Gföhl Nappe and elevating temperatures in the crustal rocks. Further Carboniferous (Viséan) subduction produced the high pressure assemblages in ultramafic (garnet peridotite), mafic (eclogite), and felsic (HP granulite) rocks. Subduction-related melts penetrated the overlying mantle wedge, producing lenses of garnet pyroxenite and eclogite in the Nové Dvory peridotite. Slab breakoff then released the subducted Moldanubian terrane and locally attached fragments of mantle wedge, allowing rapid exhumation and cooling, during which the HP rocks were retrograded to varying degrees over a range of decreasing temperatures and pressures.

Alternatively, the Mohelno peridotite and associated lithologies may have originated in a Devonian back-arc basin between Saxothuringia and Tepla-Barrandia, which was subsequently subducted beneath Tepla-Barrandia (Schulmann et al., 2005; Dörr and Zulauf, 2010). Carboniferous closure of the thermally weakened back-arc basin, due to convergence and eventual collision of Brunia, led to crustal thickening and high-pressure and high-temperature metamorphism in deeper crustal levels, which was followed by orogenic collapse and delamination of mantle lithosphere, leading to rapid exhumation during transpression or elevator tectonics.

Sm-Nd mineral isochrons for nine samples of peridotite-hosted pyroxenite and eclogite in the Gföhl Unit yield a Viséan mean age of 336 ±7 Ma (Medaris et al., 2006a). So, in either tectonometamorphic scenario, exhumation following high-temperature and high-pressure metamorphism must have been rapid, as demonstrated by the presence of Gföhl detritus in Viséan sediments of the Culm foreland basin (Hartley and Otava, 2001).

Stop 6-1 (Day 6). Nové Dvory Garnet Peridotite and Eclogite, ~400 m SW of the Nové Dvory Farmhouse, 2 km WNW of the Town of Rouchovany

Coordinates: N49°04′36.4″ E16°04′56.6″)

This locality is in the southeastern part of the Nové Dvory body, where a low ridge is supported by a large eclogite layer (Fig. 1). Garnet peridotite is exposed along the dirt track leading to the ridge and in outcrop at the western end of the ridge; eclogite is exposed along the top of the ridge and in fallen blocks at the base of the ridge.

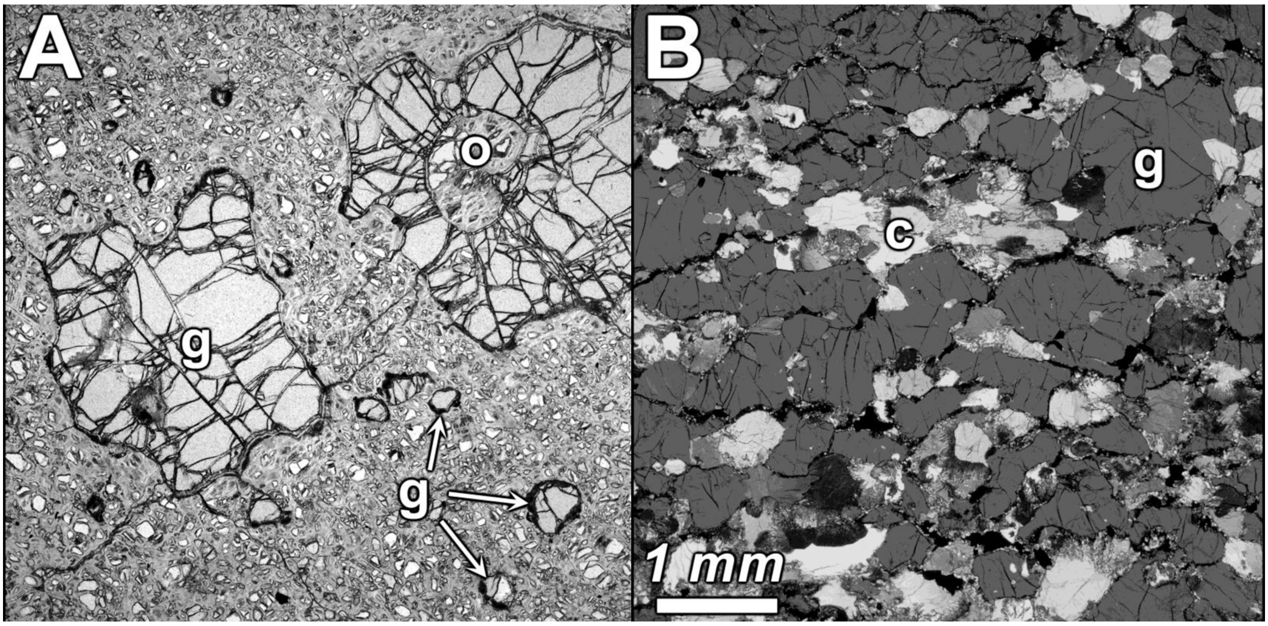

■ **Fig. 10.** Photomicrographs of Nové Dvory samples; the scale in each panel is the same. A. Inequigranular garnet peridotite; plane polarized light. Note the two grain size populations of garnet. B. Medium-grained, granoblastic eclogite; partly crossed polarizers. Abbreviations: c, clinopyroxene; g, garnet; o, olivine.

Garnet peridotite (assemblage ND1) has an inequigranular texture, in which large, irregular garnet grains (≤7 mm) are set in a fine-grained matrix (0.5–1.0 mm) of equant olivine, orthopyroxene, clinopyroxene, and garnet (Fig. 10A). Except for extensive serpentinization, post-garnet recrystallization is limited, consisting of thin kelyphite rims of fibrous spinel and amphibole around garnet (assemblage ND2, visible as dark fringes around garnet in Fig. 10A). Mg #'s are 90.3–91.1 for olivine, 91.0–91.4 for orthopyroxene, 90.0–91.1 for clinopyroxene, and garnet contains 69.9–72.9 mol% pyrope. Pyroxenes are much less aluminous than those in the Mohelno peridotite (Fig. 6), due to equibration with garnet at significantly higher pressures.

Eclogite typically has a medium-grained, granoblastic, slightly foliated texture (Fig. 10B), and some samples display prominent layering of garnet and clinopyroxene (see Fig. 2 in Medaris *et al*., 2006a), which is parallel to foliation in the surrounding peridotite. The most common assemblage in eclogite is garnet, clinopyroxene and accessory rutile, although some samples also contain orthopyroxene or kyanite. Garnet is intermediate in composition, varying among samples from $Prp_{55}Alm+Sps_{20}Grs_{25}$ to $Prp_{30}Alm+Sps_{40}Grs_{30}$, and clinopyroxene has a wide range in jadeite content, 10-50 mol%. P-T estimates for orthopyroxene eclogite, garnet websterite, and kyanite eclogite range from ~30 kbar, 800 °C to 47 kbar, 1100 °C (Nakamura et al. 2004; Medaris et al., 2006a), which lie within the field gradient defined by Nové Dvory garnet peridotite (Fig. 9).

Eclogite and garnet pyroxenite layers in the Nové Dvory and similar peridotite bodies have a wide range in elemental (major and trace) and isotopic (Nd, Sr, and O) compositions. Based on geochemical modelling, Medaris et al. (1995) demonstrated that such variation could be explained by high-pressure crystal accumulation (± trapped melt) from transient melts in a mantle wedge above a subduction zone, with a component of such melts being subducted, hydrothermally altered oceanic crust. In contrast, Obata et al. (2006) suggested that kyanite eclogite in the Nové Dvory body represents oceanic crust (cumulus gabbro) that was subducted, transformed to eclogite, and tectonically juxtaposed with garnet peridotite.

Stop 6-2 (Day 6). Mohelno Spinel Peridotite, Outcrop along the North Bank of the Jihlava River, ~870 m Upstream from the Highway 392 Bridge

Coordinates: N49°06′21.0″ E16°11′12.9″

This outcrop is representative of spinel peridotite that constitutes the interior and bulk of the Mohelno body. Although not visited during the excursion, note that the large Biskoupky peridotite to the east (Fig. 1) is a companion to the Mohelno peridotite and shares all the same characteristics.

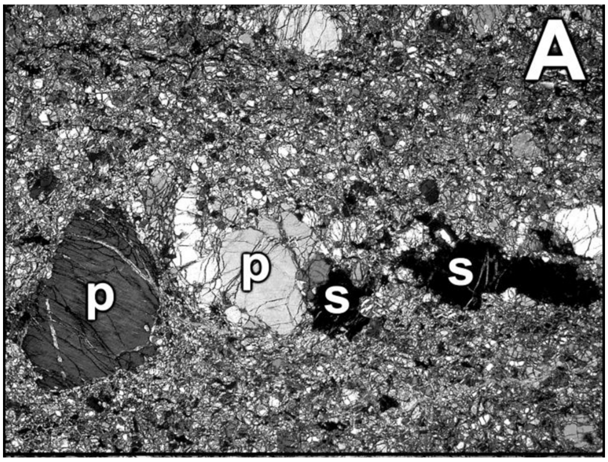

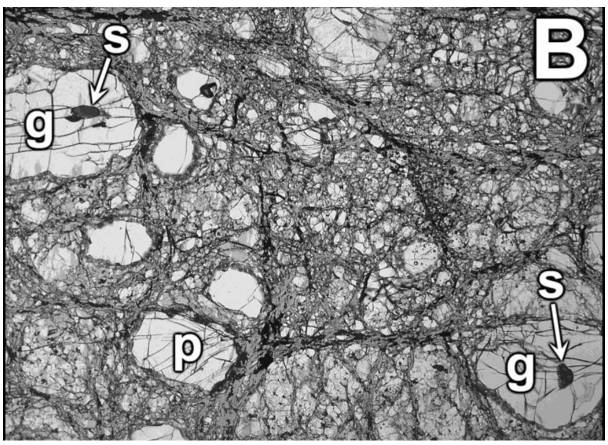

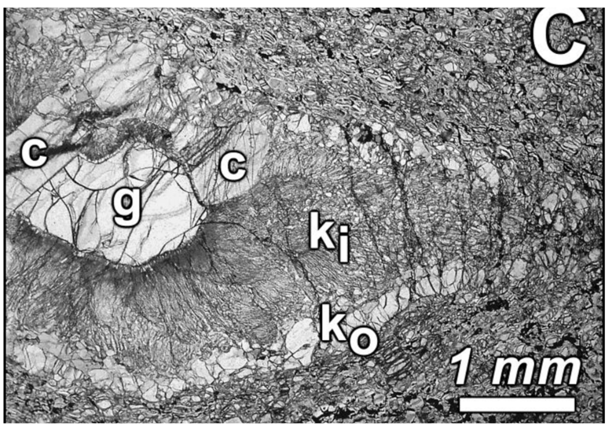

■ **Fig. 11.** Photomicrographs of Mohelno peridotite samples; the scale in each panel is the same. A. Porphyroclastic spinel peridotite; crossed polarizers. B. Porphyroclastic garnet peridotite; note spinel inclusions in garnet; plane polarized light. C. Garnet surrounded by an outer, fine-grained kelyphite (assemblage M3, spl+opx+cpx) and an inner, symplectitic kelyphite (assemblage M4, spl+opx+amp); plane polarized light. Abbreviations: c, clinopyroxene; g, garnet; k_i, inner kelyphite; k_o, outer kelyphite; p, orthopyroxene; s, spinel.

Peridotite at this locality contains a porphyroclastic M1 mineral assemblage (ol+spl+opx+cpx), in which medium- to coarse-grained pyroxene and spinel porphyroclasts reside in a fine-grained, recrystallized matrix (Fig. 11A). The peridotite exhibits a pronounced foliation, parallel to which are several cm-scale spinel pyroxenite layers and lenses. The crystal-preferred orientation (CPO) of olivine in coarse-grained spinel peridotite shows a strong concentration of [100] subparallel to mineral lineation, with [010] and [001] girdles normal to lineation, reflecting an {0kl}[100] deformation mechanism (Kamei et al., 2010).

Minerals in the M1 assemblage are magnesian, with the following Mg #'s [100× Mg/(Mg+Fe)]: olivine, 88-91; orthopyroxene, 89-91; clinopyroxene, 90-94; and spinel, 72-77. The pyroxenes are Cr-bearing and relatively aluminous, containing >5 wt% Al_2O_3 (Fig. 6). Spinel is also aluminous, being similar in composition to disseminated spinel in abyssal peridotites, with Cr #'s [100×Cr/(Cr+Al)] ranging from 13 to 19. Based on the host compositions of exsolved pyroxene porphyroclasts, samples of spinel peridotite yield *minimum* temperatures of ~1100 ºC (two-pyroxene geothermometry, Taylor, 1998; Al-in-orthopyroxene geothermometry, Witt-Eickschen and Seck 1991), and based on the compositions of spinel, *maximum* pressures of ~21-22 kbar (O'Neill, 1981).

Stop 6-3 (Day 6). Mohelno Garnet Peridotite, Outcrop along the North Bank of the Jihlava River, ~130 m Downstream from the Highway 392 Bridge

Coordinates: N49°05′55.4″ E16°11′48.9″

Illustrated at this locality is the M2 mineral assemblage (ol+grt+opx+cpx), which has an inequigranular texture with large spheroidal grains of garnet and pyroxene (up to 7 mm) set in a fine-grained matrix of olivine, pyroxene, and spinel (0.2–0.5 mm). An important feature is the common occurrence of spinel inclusions in garnet (Fig. 11B). Typically, garnet is separated from olivine by a compound kelyphite, consisting of the M3 assemblage (spl+opx+cpx) in an outer zone and the M4 assemblage (spl+opx+am) in a fibrous, inner zone (Fig. 11C).

In contrast to the olivine fabric in spinel peridotite, the CPO of olivine in garnet peridotite shows a strong concentration of [010] normal to foliation and a concentration of [100] parallel to the lineation (Kamei et al., 2010), which is ascribed to an (010)[100] deformation mechanism.

As in the M1 assemblage, minerals in the M2 assemblage are magnesian, including garnet, which contains 82.5–84.3 mol% pyrope. M2 orthopyroxene contains less Al_2O_3 than that in spinel peridotite (Fig. 6), due to its coexistence with garnet. Spinel inclusions in garnet have higher Cr #'s (27-33) than does M1 spinel (13-19), due to re-equilibation and reaction of spinel with garnet at higher pressures. The lowest Cr #'s in spinel (3-9) are found in M3 and M4 spinel in kelyphite, where spinel formed through the reaction, ol+grt=spl+opx+cpx.

It should be emphasized that garnet (the M2 mineral assemblage) only occurs at the margin of the Mohelno and Biskoupky peridotite bodies, within a few meters of the contact with surrounding felsic granulite. We suggest that the entire Mohelno and Biskoupky bodies were subjected to elevated pressures (~20–25 kbar) during subduction of oceanic lithosphere, but that the garnet-bearing M2 assemblage only developed along the margins of the bodies, where recrystallization was promoted by deformation.

References

ACKERMAN L., JELÍNEK E., MEDARIS L.G.Jr., JEŽEK J., SIEBEL W. and STRNAD L., 2009. Geochemistry of Fe-rich peridotites and associated pyroxenites from Horní Bory, Bohemian Massif: Insights into subduction-related melt-rock reactions. *Chemical Geology*, 259: 152-167.

ALTHERR R. and KALT A., 1996. Metamorphic evolution of ultrahigh-pressure garnet peridotites from the Variscan Vosges Mts. (France). *Chemical Geology*, 134: 27-47.

BEARD B.L., MEDARIS L.G.Jr., JOHNSON C.M., JELÍNEK E., TONIKA J. and RICIPUTI L.R., 1995. Geochronology and geochemistry of eclogites from the Mariánské Lázně Complex, Czech Republic : Implication for Variscan orogenesis. *Geologische Rundschau*, 84: 552-567.

BECKER H., 1997. Sm-Nd garnet ages and cooling history of high-temperature garnet peridotite massifs and high-pressure granulites from lowerr Austria. *Contributions to Mineralogy and Petrology,* 127: 224-236.

BREY G.P. and KÖHLER T., 1990. Geothermobarometry in four-phase lherzolites II. New thermobarometers, and practical assessment of existing thermobarometers. *Journal of Petrology*, 31: 1352-1378.

BREY G.P., BULATOV V.K. and GIRNIS V., 2008. Geobarometry for peridotites: experiments in simple and natural systems from 6 to 10 GPa. *Journal of Petrology*, 49: 3-24.

CHÁB J., 1973. An ancient oceanic crust and upper mantle on the recent land surface. *Věst Ústř Úst Geol.,* 48: 303-310 (In Czech).

DÖRR W. and ZULAUF G., 2010. Elevator tectonics and orogenic collapse of a Tibetan-style plateau in the European Variscides: the role of the Bohemian shear zone. *International Journal of Earth Sciences*, 99: 299-325.

FREY F.A., SUEN C.J. and STOCKMAN H. W., 1985. The Ronda high temperature peridotite: geochemistry and petrogenesis. *Geochimica et Cosmochimica Acta*, 49: 2469-2491.

GARDIEN V., TEGYET M., LARDEAUX J.M., MISSERI M. and DUFOUR E., 1990. Crust-mantle relationships in the French Variscan chain: the example of the Southern Monts du Lyonnais unit (eastern French Massif Central). *Journal of metamorphic Geology*, 8: 477-492.

HARTE S.R., 1988. Heterogeneous mantle domains: signatures, genesis and mixing chronologies. *Earth and Planetary Science Letters*, 90: 273-296.

HARTLEY A.J. and OTAVA J., 2001. Sediment provenance and dispersal in a deep marine foreland basin: the Lower Carboniferous Culm Basin, Czech Republic. *Journal of the Geological Society London*, 158: 137-150.

HÖCK V., PETRAKAKIS K. and RICHTER W., 1997. Metamorphic evolution of the Southeastern Bohemian Massif. *Mineralogy and Petrology*, 60: 267-287.

JELÍNEK E., PAČESOVÁ M., MÍSAŘ Z., MARTINEC P. and WEISS Z., 1984. Geochemistry of a dismembered metaophiolite complex, Letovice, Czechoslovakia. *Transactions of the Royal Society of Edinburgh, Earth Sciences*, 75: 37-48.

JELÍNEK E., ŠTĚDRÁ V. and CHÁB J., 1997. The Mariánské Lázně complex. In: S. VRÁNA and V. ŠTĚDRÁ (Editors), Geological model of Western Bohemia related to the KTB borehole in Germany. pp. 61-70, Czech Geological Survey, Prague.

KALT A. and ALTHERR R., 1996. Metamorphic evolution of garnet-spinel peridotites from the Variscan Schwarzwald (F.R.G.). *Geologische Rundschau*, 85: 211-224.

KALT A., ALTHERR R. and HANEL M., 1995. Contrasting P-T conditions recorded in ultramafic high-pressure rocks from the Variscan Schwarzwald (F.R.G.). *Contributions to Mineralogy and Petrology*, 121: 45-60.

KAMAEI A., OBATA M., MICHIBAYASHI K., HIRAJIMA T. and SVOJTKA M., 2010. Two contrasting fabric patterns of olivine observed in garnet and spinel peridotite from a mantle-derived ultramafic mass enclosed in felsic granulite, the Moldanubian Zone, Czech Republic. *Journal of Petrology*, 51: 101-123.

KASTL E. and TONIKA J., 1984. The Mariánské Lázně metaophiolitic complex (west Bohemia). *Krystalinikum*, 17: 59-76.

LASNIER B., 1971. Les peridotites et pyroxenolites a grenat du Bois des Feuilles (Monts du Lyonnais) (France). *Contributions to Mineralogy and Petrology*, 34: 29-42.

MACHART J., 1984. Ultramafic rocks in the Bohemian part of the Moldanubicum and central Bohemian islet zone (Bohemian massif). *Krystalinikum*, 17: 13-32.

McDONOUGH W.F. and SUN S., 1995. The composition of the Earth. *Chemical Geology*, 120:223-253.

MEDARIS L.G.Jr., 1999. Garnet peridotites in Eurasian high-pressure and ultrahigh-pressure terranes: a diversity of origins and thermal histories. *International Geology Review*, 41: 799-815.

MEDARIS L.G.Jr., WANG H.F., MÍSAŘ Z. and JELÍNEK E., 1990. Thermobarometry, diffusion modelling and cooling rates of crustal garnet peridotites: Two examples from the Moldanubian zone of the Bohemian Massif. *Lithos*, 25: 189-202.

MEDARIS L.G.Jr., BEARD B.L., JOHNSON C.M., VALLEY J.W., SPICUZZA M.J., JELÍNEK E. and MÍSAŘ Z., 1995. Garnet pyroxenite and eclogite in the Bohemian Massif: geochemical evidence for Variscan recycling of subducted lithosphere. *Geologische Rundschau*, 84: 489-505.

MEDARIS L.G.Jr., WANG H., JELÍNEK E., MIHALJEVIČ M. and JAKEŠ P., 2005. Characteristics and origins of diverse Variscan peridotites in the Gföhl Nappe, Bohemian Massif, Czech Republic. *Lithos*, 82:1-23.

MEDARIS L.G.Jr., BEARD B.L. and JELÍNEK E., 2006a. Mantle-derived, UHP garnet pyroxenite and eclogite in the Moldanubian Gföhl Nappe, Bohemian Massif: A geochemical review, new P-T determinations and tectonic interpretation. *International Geology Review*, 48: 765-777.

MEDARIS L.G.Jr., GHENT E.D., WANG H.F., FOURNELLE J.H. and JELÍNEK E., 2006b. The Spačice eclogite: constraints on the P-T-t history of the Gföhl granulite terrane, Moldanubian Zone, Bohemian Massif. *Mineralogy and Petrology*, 86: 203-220.

NAKAMURA D., SVOJTKA M., NAEMURA K. and HIRAJIMA T., 2004. Very high-pressure (>4 GPa) eclogite associated with the Moldanubian Zone garnet peridotite (Nové Dvory, Czech Republic). *Journal of metamorphic Geology*, 22: 593-603.

OBATA M., HIRAJIMA T. and SVOJTKA M., 2006. Origin of eclogite and garnet pyroxenite from the Moldanubian Zone of the Bohemian Massif, Czech Republic and its implication to other mafic layers embedded in orogenic peridotites. *Mineralogy and Petrology*, 88: 321-340.

O'NEILL H.StC., 1980. An experimental study of Fe-Mg partitioning between garnet and olivine and its calibration as a geothermometer: corrections. *Contributions to Mineralogy and Petrology*, 72: 337.

O'NEILL H.StC., 1981. The transition between spinel lherzolite and garnet lherzolite, and its use as a geobarometer. *Contributions to Mineralogy and Petrology*, 77: 185-194.

O'NEILL H.StC. and Wood B.J., 1979. An experimental study of Fe-Mg partitioning between garnet and olivine and its calibration as a geothermometer. *Contributions to Mineralogy and Petrology*, 70: 59-70.

SCHMÄDICKE E. and EVANS B.W., 1997. Garnet-bearing ultramafic rocks from the Erzgebirge, and their relation to other settings in the Bohemian Massif. *Contributions to Mineralogy and Petrology*, 127: 57-74.

SCHMÄDICKE E., GOSE J. and WILL T.M., 2010. The P-T evolution of ultra high temperature garnet-bearing ultramafic rocks from the Saxonian Granulitgebirge Core Complex, Bohemian Massif. *Journal of metamorphic Geology*, 28: 489-508.

SCHULMANN K., KRÖNER A., HEGNER E., WENDT I., KONOPÁSEK J., LEXA O. and ŠTÍPSKÁ P., 2005. Chronological constraints on the pre-orogenic history, burial, and exhumation of deep-seated rocks along the eastern margin of the Variscan Orogen, Bohemian Massif, Czech Republic. *American Journal of Science*, 305: 407-448

TAYLOR W. R. 1998. An experimental test of some geothermometer and geobarometer formulations for upper mantle peridotites and application to the thermobarometry of fertile lherzolite and garnet websterite. *Neues Jahrbuch Mineralogische Abhandlung*, 172: 381-408.

WITT-EICKSCHEN G. and SECK H. A., 1991. Solubility of Ca and Al in orthopyroxene from spinel peridotite: an improved version of an empirical geothermometer. *Contributions to Mineralogy and Petrology*, 106: 431-439.

WU C.M. and ZHAO G.C., 2007. A recalibration of the garnet-olivine geothermometer and a new geobarometer for garnet peridotites and garnet-olivine-plagioclase-bearing granulites. *Journal of metamorphic Geology*, 25: 497-505.

Stop 6-4 (Day 6). Peridotite and Pyroxenite Boudins in the Bory Granulite, Horní Bory

Coordinates: N49°25′28.6″ E16°02′28.2″

Lukáš ACKERMAN[1,2], Emil JELÍNEK[3], L. Gordon MEDARIS Jr.[4]

[1] Institute of Geology v.v.i., Academy of Sciences of the Czech Republic, Rozvojová 269, 165 00, Praha 6, Czech Republic
[2] Czech Geological Survey, Geologická 6, Praha 5, 150 00, Czech Republic
[3] Institute of Geochemistry, Mineralogy and Mineral Resources, Faculty of Science, Charles University, Albertov 6, 128 43, Praha 2, Czech Republic
[4] Department of Geoscience, University of Wisconsin-Madison, WI 53706, USA

The Bory granulite is part of the Gföhl unit and contains numerous boudins of peridotite pyroxenite, and eclogite, which range from centimeters to meters in size (Fig. 1) (Mísař and Jelínek, 1981; Mísař et al., 1984). The granulite is characterized by a layered structure defined by the alternation of light-colored (biotite-poor) and dark-colored (biotite-rich) layers, which are isoclinally folded and parallel to the metamorphic foliation. The ultramafic boudins are concentrated along several horizons that are parallel to the predominant trend of granulite foliation, but internal structures of the boudins have variable orientations with respect to metamorphic foliation in the granulite, ranging from approximately parallel, to oblique, to perpendicular, i.e. parallel to remnants of an older vertical foliation in granulite (Hrouda et al., 2009). The ultramafic boudins consist of a variety of lithologies, including dunite, harzburgite, wehrlite, lherzolite, websterite, olivine pyroxenite, and eclogite, most of which are garnetiferous. All boudins have biotite- and amphibole-rich reaction rims of variable thicknesses at contacts with granulite, reflecting the chemical incompatibility between phases in the ultramafic boudins and granulite.

Based on mineralogy and geochemistry (Fig. 2), three types of ultramafic boudins have been distinguished (Medaris et al., 2005; Ackerman et al., 2009): (1) Mg-lherzolite with Mg-numbers from 91 to 89, (2) Fe-dunite/wehrlite with Mg-numbers from 88 to 81, and (3) pyroxenite with Mg-numbers from 77 to 85. The Mg-lherzolite is a strongly serpentinized, five-phase peridotite, consisting of variable proportions of olivine (61–78 %), orthopyroxene (13–23 %), clinopyroxene (5–13 %), Cr-spinel (3 %), and garnet (5–7 %). Spinel occurs as discrete, intergranular grains and as inclusions in garnet, indicating the stable coexistence of spinel and garnet (Fig. 3). Garnet is extensively replaced by kelyphite Fe-dunite/wehrlite is the predominant type of ultramafic boudin in the Horní Bory quarry. It has a slightly foliated, equigranular texture and, locally, a layered aspect due to thin layers of clinopyroxene in dunite and wehrlite. The Fe-dunite/wehrlite consists of olivine (83–88 %), orthopyroxene (0–5 %), clinopyroxene (4–11 %) and spinel+garnet (2–7 %). In contrast to Mg-lherzolite, Fe-dunite/wehrlite contains abundant ilmenite (Fig. 4) and thin veins of secondary clinopyroxene, tremolite, carbonate, and chlorite (after phlogopite) parallel to foliation and layering. Some Fe-dunite/wehrlite boudins have a composite structure with interlayering of Fe-dunite/wehrlite and pyroxenite on a scale of 1 to 6 cm.

The pyroxenite boudins are clinopyroxenite and websterite, which contain clinopyroxene, orthopyroxene, garnet, and small or accessory amounts of olivine, ilmenite, rutile, phlogopite, and secondary amphibole. The clinopyroxenite has a porphyroclastic texture, in which large clinopyroxene porphyroclasts are set in a fine-grained equigranular matrix of clinopyroxene, orthopyroxene, and garnet. Locally, clinopyroxene porphyroclasts contain garnet and orthopyroxene lamellae, as well as ilmenite rods, that are oriented parallel to the (100) planes of the porphyroclasts (Sanc and Rieder, 1981; Faryad et al., 2009).)

Modeling of Mg-Fe exchange between Mg-lherzolite and Fe-rich melt reveals that the modal and chemical compositions of the Fe-dunite/wehrlite suite can be produced by melt-rock reaction between Mg-lherzolite and SiO_2-undersaturated melts of basaltic composition at melt/rock ratios ranging from 0.3 to 2 (Ackerman et al., 2009). The Fe-rich suite is significantly enriched in large-ion lithophile elements (LILE), depleted in high field strength elements (HFSE) and has radiogenic $^{87}Sr/^{86}Sr$ ratios (Fig. 5), all of which point to a significant component of subducted(?) crustal material. Following this model, the pyroxenites could represent crystal cumulates (± trapped liquid) from melts migrating along conduits, and reacting with, peridotite in a mantle wedge above a Variscan subduction zone.

P-T conditions were calculated for peridotites by using the olivine-garnet Fe-Mg exchange geothermometer of O'Neill and Wood (1979) and O'Neill (1980) and the Al-in-Opx geobarometers of Brey and Köhler (1990) and Nickel and Green (1985). Mg-lherzolite yields an average P-T estimate of 905 °C, 37.7 kbar, and two samples of Fe-dunite/wehrlite yield 885 °C, 28.7 kbar and 965 °C, 25.5 kbar (Fig. 6). For one sample of clinopyroxenite, Faryad et al (2009) provided analyses of an exsolved clinopyroxene host and its orthopyroxene and garnet lamellae, the reintegrated clinopyroxene porphyroclast, which contains 18.25 wt% CaO and 5.87 wt% Al_2O_3, and matrix orthopyroxene, clinopyroxene, and garnet. The clinopyroxene porphyroclast likely crystallized at ~1400 °C, 23 kbar (Fig. 6), by comparison of its reintegrated composition with the thermodynamic model of Gasparik (2000). Note however, that this P-T estimate is semi-quantitative, because it is unlikely that the clinopyroxene porphyroclast was in equilibrium with orthopyroxene and garnet at the time of its crystallization, which is required for direct application of the Gasparik model. P-T conditions for the exsolved and matrix phases in clinopyroxenite were obtained from application of the Fe-Mg exchange geothermometers for Opx-Grt (Halley, 1984) and Cpx-Grt (Powell, 1985), three 2-Px geothermometers (Brey and Köhler, 1990; Bertrand and Mercier, 1985; Tailor, 1998) and the Al-in-Opx

■ **Fig. 1.** Large boudin of layered Fe-dunite/wehrlite and pyroxenite in granulite, Horní Bory quarry.

geobarometers of Brey and Köhler (1990) and Nickel and Green (1985). The average P-T estimate for clinopyroxene host and its orthopyroxene and garnet lamellae is 830 °C, 24.0 kbar, similar to that for Fe-dunite/wehrlite, and for matrix clinopyroxene, orthopyroxene, and garnet is 830 °C, 13.5 kbar (Fig. 6).

The geochemical and P-T characteristics of ultramafic boudins in felsic granulite in the Horní Bory quarry are consistent with their derivation from a suprasubduction mantle wedge. The Mg-lherzolite may represent deeper portions of the wedge that were brought to shallower levels, where transient melts, origi-

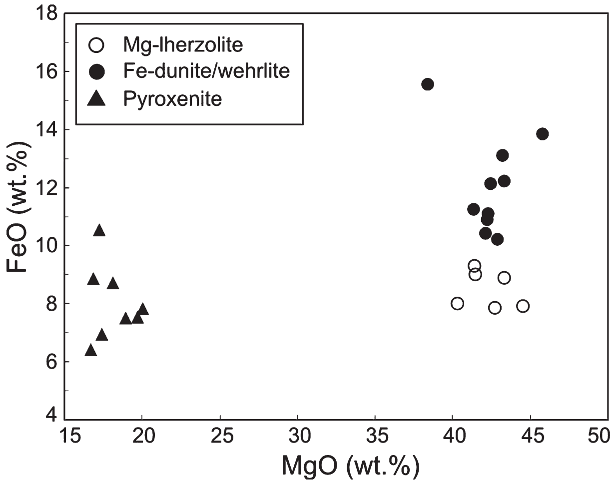

■ **Fig. 2.** Plot of MgO (wt. %) *vs*. FeO (wt. %), illustrating the compositional differences among ultramafic rock types in the Horní Bory quarry.

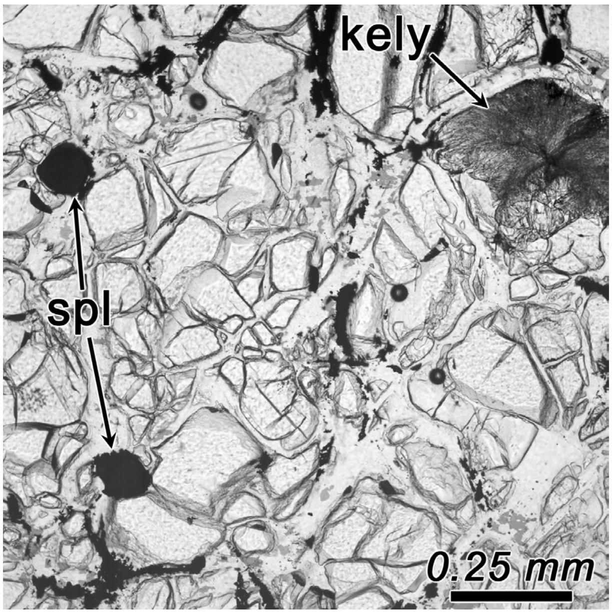

■ **Fig. 3.** Photomicrograph of Mg-lherzolite (plane polarized light). This view illustrates mostly olivine, with kelyphite (kely) after garnet and interstitial spinel (spl).

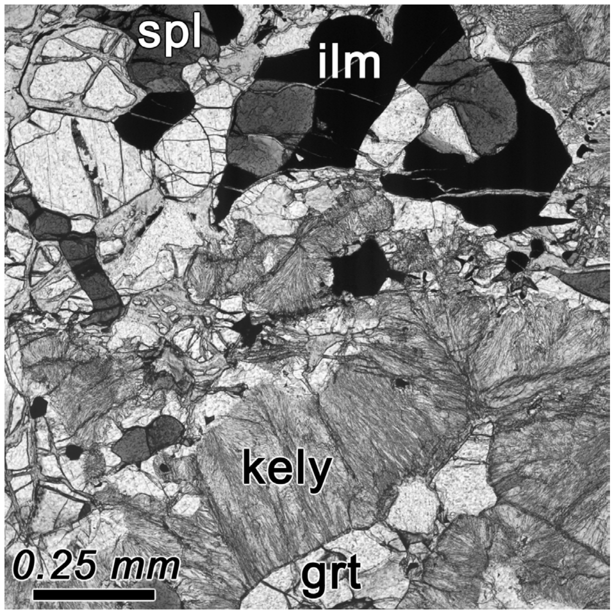

■ **Fig. 4.** Photomicrograph of Fe-dunite/wehrlite (plane polarized light), illustrating moasaic-textured olivine (unlabelled), spinel (spl), ilmenite (ilm), and garnet (grt) partly replaced by kelyphite (kely).

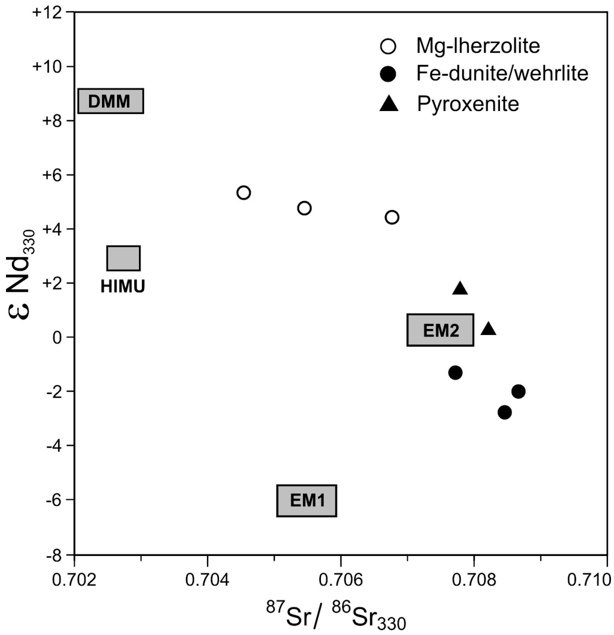

■ **Fig. 5.** εNd *vs*. $^{87}Sr/^{86}Sr_i$ of clinopyroxenes from Horní Bory peridotites and pyroxenites. Abbreviations: DMM, depleted MORB mantle; EM1, enriched mantle 1; EM2; HIMU, high Mu mantle. Data from Ackerman et al. (2009).

nating from the subduction zone, intruded and reacted with Mg-lherzolite to produce the Fe-dunite/wehrlite suite and associated pyroxenite dikes (now layers). Such reaction was accompanied by extensive recrystallization, which continued at lower pressures during entrainment by granulite and subsequent exhumation of the entire lithologic package.

References

ACKERMAN L., JELÍNEK E., MEDARIS G., JEŽEK J., SIEBEL W. and STRNAD L., 2009. Geochemistry of Fe-rich peridotites and associated pyroxenites from Horni Bory, Bohemian Massif: Insights into subduction-related melt-rock reactions. *Chem. Geol.*, 259: 152-167.

BERTRAND P. and MERCIER J.-C.C., 1985.The mutual solubility of coexisting ortho- and clinopyroxene: toward an

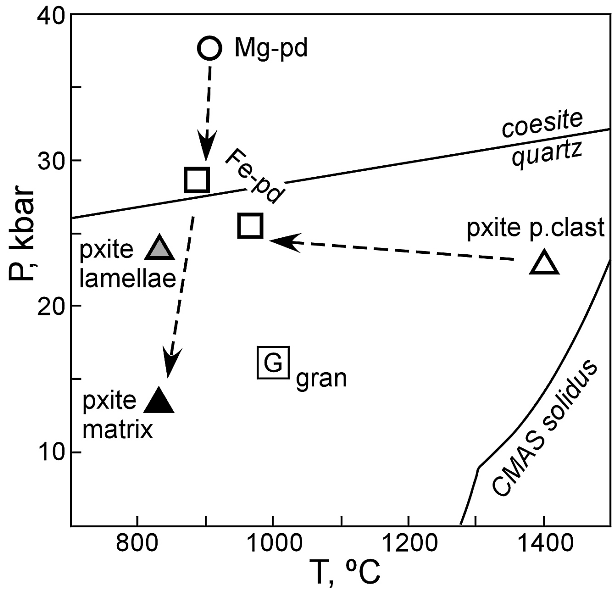

■ **Fig. 6.** P-T estimates for Mg-lherzolite (circle, Mg-pd), Fe-dunite/wehrlite (squares, Fe-pd), reconstituted clinopyroxene porphyroclast in pyroxenite (open triangle, pxite p.clast), orthopyroxene and garnet lamellae and host clinopyroxene in pyroxenite (gray triangle, pxite lamellae), and matrix orthopyroxene, clinopyroxene, garnet in pyroxenite (filled triangle, pxite matrix), and Gföhl felsic granulite (G, gran). See text for methods and discussion.

absolute geothermometer for the natural system? *Earth and Plantary Science Letters*, 76:109-122.

BREY G.P. and KÖHLER T., 1990. Geothermobarometry in four-phase lherzolites: II. New thermobarometers, and practical assessment of existing thermobarometers. *J. Petrol.*, 31: 1352-1378.

FARYAD S.W., DOLEJŠ D. and MACHEK M., 2009. Garnet exsolution in pyroxene in clinopyroxenites in the Moldanubian zone: constraining the early pre-convergence history of ultramafic rocks in the Variscan orogen. *J. Metamorphic Geol.*, 27: 655-671.

GASPARIK T., 2000. An internally consistent thermodynamic model for the system CaO-MgO-Al_2O_3-SiO_2 derived primarily from phase equilibrium data. *Journal of Geology*, 108: 103-114.

HROUDA F., FARYAD S.W., JEŘÁBEK P., CHLUPÁČOVÁ M. and VITOUŠ P., 2009. Primary magnetic fabric in an ultramafic body (Moldanubian Zone, European Variscides) survives exhumation-related granulite-amphibolite facies metamorphism. *Lithos*, 111: 95-111.

FARYAD S.W., 2009. The Kutná Hora Complex (Moldanubian zone, Bohemian Massif): A composite of crustal and mantle rocks subducted to HP/UHP conditions. *Lithos*, 109: 193-208.

HARLEY S. 1984. Comparison of the garnet-orthopyroxene-geobarometer with recent experimental studies, and applications to natural assemblages. *Journal of Petrology*, 25: 697-712.

MEDARIS L.G., WANG H., MÍSAŘ Z. and JELÍNEK E., 1990. Thermobarometry, diffusion modelling and cooling rates of crustal garnet peridotites: Two examples from the Moldanubian zone of the Bohemian Massif. *Lithos*, 25: 189-202.

MEDARIS Jr.L.G., WANG H., JELÍNEK E., MIHALJEVIČ M. and JAKEŠ P., 2005. Characteristics and origins of diverse Variscan peridotites in the Gföhl Nappe, Bohemian Massif, Czech Republic. *Lithos*, 82: 1-23.

MÍSAŘ Z., JELÍNEK E. and JAKEŠ P., 1984. Inclusions of peridotite, pyroxenite and eclogite in granulite rocks of pre-Hercynian upper mantle and lower crust in the eastern Bohemian Massif (Czechoslovakia). *Ann. Sci. Univ. Clermont-Ferrand II*, 74: 85-95.

MÍSAŘ Z. and JELÍNEK E., 1981. Inclusions of peridotites, pyroxenites, eclogites and opals in the leptynites of the Moldanubicum at the locality Bory (SW Moravia) (in Czech). *Věst. Ústř. Úst. Geol.*, 56: 13-20.

NAEMURA K., HISASHIMA H., HIRAJIMA T. and SVOJTKA M., 2009. An ultra-high-pressure metamorphic condition and isothermal decompression path obtained from a garnet-pyroxenite in the Horni Bory granulite of the Bohemian Massif. *J. Mineral. Petrol. Sci.*, 104: 168-175.

NICKEL K.G. and GREEN D.H., 1985. Empirical geothermobarometry for garnet peridotites and implications for the nature of the lithosphere, kimberlites and diamonds. *Earth and Planetary Science Letters*, 73: 158-170.

O'NEILL H.ST.C. and WOOD B.J., 1979. An experimental study of Fe-Mg partitioning between garnet and olivine and its calibration as a geothermometer. *Contrib. Mineral. Petrol.*,70: 59-70.

O'NEILL H.St.C., 1980. An experimental study of Fe–Mg partitioning between garnet and olivine and its calibration as a geothermometer: corrections. *Contrib. Mineral.Petrol.*, 72:337.

POWELL R., 1985. Regression diagnostics and robust regression in geothermometer/geobarometer calibration: the garnet-clinopyroxene geothermometer revisited. *Journal of Metamorphic Geology*, 3: 231-243.

ŠANC I. and RIEDER M., 1983. Lamellar pyroxenes and their petrogenetic significance: Three examples from the Czech Massif. *Contributions to Mineralogy and Petrology*, 84: 73-83.

TAYLOR W.R., 1998. An experimental test of some geothermometer and geobarometer formulations for upper mantle peridotites with application to the thermobarometry of fertile lherzolite and garnet websterite. *Neues Jahrb. Mineral. Abh.*, 172: 381-408.

HP/UHP Rocks in the Kutná Hora Complex and Adjacent Monotonous Unit

Shah Wali FARYAD[1], Matěj MACHEK[1,2], Radka NAHODILOVÁ[1,3] and David DOLEJŠ[1]

[1] Institute of Petrology and Structural Geology, Charles University, Prague, Czech Republic
[2] Geophysical Institute of the Academy of Sciences of the Czech Republic, Boční II/1401, 141 31 Praha 4, Czech Republic
[3] Czech Geological Survey, Klárov 3, Prague, Czech Republic

During the final day of the field trip we will visit garnet peridotite, garnet pyroxenite, eclogite and surrounding garnulite in the Kutná Hora complex (stops 7.1–7.3, Fig. 1) and one eclogite occurrence in serpentinized spinel peridotite in the Monotonous unit (stop 7.4). The field trip localities can be reached by Highway 38 to Časlav and taking Highways 337 and 345 to Villémov and Borek, respectively.

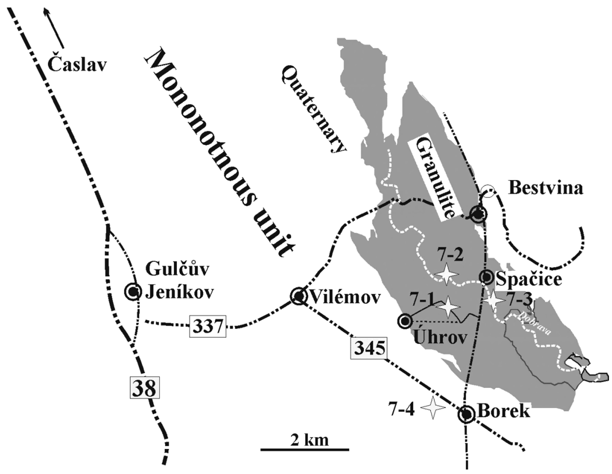

Fig. 1. Localities of field trip stops 7-1 to 7-3 in garnet peridotites and eclogites in the Kutná Hora complex and stop 7-4 in eclogite in the Monotonous unit (area C in Fig. 1 of the Introduction to post-conference excursion).

High-grade metamorphic rocks of the Kutná Hora Complex are exposed in an ~50-km-long NW-SE-oriented belt near the town of Kutná Hora, where the high-grade metamorphic rocks structurally overlie a medium-grade, paragneiss sequence of the Monotonous unit (Fig. 2). Based on its lithology and high-grade metamorphism, the Kutná Hora Complex has been correlated with the Gföhl unit in the eastern part of the Moldanubian zone (Synek and Oliveriová, 1993). The complex consists of two superposed tectonic units: at the top are granulites, granulite gneisses and migmatites with amphibolized and serpentinized mafic and ultramafic rocks and skarns, below which are micaschists with lenses of amphibolites. The largest granulite body (the Běstvina granulite) consists mainly of retrogressed felsic granulites, biotite gneisses, migmatites, and several small, isolated bodies of peridotite and eclogite (Pouba et al., 1987; Synek and Oliveriová, 1993; Vrána et al., 2006). Three stages of deformation can be recognized in the high-grade rocks of the Kutná Hora Complex (Synek and Oliveriová, 1993). D1, the oldest event, is contemporaneous with eclogite-facies metamorphism of metabasic protoliths, metamorphic crystallization of HP/HT granulites, and (re)crystallization of garnet lherzolites. An earlier S1 fabric in granulite occurs within low-strain domains surrounded by a regionally developed penetrative S2 fabric formed during the D2 stage of deformation, (Machek et al., 2009). S1 foliation in felsic granulites dips steeply to the SE or NW and is usually preserved in the vicinity of peridotite and eclogite bodies. S2 foliation dips generally to the ENE at medium to high angles. Occasionally, S1 foliation is transposed into the S2 foliation by symmetrical S2 folds, in which folds, axial planes, and S2 foliation are parallel. D2 deformation was accompanied by extensive partial melting and migmatization that generated kyanite-bearing granitic leucosomes. D3 is a late stage of reactivation, which generated low-temperature mylonites that locally overprint earlier structural patterns and migmatitic features.

The ultramafic rocks show a deformational fabric concordant with relic S1 granulite fabric. It is the youngest fabric in the mantle rocks because it cross-cuts or reworks other observed fabrics. The peridotite fabric is recorded by the LPO of olivine, which displays an (010)[001] slip system (Machek et al., 2009). The LPO in olivine defines an E-W trending and steeply dipping foliation, which is discordant to the S1 foliation in granulites with clinopyroxenites, and which might be interpreted as the original mantle fabric S0. The LPOs of clinopyroxene and quartz measured in clinopyroxenites and coarse-grained granulites, respectively define a subvertical foliation S1 and stretching lineation L1. In peridotite from stop 7.1, LPO data show an olivine fabric closely concordant to S0 in the peridotite at stop 7.2 , as well as a NE-SW striking, sub-vertical fabric that corresponds to the S1 foliation. The [001] slip direction of all minerals defines a steeply plunging stretching lineation in the S0 foliation plane, while S1 is a strongly planar fabric with weak, variable lineation. This indicates a reworking of the S0 fabric, producing(?) a sub-vertical stretching lineation in response to an oblate strain pattern during development of the S1 fabric.

The Monotonous unit beneath the Kutná Hora Complex is represented by partly migmatized kyanite/sillimanite+biotite±muscovite±cordierite paragneiss. At the contact with the micaschist zone of the Kutná Hora complex, the Monotonous unit paragneiss encloses several bodies of serpentinized peridotites, eclogites and garnet amphibolites (Synek and

Oliveriová, 1993). The surrounding paragneiss exhibits a penetrative deformational fabric defined by a medium grade foliation dipping at moderate angles towards the NE. This foliation is concordant to the S2 fabric observed in the Běstvina formation (Machek et al., 2009) and the contact between the Monotonous unit and Běstvina formation. The structural relation of this fabric to the peridotite body is unclear. The mafic and ultramafic bodies in the Monotonous unit may have been extruded along the shear zone between the Monotonous and Běstvina units.

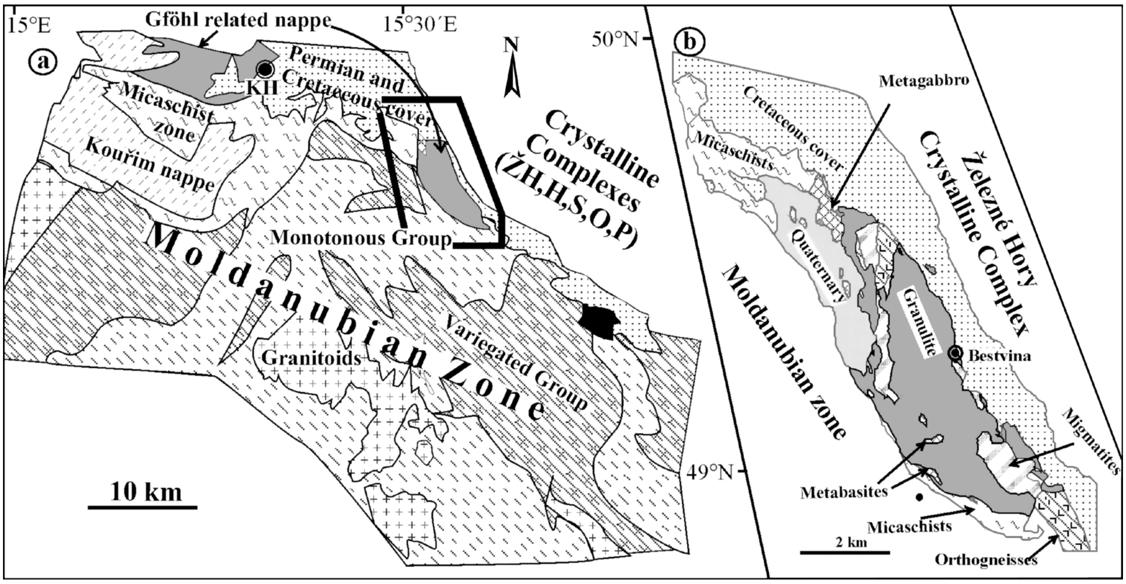

■ **Fig. 2.** (a) Simplified geological map of the north-eastern part of the Moldanubian zone and locations of the Gföhl-related units in the Kutná Hora Complex (after Synek and Oliveriová, 1973); Abbreviations: KH, the town of Kutná Hora; ZH, Zelezne Hory complex; H, Hlinsko zone; S, Svratka crystalline complex; O, Oheb crystalline complex; and P, Podohorany crystalline complex. (b) The Bestvina granulite body with associated garnet peridotites and eclogites to be visited on the excursion.

Stop 7-1 (Day 7). Garnet Peridotite and Eclogite, Úhrov, ca. 1 km East from the Village of Úhrov

Coordinates: N49°48′39.5″ E15°33′32.5″

Stop 7-1 can be reached by an asphalt road from Borek to Spačice, but before Spačice turn left on the dirt road to Úhrov, and after 300 m turn northwest (Fig. 1). It is a small outcrop of garnet peridotite with boulders of eclogite in an overgrown, abandoned quarry in serpentinized garnet peridotite.

The garnet peridotite is strongly serpentinized, but contains garnet crystals (up to 5 mm in size) that are mostly rimmed by a thick kelyphitic corona of clinopyroxene ± orthopyroxene + amphibole + spinel (Faryad, 2009). Garnet is rich in Mg ($Prp_{66\text{-}78}$, Fig. 3), with relatively low Fe and Ca contents ($Alm_{16\text{-}23}$, $Grs_{12\text{-}17}$), and the spessartine component is below

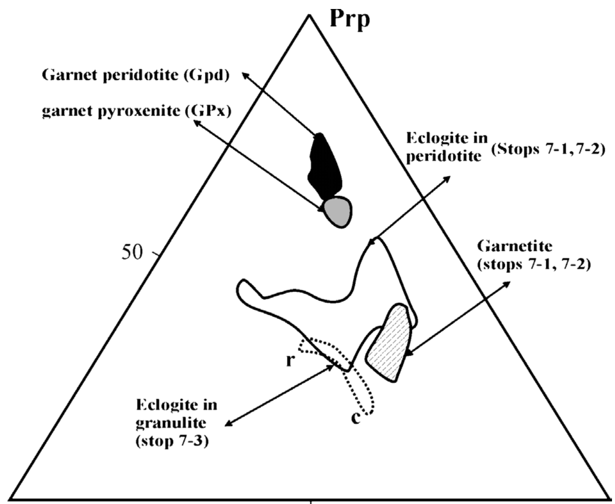

■ **Fig. 3.** Compositions of garnet from garnet peridotite, garnet clinopyroxenite, garnetite, and eclogite from the Kutná Hora complex. Dotted field shows the range of prograde compositional zoning in garnet (c, core; r, rim) from eclogite within granulite (stop 7-3).

2 mol%. The uvarovite content mostly ranges between 4 and 8 mol%, but it may reach 13 mol% near the contact with Cr-spinel inclusions (Fig. 4a). Garnet crystals are mostly homogeneous with diffusion zoning at grain boundaries as a result of decompression and cooling. However, some garnet grains exhibit grain-scale zoning with a decrease in Mg and an increase of Fe and Cr toward the rims (Fig. 4b). The garnet peridtotite also contains clinopyroxene ($Jd_{2–10}$), orthopyroxene (Al_2O_3 = 0.5 to 1.7 wt%), olivine (Fo = 0.90–0.92), and spinel (X_{Al} = Al/(Cr + Al + Fe^{3+} = 0.38–0.62. Cr-rich spinel with X_{Al} = 0.38 occurs as inclusions in garnet or in the serpentine matrix, but more aluminous spinel (X_{Al} = 0.52–0.55 and 0.61–0.68) occurs as fine grains in kelyphitic coronas around garnet. Amphibole (pargasite) is a retrograde phase and occurs within intergranular spaces between garnet and pyroxene, where it may form individual crystals in the serpentine matrix or partly overgrow clinopyroxene + spinel kelyphite around garnet.

Thin layers of pyroxenite (websterite) are present in the outcrop of garnet peridotite. In contrast to clinopyroxenite from other localities, this pyroxenite contains orthopyroxene with exsolution lamellae of garnet and clinopyroxene (Fig. 5b). The orthopyroxene forms porphyroclasts in a fine-grained, recrystallized matrix, consisting of orthopyroxene, clinopyroxene, and small amounts of garnet and amphibole (Fig. 5a). The orthopyroxene porphyroclasts contain garnet and clinopyroxene lamellae that are orientated parallel to the (100) planes of the host porphyroclasts. The lamellar clinopyroxene and garnet are partially replaced by secondary amphibole.

Two varieties of **eclogite**, forming small boudins within garnet peridotite, are present. The most abundant is eclog-

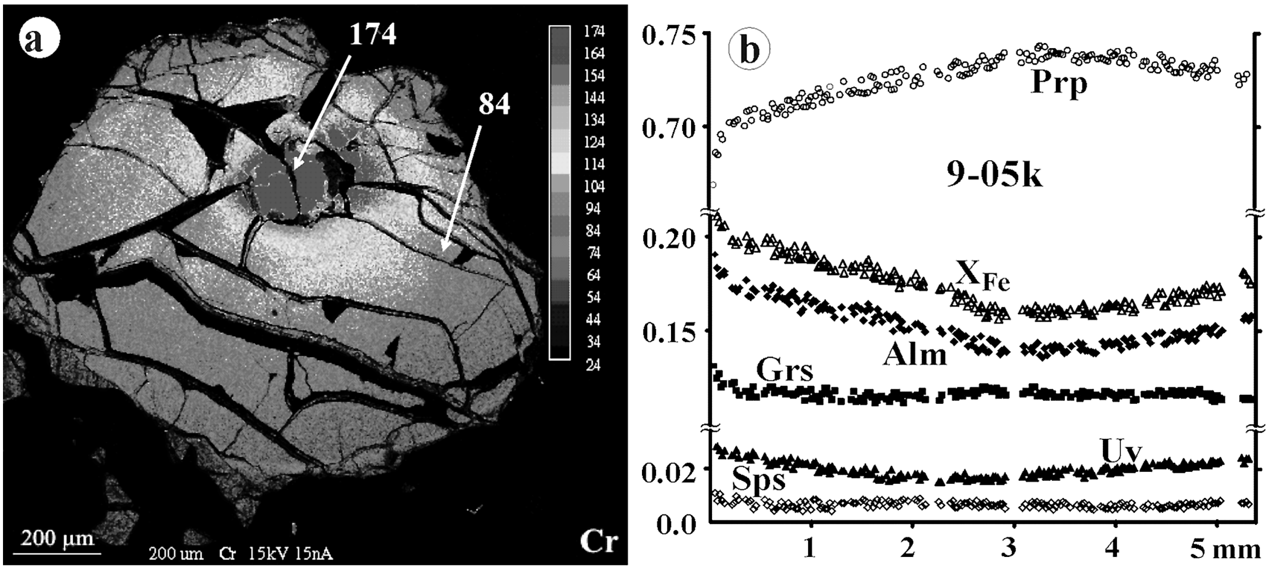

■ **Fig. 4.** (a) Cr X-ray map of garnet with inclusion of Cr-spinel in sample 9b. (b) Compositional profile (rim to rim) of garnet in garnet peridotite showing a rimward increase in Cr and Fe contents and decrease in Mg (sample 9-05k).

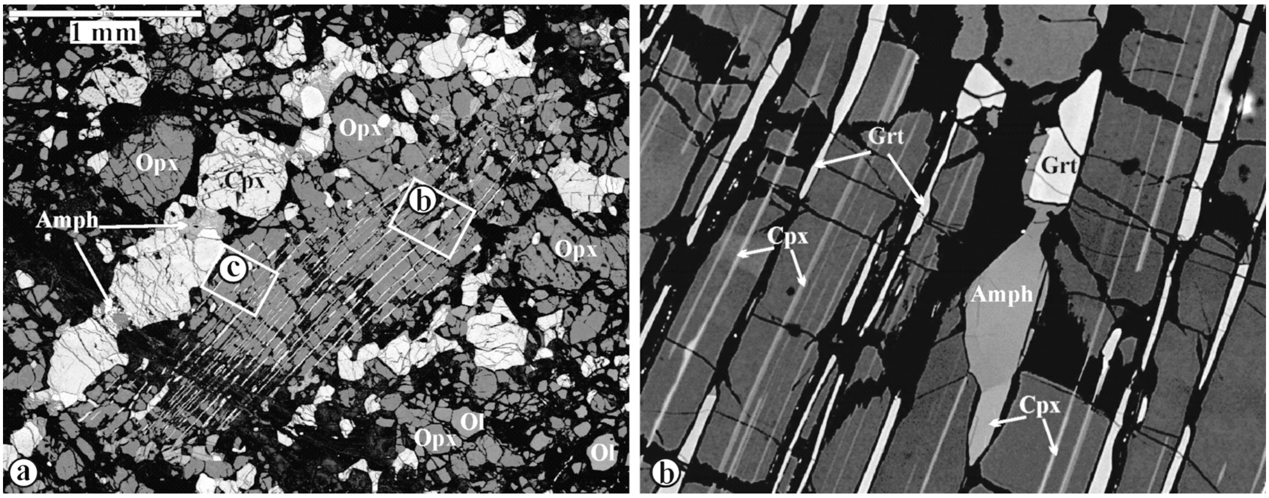

■ **Fig. 5.** Backscattered electron images of orthopyroxene porphyroclasts with exsolution products. (a) low magnification view of an orthopyroxene porphyroclast that contains garnet and clinopyroxene lamellae (Faryad et al., 2009). Bright coloured coarse grains are clinopyroxene and garnet. (b) exsolution lamellae of clinopyroxene and garnet in orthopyroxene. Amphibole forms by replacement of clinopyroxene and garnet in the lamellae.

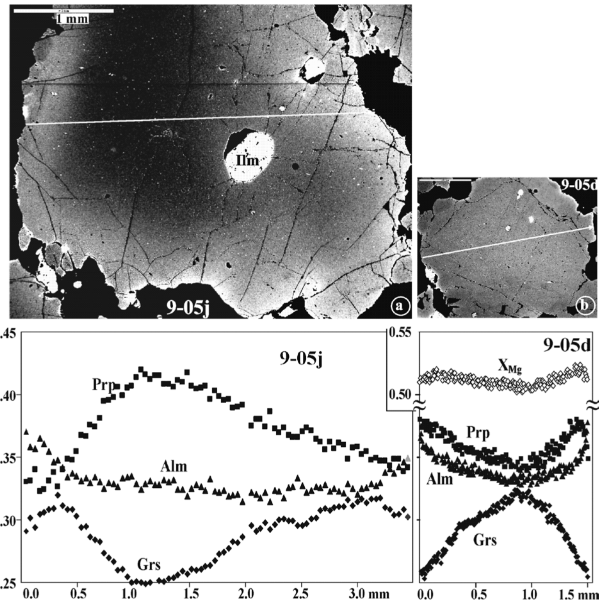

■ **Fig. 6.** Backscatter electron images illustrating contrasting compositional zoning patterns of garnets from eclogite (type II) within the garnet peridotites. In general, garnets (a) and (b) show the opposite sense of core to rim zoning for Grs and Prp.

ite (type I) with garnet (40–60 wt%), omphacite (40–60 wt%), and accessory rutile and apatite, but kyanite-bearing eclogite (type II) also occurs. Garnet is rimmed by a corona of diopsidic clinopyroxene, plagioclase, and amphibole and kyanite is surrounded by a corona of plagioclase, amphibole, and spinel. Garnet from eclogite forms relatively large (1–4 mm) crystals and contains small, oriented rutile needles. Its composition varies from sample to sample ($Prp_{37\text{-}50}$, $Grs_{15\text{-}34}$, $Alm_{18\text{-}37}$) with <1 mol% spessartine and uvarovite contents. The most Mg-rich garnet comes from kyanite-bearing variety. Apart from a systematic rimward increase in Fe and decrease of in Ca in garnet from type I and II, compositional zoning in garnet from type II is different in the different samples (Fig. 6). In some cases, Ca shows an increase in the core with a decrease toward the rim. Omphacite forms up to 1-mm grains that may contain quartz rods. The jadeite content in omphacite ranges from 24 to 28 mol%. The most Jadeite-rich omphacite occurs in type II eclogite. Exsolution lamellae of garnet occur in omphacite from one sample of kyanite-bearing eclogite.

Stop 7-2 (Day 7). Garnet Peridotite, Garnet Pyroxenite, Garnetite and Eclogite. West Bank of the Doubrava River, ca 2 South from the Village of Úhrov

Coordinates: N49°48′33.1″ E15°33′23.9″

At Stop 7-2, outcrops of garnet peridotite and granulite are exposed along the banks of the Doubrava River. Garnet peridotite occurs in two ca. 100 × 30 m lens-shaped bodies surrounded by coarse-grained and retrogressed granulites. The **garnet peridotite** contains several eclogite bodies (ca. 10–60 cm × 1.8 m in size), but because of poor exposure and small outcrops it is not possible to discern the exact dimensions of these bodies. In contact with, or close to, the eclogites, parallel layers of garnet clinopyroxenite and rarely garnetite with garnet peridotites are present, which are oriented parallel to the shapes of the eclogite bodies. Contacts between garnet peridotite and clinopyroxenite layers are mostly sharp. Although garnet peridotite is strongly serpentinized, fine-grained relics of garnet, olivine, and clinopyroxene are preserved. Minerals in the peridotite at stop 7-2 have a slightly lower Mg/Fe ratio than do those in peridotite at stop 7-1.

Garnet pyroxenite is medium-grained and contains clinopyroxene (90–95 vol%), garnet (5–10 vol%), and small amounts of olivine and accessory spinel. Contacts between the pyroxenite layers and serpentinized garnet peridotites are sharp, and no deformation or metasomatic textures occur along their boundaries. Garnet in pyroxenite has a slightly lower Mg content compared to that in peridotite, (Fig. 3). In clinopyroxenite, olivine occurs interstitially between clinopyroxene grains and as inclusions in garnet and clinopyroxene.

Garnetite with up to 98 vol% garnet and small amounts of apatite and clinopyroxene, locally altered to amphibole, occurs adjacent to garnet pyroxenite. In addition, magnesiotaramite and associated quartz and biotite occur as inclusions in garnet. Apatite contains exolution lamellae of monazite.

Eclogite at this locality is largely bimineralic, consisting of omphacite (Jd_{33}), garnet $Prp_{37}Grs_{16}Alm_{45}$), and accessory rutile, and symplectites of amphibole (diopside) + plagioclase.

P-T estimates were made for garnet peridotites using the Fe-Mg garnet-olivine exchange geothermometer (O'Neill and Wood, 1981), two two-pyroxene geothermometers (Tailor, 1998, Brey and Köhler, 1990), the Al-in-Opx and Cr-in-Cpx geobarometers (Brey and Köhler, 1990), and the spinel-garnet transition (O'Neill and Wood 1980). The results are approximately 4.0 GPa and 850–900 °C for garnet peridotite at stop 7-1 (Fig. 7) and 3.0 at 900 °C for stop 7-2 (not illustrated).

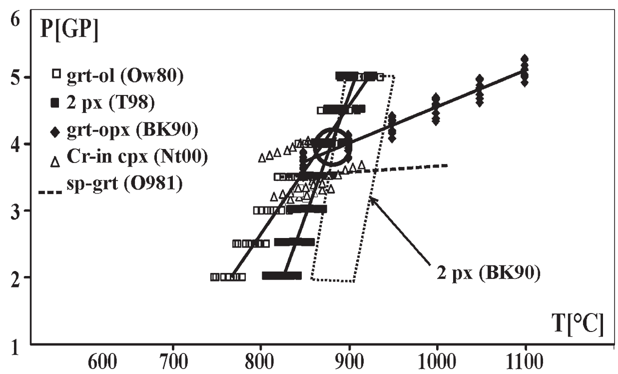

■ **Fig. 7.** Results of PT calculations for garnet peridotite at stop 7-1 (Faryad, 2009) obtained using different thermobarometers: BK90 – Brey and Kohler (1990), T98 – Taylor (1998), NT00 – Nimis and Taylor (2000), OW80 – O'Neill and Wood (1980) and O81 – O'Neill (1981).

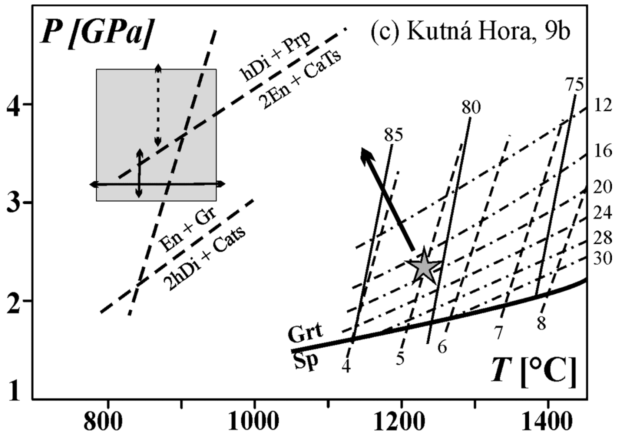

■ **Fig. 8.** P-T plot illustrating garnet-clinopyroxene-orthopyroxene equilibria for reintegrated and exsolved orthopyroxenes in the system $CaO-MgO-Al_2O_3-SiO_2$. (Faryad et al., 2009). Dash-dotted curves labeled 12 through 30 are isopleths of Al content in pyroxene expressed in cation per cent per six oxygen formula unit. Thin solid and dashed curves are isopleths of Ca contents in clinopyroxene (75 through 85) and orthopyroxene (4 through 8), respectively, expressed in cation per cent per six oxygen formula unit (Gasparik, 2000, 2003). Pressure-temperature ranges calculated for exsolved pyroxenes are shown by gray rectangles and double headed arrows (calculated at 800 and 950 °C), computed using the clinopyroxene, orthopyroxene and garnet compositions and the internally consistent thermodynamic data of Gasparik (2000) and non-ideal mixing models of Gasparik (2003).

Kyanite-bearing eclogites within garnet peridotites (stop 7.1) yield using the calibration of Ravna and Terry (2004) a pressure of 3.3 GPa at 900–960 °C. The composition of reintegrated orthopyroxene indicates that primary orthopyroxene megacrysts crystallized at 1200–1250 °C and 2.2–2.5 GPa (Fig. 8). Unmixing and exsolution of garnet and clinopyroxene occurred in response to cooling and pressure increase before the peak pressure of 4.5 GPa was reached at approximately 900 °C. This scenario is consistent with burial of hot upper-mantle ultramafics into a cold subcratonic environment, followed by exhumation through $T = 900$ °C and $P = 2.2$–3.3 GPa, when the pyroxenites were partly recrystallized during tectonic incorporation into eclogites and felsic granulites (Faryad et al. 2009).

Stop 7-3 (Day 7). Eclogite and Granulite, Spačice

Coordinate: N49°48′57.3″ E15°35′49.4″

Eclogite and granulite

The eclogite forms a ca. 10- × 50-m body within granulite that is exposed along the northern bank of the Doubrava River near the village of Spacice (Fig. 1). The eclogite shows isoclinal folding that is defined by alternating thin, fine-grained garnet-rich layers and coarse-grained layers of clinopyroxene and porphyroblastic garnet. In the Spačice eclogite, clinopyroxene LPOs show an LS-type fabric in the coarse-grained layers and an S-type fabric in the fine-grained layers. Foliations in both microstructural types are parallel to the limbs of upright, tight-to-isoclinal folds, the axial plane of which is parallel to the S_1 fabric. A stretching lineation, defined by a maximum in the distribution of clinopyroxene [001] axes, rotates from a sub-vertical position in the coarse-grained layers to a gently plunging orientation in the fine-grained layers, parallel to the fold hinge.

The eclogite is kyanite-bearing and has the composition of subalkaline to tholeiitic basalt (Medaris et al., 1998, 2006). It contains garnet and omphacite (40–60 vol% each), kyanite (up to 10 vol%), and accessory rutile. Variable amounts of diopsidic clinopyroxene, plagioclase, spinel, and amphibole in symplectites around garnet or coronae around kyanite depend upon the degree of retrogression. The eclogite contains two textural and compositional varieties of garnet. The first variety, coexisting with omphacite and kyanite, forms large crystals (garnet I) and is rich in Mg (Prp_{39}, Grs_{26}, Alm_{30}, Sps_5). It shows prograde compositional zoning with relatively flat core profiles and a rimward decrease in Mn and Fe and increase in Mg and Ca (Fig. 9). The second variety (garnet II) forms small grains that either occur in the plagioclase + diopsidic clinopyroxene ± amphibole matrix or overgrows the large garnet I grains. It has high Ca and low Mg contents ($Grs_{55\text{-}66}$, $Prp_{10\text{-}15}$), but its Alm is similar to that in garnet I ($Alm_{28\text{-}30}$). The Mn content is 2–3 times higher than that in garnet I rims. Omphacite has a jadeite content of 24–29 mol%, Ca-tschermak of ca. 6–12 mol%, and the remainder is diopside $Di_{50\text{-}54}$ and hedenbergite Hd_7. The jadeite content decreases at the rims of clinopyroxene grains. Plagioclase (up to An_{99} in symplectite after kyanite) and pargasitic amphibole are common secondary phases in retrogressed eclogite.

The **HP felsic granulite** with lenses of eclogite in stop 7-3 and with garnet peridotites in stop 7-2 are fine- to medium-grained, with a foliation that is highlighted by modal layering of quartzofeldspathic layers alternating with garnet-rich layers. The granulite consists of ternary feldspar, quartz, garnet, kyanite, and rutile. Rarely, inclusions of phengite with a high Ti content (TiO_2=3.0–3.1 wt.%) occur in garnet (Fig. 10). Similar to other granulites, it has a layered structure, in which light-coloured, 1- to 10-cm-wide layers enriched in quartz and feldspar, as result of melt infiltration, alternate with grey-coloured granulite layers. Garnet shows a zoning profile that is characterized by a decrease of Ca and an increase of Mg from the core (Grs_{41} $Prp_{08}Alm_{47}$) toward the rim ($Grs_{29}Prp_{15}Alm_{47}$); Mn content is very low (less than 1 mol%) and decreases slightly toward the rim.

P-T conditions of 3.2 GPa and 910 °C (Fig. 11) were obtained using the method of Ravna and Terry (2004) for the Spačice kyanite eclogite enclosed in granulite (Faryad, 2009).

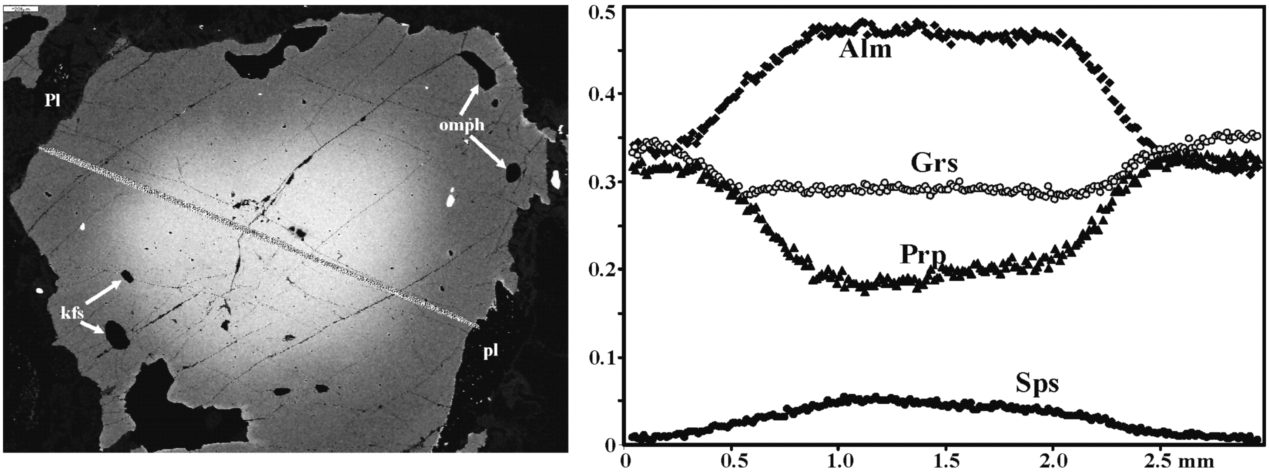

■ **Fig. 9.** Back-scattered electron image and compositional zoning profile of garnet from kyanite-bearing eclogite within granulite (stop 7.3), indicating a prograde metamorphic evolution. Abbreviations: kfs, K-feldspar; omph, omphacite; pl, plagioclase.

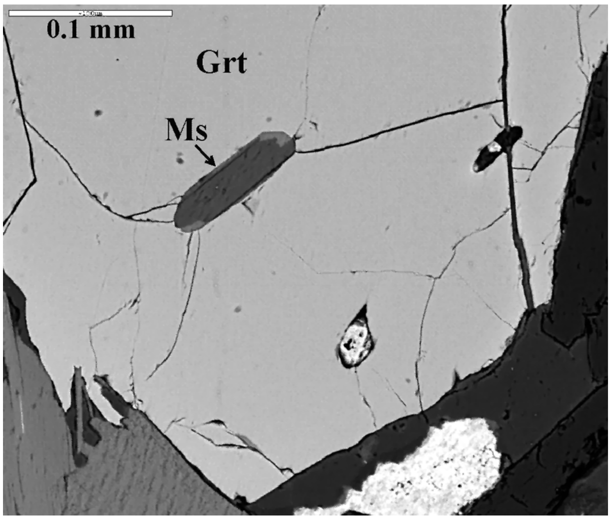

■ **Fig. 10.** Back-scattered electron image of garnet with inclusion of Ti-rich phengite from the Běstvina felsic granulite.

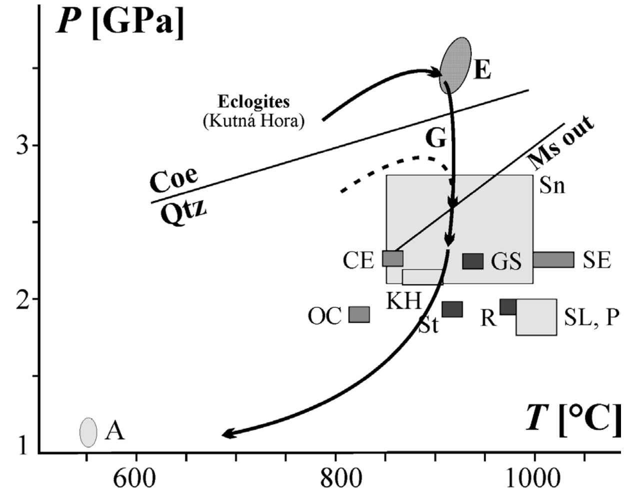

■ **Fig. 11.** PT paths and peak pressure and temperature conditions for kyanite-bearing eclogite (E) in HP felsic granulite near Spačice village (stop 7.3) (Faryad, 2009). Area A: PT conditions for formation of Ca-rich garnet (II) in eclogite. The bold letter, G, indicates the transition from eclogite to granulite facies conditions, calculated for felsic granulites of the Kutná Hora complex. Pressure-temperature estimates for other high-pressure granulites from the central European Variscides are plotted for comparison. Abbreviations for the Moldanubian Zone (light gray fields): KH – Kutná Hora Complex (Vrána et al., 2006), BL – Blanský Les Massif (O'Brien, 1999), SL – St. Leonhard Massif (Carswell and O'Brien, 1993; Cooke, 2000), P – Prachatice Massif (Kröner et al., 2000), St – Strážek Unit (Tajčmanová et al., 2006); Saxothuringian Zone (dark gray fields): SE – Saxonian Erzgebirge (Rötzler et al., 2004), CE – Central Erzgebirge (Willner et al., 1997), OC – Ohře Crystalline Complex (Kotková, 1993); Sudetes (medium gray fields): Sn – Snieznik (Kryza et al., 1996; Klemd and Bröcker, 1999), GS – Gory Sowie (Kryza et al., 1996), R – Rychleby (Štípská et al., 2004). The P-T path inferred for the Kutná Hora granulite (dashed curve) is compared to that of the kyanite eclogite lens (E) (Faryad, 2009).

A pressure of 1.1 GPa at 720 °C was obtained for Ca-rich (type II) garnet that rims eclogite facies garnet (Type I) and occurs with diopside and plagioclase in the matrix. For felsic granulite, P-T conditions of 2.2 GPa and 900 °C GPa were obtained using GASP thermobarometry (Vrána et al., 2005). The results of thermodynamic calculations and phase equilibrium experiments indicate that granulite experienced eclogite facies metamorphism in or near the coesite stability field, and that the modal layering was a result of high-pressure partial melting at 2.2 GPa and 900 °C during decompression to granulite facies conditions (Faryad et al., 2010). Both the thermodynamic calculations and phase equilibrium experiments suggest that the partial melt was produced by the dehydration melting reaction: muscovite + omphacite + quartz = melt + K-feldspar + kyanite (Nahodilová et al., 2010).

Stop 7-4 (Day 7). Eclogite, Borek

Coordinates: N49°47′34.3″ E15°34′41.3″

Eclogite at this stop is enclosed by serpentinite and located in the medium-grade Monotonous unit (Synek and Oliveriová, 1993). The eclogite and serpentinite occur in a ca. 400 × 250 lens-shaped body in an abandoned quarry, now used as a water reservoir, about 900 m west of the village of Borek. Two sets of fabrics, dipping steeply to the NW and SW, occur within the strongly serpentinised peridotite. Their origin and mutual relations are unclear due to strong serpentinization. The SW dipping fabric is parallel to the orientation of the eclogite layer, which occurs along the SW margin of the peridotite. The eclogite exhibits a foliation defined by the alignment of garnet grains and compositional layering and is concordant with the NW fabric in the peridotite.

Omphacite occurs as relics surrounded by symplectite in the matrix but may occur as inclusions in the rims of garnet. It has a jadeite content between 32–37 mol% and about 10–13 mol% aegirine content. Amphibole enclosed in garnet is taramite, in which the B site is occupied by 0.51 to 0.76 Na atoms per formula unit (a.f.u.) and the A site contains 0.6-0.8 Na+K a.f.u. (the ferric/ferrous ratio in amphibole was calculated by normalization to 13 cations and 46 charges). The $X_{Mg} = Mg/(Mg+Fe^{2+})$ ratio is about 0.5.

The pattern of compositional zoning and the presence of Na-Ca amphibole inclusions in garnet from eclogite suggest a prograde metamorphism from high-temperature blueschist

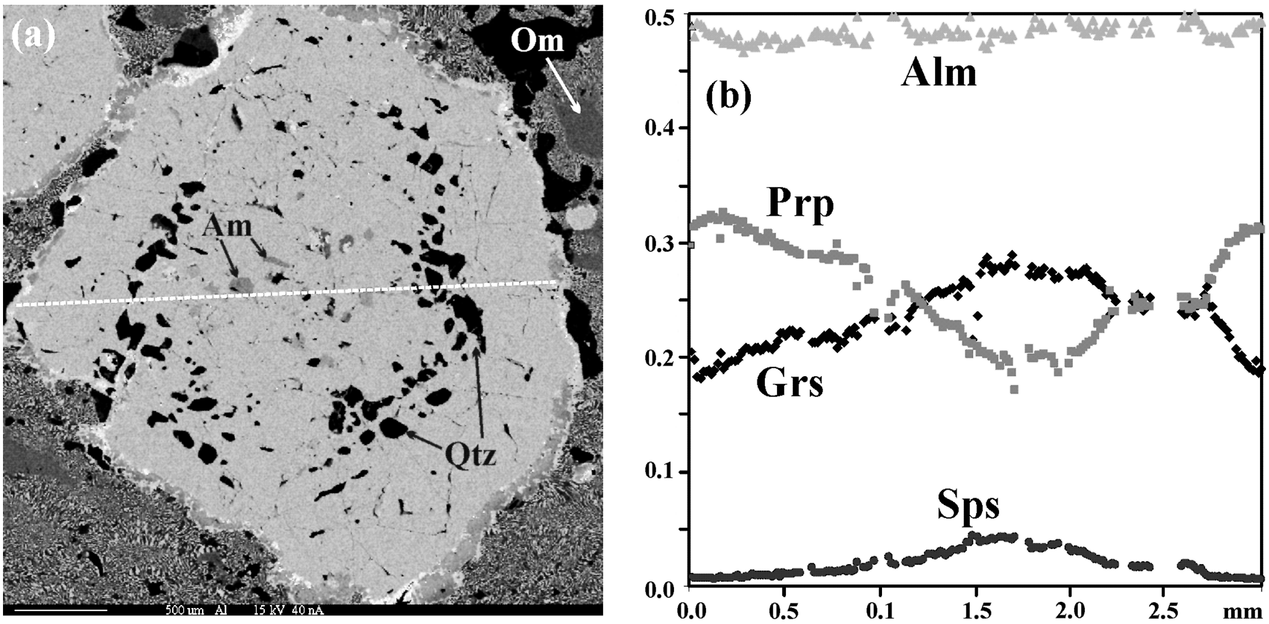

■ **Fig. 12.** (a) Al X-ray map of a garnet porphyroblast with inclusions of quartz (black) and Na-Ca amphibole (dark-grey) from the Borek eclogite. The matrix omphacite is replaced by amphibole+plagioclase symplectuite. (b) Rim-to-rim compositional profile for garnet prophyroblast in (a), illustrating variations in mol fractions of almandine, pyrope, grossular and spessartine.

The serpentinized peridotite consists of harzburgite with minor lherzolite and dunite (Fiala and Jelínek, 1992). In addition to olivine (Fo90) it contains orthopyroxene (En90), minor diopsidic clinopyroxene and accessory spinel. The eclogite forms a 60–70 m thick lens-like body in the serpentinite. Eclogite has the composition of tholeitic basalt and consists of garnet, omphacite, and quartz, with Na-Ca amphibole inclusions in garnet. The eclogite has been partly retrogressed, resulting in the replacement of omphacite by amphibole-plagioclase symplectite and the development of thin coronas of plagioclase and amphibole around garnet.

Garnet contains abundant inclusions of quartz and Na-Ca amphibole (Fig. 12a). It shows prograde zoning with high Mn and Ca in the core ($Grs_{28}Prp_{20}Alm_{48}Sps_4$) and high Mg at the rim ($Grs_{19}Prp_{32}Alm_{48}Sps_1$), while Fe is almost constant (Fig. 12b).

facies to eclogite facies conditions. Temperatures of 632 ±23, 616 ±34 and 690 ±46 °C, calculated at 2.2 GPa, were obtained using the garnet-pyroxene thermometers of Ravna (2000), Ai (1994) and Ganguly et al. (1996), respectively. Using the compositions of amphibole inclusionsnband adjacent garnet and omphacite, a pressure of 2.3 GPa at 590 °C is calculated, based on end-member reactions and the PTGIBS program (Brandelik and Massonne, 2004) (Fig. 13).

Summary

The lithological and metamorphic characteristics of HP/UHP rocks from the Kutná Hora complex and the adjacent Monotonous unit suggest subduction of crustal and mantle fragments from different geotectonic positions. Some garnet peridotites with layers of garnet pyroxenites and lenses of eclogites seem to represent fragments of lithospheric mantle that were incorporated in the subduction zone, where they crossed the spinel stability field to the garnet stability field and reached a maximum pressure of 4.0 GPa/1000 °C (Fig. 14). Different rock compositions and garnet zoning in eclogite within garnet peridotite indicate that some eclogites could have been tectonically emplaced into peridotite during different stages subduction and exhumation. Calculated PT conditions (~3.5 GPa, 950 °C) and the preservation of prograde-zoned garnet in kyanite-bearing eclogites within granulite suggest their subduction to the coesite stability field, followed by rapid exhumation and cooling, as indicated by the coexistence of retrograde high-grossular garnet with amphibole and plagioclase (point A in Fig. 11). In contrast, the present mineral assemblages in granulite indicate maximum pressures of 2.2–2.3 GPa at 900 °C. However, the association of granulite with eclogite and the preservation of zoning and inclusion patterns in garnet (Faryad et al., 2010) suggest that some granulites could have reached deeper levels in the subduction zone than that indicated by their calculated P-T conditions. During subsequent, buoyancy-enhanced *exhumation,* granulite could have entrained denser *mantle* rocks during their return flow up the subduction channel. The presence of the Borek MT eclogite in the Monotonous unit suggests that this may have been part of an accretionary wedge into which the HP/UHP Kutná Hora Complex was tectonically emplaced.

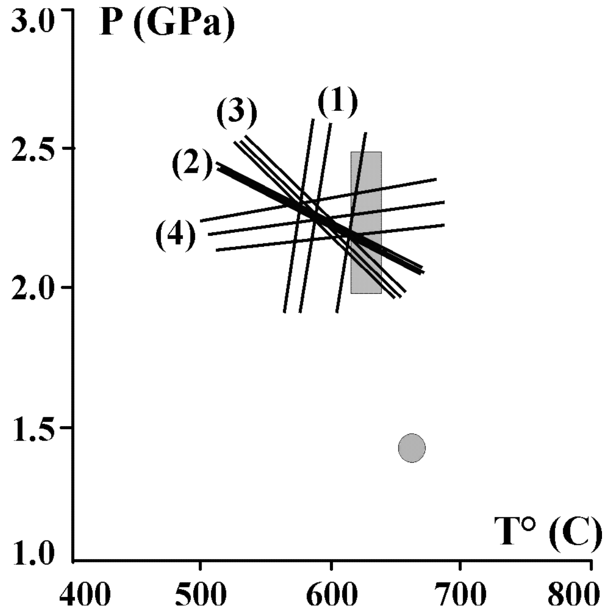

■ **Fig. 13.** Results of PT calculations for the Borek eclogite using PTGIBS software (Brandelik and Massonne, 2004) for reactions 1-4 and garnet-clinopyroxene thermometry (box) from calibrations of Ravna (2000) and Ai (1994). Reactions 1-4:
(1) prp + hed = di + alm
(2) parg + q = prp + gr + di + jd + H_2O
(3) parg + alm + q = prp + gr + jd + hed + H_2O
(4) parg + hed + q = gr + di + jd + alm + H_2O
Circle shows the minimum P-T conditions, estimated for the Borek eclogite by Medaris et al (1995)

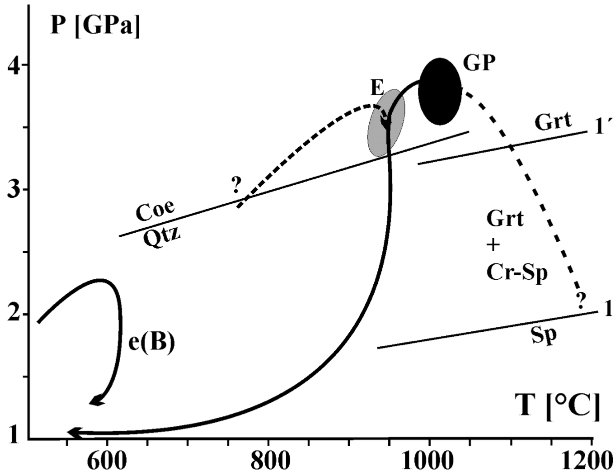

■ **Fig. 14.** PT conditions and proposed metamorphic evolution of garnet peridotites (GP) and eclogites (E) from the Kutná Hora Complex (Bohemian massif) (Faryad, 2009, simplified). e(B) is the possible PT path for eclogite in spinel peridotite at Borek. Lines 1 and 1' indicate spinel-garnet transition curves from Klemme and O'Neill (2000) and calculated for the compositions of spinel and garnet in the analyzed rocks.

References

AI Y., 1994. A revision of the garnet-clinopyroxene Fe^{2+}-Mg exchange geothermometer. *Contribution to Mineralogy and Petrology,* 115: 467–473.

BRANDELIK A. and MASSONNE H.J., 2004., PTGIBBS – an EXCEL (TM) Visual Basic program for computing and visualizing thermodynamic functions and equilibria of rock-forming minerals. *Computers & Geosciences,* 30: 909–923.

BREY G.P. and KÖHLER T.P., 1990. Geothermobarometry in 4-phase lherzolites. 2. New thermobarometers, and practicle assesment of existing thermometers. *Journal of Petrology*, 31: 1353–1378.

CARSWELL D.A. and O'BRIEN P.J., 1993. Thermobarometry and geotectonic significance of high- pressure granulites: examples from the Moldanubian Zone of the Bohemian Massif in Lower Austria. *Journal of Petrology,*34:427-459.

COOKE R.A., 2000. High-pressure/temperature metamorphism in the St. Leonhard Granulite Massif, Austria: evidence from intermediate pyroxene-bearing granulites. *International Journal of Earth Sciences,* 89: 631-651.

ELLIS D.J. and GREEN D.H., 1979. An experimental study of the effect of ca. upon garnet-clinopyroxene Fe-Mg exchange equilibria. *Contribution to Mineralogy and Petrology,* 71: 13–22.

FARYAD S.W., 2009. The Kutná Hora Complex (Moldanubian Zone, Bohemian Massif): A composite of crustal and mantle rocks subducted to HP/UHP conditions. *Lithos,* 109: 193–208.

FARYAD S.W., DOLEJŠ D. and MACHEK M., 2009. Garnet exsolution in pyroxene from clinopyroxenites in the

Moldanubian zone: constraining the early pre-convergence history of ultramafic rocks in the Variscan orogen. *Journal of Metamorphic Geology*, 27: 655-671.

FARYAD S.W, NAHODILOVÁ R. and DOLEJŠ D., 2010. Incipient eclogite facies metamorphism in the Moldanubian granulite recorded by inclusion patterns in garnet. *Lithos,* 114: 54-69.

GANGULY J. CHENG W. and TIRONE M., 1996. Thermodynamics of alumosilicate garnet solid solution: New experimental data, an optimized model, and thermodynamic application. *Contribution to Mineralogy and Petrology,* 126: 137–151.

FIALA J. and JELÍNEK E., 1992. The Borek qurarry near Chotěboř. Internationa workshop, high-pressure granulites-lower crustal metamorphism. Excursion guide. Czech Geologica Survey, 42-47.

GASPARIK T., 2000. An internally consistent thermodynamic model for the system CaO-MgO-Al_2O_3-SiO_2 derived primarily from phase equilibrium data. *Journal of Geology*, 108: 103-114.

GASPARIK T., 2003. Phase diagrams for geoscientists, An atlas of the Earth's Interior. Springer, 462 p.

KLEMD R. and BROCKER M., 1999. Fluid influence on mineral reactions in ultrahigh-pressure granulites: a case study in the Snieznik Mts. (West Sudetes, Poland). *Contributions to Mineralogy and Petrology*, 136: 358-373.

KLEMME S. and O'NEILL H.S.C., 2000. The effect of Cr on the solubility of Al in orthopyroxene: experiments and thermodynamic modeling. *Contribution to Mineralogy and Petrology*, 140: 85–98.

KOTKOVÁ J., 1993. Tectonometamorphic history of lower crust in the Bohemian Massif – example of north Bohemian granulites. Czech Geological Survey Special Pápera*,* 2: 56 p.

KRÖNER A., O'BRIEN P.J., NEMCHIN A.A. and PIDGEON R.T., 2000. Zircon ages for high pressure granulites from South Bohemia, Czech Republic, and their connection to Carboniferous high temperature processes. *Contributions to Mineralogy and Petrology,* 138: 127-142.

KRYZA R., PIN C. and VIELZEUF D., 1996. High-pressure granulites from Sudetes (south-west Poland): Evidence of crustal subduction and collisional thickening in the Variscan Belt. *Journal of Metamorphic Geology*, 14: 531-546.

MACHEK M., ULRICH S. and JANOUSEK V., 2009. Strain coupling between upper mantle and lower crust: natural example from the Běstvina granulite body, Bohemian Massif. *Journal of metamorphic Geology*, 27: 721-737.

MEDARIS L.G., FOURNELLE J.H., GHENT E.D., JELINEK E. and MÍSAŘ Z., 1998. Prograde eclogite in the Gföhl Nappe, Czech Republic: New evidence on Variscan high-pressure metamorphism. *Journal of Metamorphic Geology,* 16: 563–576.

NAHODILOVÁ R., FARYAD S.W., DOLEJŠ D. and TROPPER P., 2010. Decompresion and partial melting of subducted continental crust rocks; example from felsic high-*PT* granulites in the Bohemian Massif. IMA, Budapest, abstract volume.

NIMIS P. and TAYLOR W.R., 2000. Single clinopyroxene thermobarometry for garnet peridotites. Part I. Calibration and testing of a Cr-in-Cpx barometer and an enstatite-in-Cpx thermometer. *Contributions to Mineralogy and Petrology*, 139: 541–554.

O'BRIEN P.J., 1999. Asymmetric zoning profiles in garnet from HP-HT granulite and implications for volume and grain-boundary diffusion. *Mineralogical Magazine,* 63: 227-238.

O'NEILL H.S.C.,1981. The transition between spinel lherzolite and garnet lherzolite, and its use as a geobarome. *Contribution to Mineralogy and Petrology*, 77: 185–194.

O'NEILL H.S.C. and WOOD B.J., 1980. An experimental study of Fe-Mg partitioning between garnet and olivine and its calibration as a geothermometer. *Contribution to Mineralogy and Petrology*, 70: 59–70*; erratum in Contribution to Mineralogy and Petrology, 72: 337*.

POUBA Z., FIALA J., PADĚRA K., 1987. The granulite body near Běstvina in the Železné hory Mts. *Časopis pro Mineralogy Geology*, 32: 73–78

POWELL R., 1985. Regression diagnostics and robust regression in geothermometer/ geobarometer calibration: the garnet-clinopyroxene geothermometer revisited. *Journal of Metamorphic Geology,* 3: 231–243.

RAVNA E.J.K., 2000. The garnet-clinopyroxene Fe^{2+}-Mg geothermometer: An updated calibration. *Journal of metamorphic Geology,* 18: 211–219.

RAVNA E.J.K. and TERRY M.P., 2004. Geothermobarometry of UHP and HP eclogites and schists—an evaluation of equilibria among garnet-clinopyroxene-kyanite-phengite-coesite/quartz. *Journal of Metamorphic Geology,* 22: 579-592.

RÖTZLER J., ROMER R.L., BUDZINSKI H. and OBERHÄNSLI R., 2004. Ultrahigh-temperature high-pressure granulites from Tirschheim, Saxon Granulite Massif, Germany: P-T-t path and geotectonic implications. *European Journal of Mineralogy,* 16: 917–937.

SYNEK J. and OLIVERIOVÁ D., 1993. Terrane character of the northeast margin of the Moldanubian Zone—the Kutná Hora crystalline complex, Bohemian Massif. *Geologische Rundschau*, 82: 566–582.

ŠTÍPSKÁ P., SCHULMANN K. and KRÖNER A., 2004. Vertical extrusion and middle crustal spreading of omphacite granulite: a model of syn-convergent exhumation (Bohemian Massif, Czech Republic). *Journal of Metamorphic Geology,* 22: 179-198.

TAYLOR W.R., 1998. An experimental test of some geothermometer and geobarometer formulations for upper mantle peridotites with application to the thermobarometry of fertile lherzolite and garnet websterite. *Neues Jahrbuch fuer Mineralogie Abh*., 172: 381–408.

VRÁNA S., ŠTĚDRÁ V. and FIŠERA M., 2006. Petrology and geochemistry of the Běstvina granulite body metamorphosed at eclogite facies conditions, Bohemian Massif. *Journal of the Czech Geological Society,* 50: 81–94.